UNIVERSITY OF TWENTE.

Faculty of Behavioural Management and Social sciences
Financial engineering and management

Assessing the Economic Implications of Physical Climate Risks on Dutch Banks: A Case Study

Master Thesis

Ir. Erwin H. Siegers
S2038005
2 October 2023

MSc graduation committee:

Chair:
Prof. Dr. Ir. L. Spierdijk
Second adjudicator:
Prof. Dr. Ir. A. Bruggink
External member:
MSc. FRM J.J. Noordegraaf

Abstract

Climate change is one of the greatest challenges currently faced by humanity. Currently, initiatives are being developed to achieve net-zero carbon emissions by 2050. Nevertheless, the impacts of these emissions are already being experienced, exerting an ever-increasing influence on the climate. These impacts are also being felt by financial institutions and are encompassed in the ESG governance. The Netherlands is no exception to these challenges, facing increased risks regarding floods and ecological/geographical risks due to extended drought periods. Banks are increasingly compelled to study the impacts of climate change on their loan portfolios since these phenomena can devalue underlying assets or reduce creditworthiness of borrowers. Currently, a significant portion of loans comprises private residential mortgages. Typically, these loans are secured by residential properties that are vulnerable to the amplified climate threats. Unfortunately, there is a very limited literature available that quantifies these threats to the residential mortgage portfolio. Therefore, the following research question is formulated to fill the identified gap in the current literature:

What is the predicted increase in Loss Given Default up to 2050 for the residential mortgage portfolio in the banking sector in the Netherlands, resulting from physical climate risks such as flooding, pile rot, and settlement?

The existing literature on the impact of extended drought periods is rather limited. While drought periods are known to induce pile rot in houses built on wooden pole foundations and can cause settling damage due to uneven foundation settlement, the quantification of these effects remains constrained. One methodology, proposed by Costa et al., has developed a Hazard-Exposure-Vulnerability framework to predict damages to properties resulting from these phenomena.

While the current literature lacks the quantification of flood and drought risks to a residential mortgage portfolio, several papers have been published that attempt to model the impact of floods on floodplain areas predominantly consisting of residential properties. Some of these methodologies employ a Bernoulli trial approach to determine whether a flood has occurred. By combining this methodology, with a damage model dependent on the property's area and a set of inundation depth-damage functions, it becomes possible to predict the damage to residential properties.

The methodology employed in this research combines a synthesis of previously conducted studies. A Bernoulli trial approach based on charts from the Klimaateffectatlas is employed, alongside a custom set of inundation depth-damage functions specific to the Netherlands provided by Deltares. This combined method predicts damages resulting from flooding. To forecast damages from settling and pile rot up to 2050, the Hazard-Exposure-Vulnerability framework proposed by Costa et al. is utilised. Based on these incurred damages, the implication of physical climate risk on the value-to-loan ratio and the loss given default can be predicted for the upcoming 30 years.

The research presents several realistic predictions, with the simulation involving a given inundation depth of 0.5m and a high settling and pile rot scenario resulting in the highest estimated amount of damage. For a dummy portfolio comprising 4116 mortgages, the average flood damage incurred amounted to €826,308. The average settling damage is €332,523, whereas the average pile rot damage is €1,035,242. Considering both direct and indirect damages, the VtL decreased from the average baseline of 1.3068 to 1.3040 when the average incurred damages are used. Further reduction occurred when the 99.9% VaR is utilised, lowering the VtL to 1.3029. Simultaneously, these damages increased the LGD from the average baseline of 16.78% to 16.88% for the average incurred damage and to 16.94% for the 99.9% VaR damage. The reduction of the VtL and LGD are both primarily concentrated around the Randstad, with physical risks being particularly high in Amsterdam. However, when points proximity is disregarded the overall reduction in LGD is observed in the municipality of Landsmeer.

Additionally, an extreme prediction is conducted, wherein the incurred flood damages exceeded the indirect damages by a factor of 12. While this scenario is highly unrealistic, it could become relevant if incentives to comply with the Waterwet 2050 are disregarded. In this hypothetical scenario, the average incurred flood damages totaled €9,630,762. These damages lead to a decrease in the VtL to 1.2924 and 1.2867 for the average case and the 99.9% VaR case, respectively. Simultaneously, the LGD increased to 17.34% and 17.80% for the average case and the 99.9% VaR case, respectively. The domination of direct damages focuses the physical climate risk more around the major rivers, where the inundation depths are the highest.

In summary, the realistic prediction exhibited a limited impact on the VtL and LGD due to physical climate risks. Conversely, the extreme scenario does reveal significant decreases in the VtL and an increase in the LGD. This emphasises that while physical climate risks might not have a significant impact in average cases, the risks could play a crucial role in extreme scenarios. Therefore, conducting stress testing becomes essential to thoroughly evaluate these tail risks.

Contents

List of Figures

List of Tables

List of Symbols

Symbol	Function	Unit
p	Property price	e
β_i	Regression coefficient i	-
D^{dir}	Total direct damage in the area under consideration	e
D^{max}	Value at risk for land-use category i	e
Z	Z-score	-
N	Population size of the original portfolio	-
ϵ	Margin of error	-
P	Population proportion	-
S_i	Incurred damages on building i	e
SA_i	Surface area of building i	m^2
SN	Base rate per square meter	e
r	Risk-free rate	-
σ	Standard deviation	-
β	Haircut	-
a	Damage factor	-

List of Abbreviations

Abbreviation	Description
BAG	Basisregistratie Adressen en Gebouwen
BPS	Basis points
CDF	Cumulative distribution function
CET1	Common equity tier 1
CSRD	Corporate Sustainability Reporting Directive
DiD	Difference-in-difference
EAD	Estimated annual damages
EBA	European Banking Agency
ECL	Expected credit loss
EL	Expected loss
EPSG	European Petroleum Survey Group
ES	Expected shortfall
ESG	Environmental, Social, and Governance
FS	First street
GDP	Gross domestic product
GHG	Greenhouse gasses
Gl	Gematigd laag
HPM	Hedonic pricing model
IFRS	International Financial Reporting Standards
INSYDE	In-depth Synthetic Model for Flood Damage Estimation
I-O	Input-output
IRB	Internal rating based
ITS	Implementing technical standards
JRC	Joint research centre
KNMI	Koninklijk Nederlands Meteorologisch Instituut
LGD	Loss given default
NDC	nationally determined contributions
NGFS	Network of Central Banks and Supervisors for Greening the Financial System
NPV	Net present value
PD	Probability of default
ROE	Return on equity
RCP	Representative Concentration Pathway
SFDR	Sustainable Finance Disclosure Regulation
TIFF	Tag Image File Format
UNEP FI	United nation environment program finance initiative
VaR	Value at risk
VtL	Value-to-loan
Wh	Warm hoog
WOZ	Wet waardering onroerende zaken

1 Introduction

1.1 Problem context

Climate change represents one of the greatest challenges humanity has ever encountered. Currently, human activities contribute to the rising levels of greenhouse gases (GHG), accelerating the pace of climate change. Governments worldwide are striving to reduce carbon emissions, aiming for a net-zero ambition by 2050. However, the impacts of climate change are already being experienced globally, causing extensive damage. These climate changes, coupled with evolving regulations on GHG emissions, have led to a rapidly changing economic landscape and substantial financial risks. Financial institutions, in particular, face significant risks on both their assets and liabilities. To address these challenges, over 100 financial institutions worldwide have established the Network of Central Banks and Supervisors for Greening the Financial System (NGFS), with the goal of developing an environment and climate risk management framework for the financial sector.

In addition to their own commitment, financial institutions are guided by the Basel Committee's publication of 18 principles for the effective management and supervision of climate-related risks [1]. These principles encompass the integration of Environmental, Social, and Governance (ESG) factors and associated risks into financial practices. The ESG framework focuses on non-financial factors and aims to be incorporated into companies to identify material risks and growth opportunities. While these directives are currently not mandatory, they are likely to be integrated into the Basel framework in the coming years. As a result, banks and insurers are actively working on addressing the associated capital requirements. The significance of this topic is evident in its central position in financial research, as depicted by the most frequently used keywords in the field, shown in Figure 1.1.

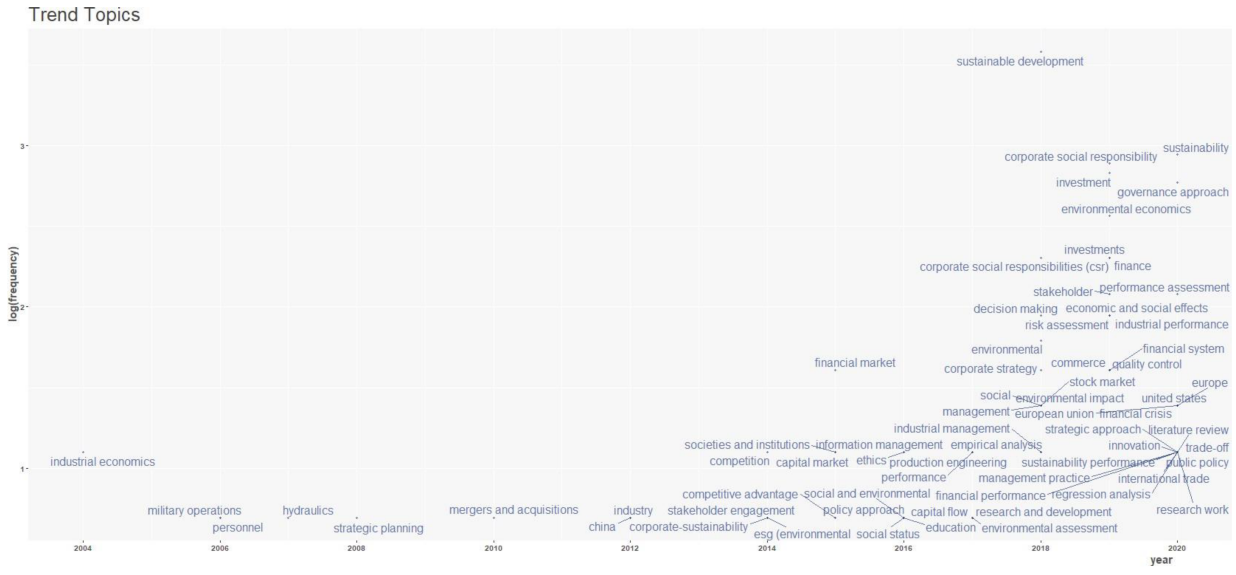

Figure 1.1: *Keyword search trends on Scopus regarding the financial sector [2].*

A significant aspect of ESG risk is associated with climate risks. Therefore, the assigned task at Mount Consulting focuses on the climate risk component within the ESG framework. Mount Consulting provides consultancy services to several prominent banks and insurers in the Netherlands, primarily focusing on qualitative aspects of the sector. Their expertise lies in areas such as EU taxonomy, data separation during takeovers, and data vendor selection. Recently, there has been a growing interest in the quantitative aspect of ESG, particularly in climate risk modeling.

As the importance of ESG continues to grow, Mount Consulting also needs to gather information on this topic. Currently, other employees in the company are qualitatively assessing the regulatory aspects of ESG. However, these regulatory frameworks do not provide guidelines regarding estimates for the required risk capital. To improve the knowledge regarding the analytical part of this topic, the internship aims to quantify these risks, primarily focusing on the physical risks associated with climate change.

Mount Consulting primarily serves banks and insurers within the Netherlands, so the scope of the internship is limited to assets located in this region. By narrowing down the research area, the quantification of physical risks becomes more realistic, considering that different parameters are relevant in different parts of the world. For instance, physical climate risk modeling in the USA and the Caribbean focuses on earthquakes and hurricanes [3, 4], which do not pose a threat of physical damage in the Netherlands. Nevertheless, a similar approach is required to identify and quantify potential damages to underlying assets, such as loans.

1.2 Core problem

The Netherlands is situated 26% below sea level, with an additional 33% of the country prone to flooding [5]. This area primarily encompasses the densely populated regions, making the failure of water defenses a significant concern. It could lead to a major loss of life and extensive damage to everything located within this vulnerable area. Throughout history, the threat of flooding has been ever-present, with the most memorable incidents being the North Sea floods in 1953. Since then, the government has made significant improvements to flood defenses and demonstrated a strong commitment to long-term defense measures through the enactment of the Waterwet 2050. However, the current rate of climate change predicts a sea level rise of 26cm to 82cm [6], which endangers the effectiveness of the existing primary flood defenses. Additionally, climate change brings about more extreme weather events, including heavy rainfall, hailstorms, and prolonged periods of drought. These droughts cause groundwater levels to drop, exposing wooden foundations to oxygen and resulting in rotting. Moreover, these dry periods can induce uneven settlement of foundations, causing damage to houses. These climate effects are expected to intensify in the coming years as climate change worsens.

Banks are increasingly compelled to study the effects of climate change on their loan portfolios, as such phenomena can devalue underlying assets and reduce the creditworthiness of borrowers who bear the responsibility for the resulting damages. Furthermore, with the introduction of technical standards for ESG by the European Banking Authority (EBA) and the implementation of other ESG-related regulatory frameworks like the Corporate Sustainability Reporting Directive (CSRD) and the Sustainable Finance Disclosure Regulation (SFDR), regulatory bodies are preparing to incorporate directives related to this topic into the Basel framework. This could lead to additional credit risks and may also influence operational risks [7]. As a result, banks are required to hold higher levels of risk capital. Consequently, policymakers and bank boards of directors are keen to obtain approximate figures regarding the expected physical damage and accompanying credit risks [8].

This thesis primarily focusses on the residential mortgage portfolio, which constitutes 50% of ING Bank's total loan book [9]. For banks that predominantly specialise in this type of mortgage, like Volksbank, the residential mortgage portfolio represents an even higher percentage [10]. Therefore, this portfolio has a significant influence on the bank's balance sheet.

Currently, there is ample literature available regarding the incurred damage from acute physical climate risks in the Netherlands [11, 12]. Additionally, the indirect implications of these acute events have been extensively researched, with several papers examining the decline in house prices following such weather events [13, 14]. However, this literature primarily focuses on the extent of the damage and does not address the credit risks faced by banks in relation to these risks. Hence, there is a need for more empirical research that explores the economic implications of these physical risks on mortgage default rates, loss given default, and the overall creditworthiness of borrowers.

In addition to acute threats, chronic climate events also cause damage to residential homes. However, research in this area is currently limited due to its limited generalisability beyond the Netherlands and its limited practical relevance for other countries. Although Costa et al. have proposed a modeling methodology for pile rot and settling [15], there is a lack of research in the available literature that examines the actual damages resulting from these chronic climate events and their implications on parameters such as probability of default (PD) and loss given default (LGD). This research gap highlights the need for further investigation into the assessment and quantification of damages caused by pile rot and settling, as well as their subsequent impact on credit risk metrics.

Therefore, by quantifying the physical risks on the residential mortgage portfolio, this research aims to bridge the gap between the incurred damages from acute and chronic climate risks and their implications on credit metrics. Additionally, it will contribute to answering questions about the potential exposure of banks to climate change risks concerning their residential mortgage portfolios.

1.3 Problem approach

In order to address the core problems identified earlier, this research aims to develop an accurate modeling framework that allows for an evaluation of the financial implications associated with physical climate risks, with a specific focus on the residential mortgage portfolio. The primary objective is to investigate the specific effects of flooding, pile rot, and settlement on loan default rates and loss given default rates. The research approach will consist of the following key components.

The first step in this research is to acknowledge the regulatory framework that governs financial institutions across Europe, known as the Basel framework. The Basel framework consists of three pillars that guide risk management practices within the financial sector. It is crucial to recognise that climate risk is considered a material risk and should be integrated into Pillar I, as emphasised by Genest et al. [16].

However, it is important to note that the current Basel framework does not explicitly include environmental, social, and governance risks. Nevertheless, recognising the significance of ESG risks, the EBA has already issued directives regarding these risks. This highlights the evolving regulatory landscape and the increasing recognition of the importance of incorporating climate-related factors into financial risk management practices. Based on these directives a foundation for a prediction model can be established.

Building upon this regulatory context, a literature review will explore the current knowledge on physical climate risks in the Netherlands. It will cover different climate scenarios and identify the specific climate risks that apply to the Netherlands. The review will examine existing studies and methodologies, presenting current efforts to quantify both acute climate events, such as floods, and chronic events, such as pile rot and settling. Additionally, it will explore current efforts made to connect climate risks with mortgage credit risk. The literature review aims to identify gaps in knowledge and contribute to understanding which methodologies to employ in the subsequent sections of the thesis.

Constructing a representative portfolio that closely resembles an actual bank's residential mortgage portfolio is a crucial step in addressing the core problem. Due to the confidentiality of residential mortgage data, obtaining an actual bank's portfolio is unattainable. However, by carefully selecting and constructing a portfolio that captures key characteristics and risk profiles, a representative portfolio can be created. This representative portfolio will enable a comprehensive analysis of the impacts of physical climate risks on loss given default rates.

To address the problem of identifying potential damages that may occur in the next few decades, it is necessary to translate the qualitative concept of "climate change" into a quantitative set of variables. This set of variables should specifically capture the risks and hazards relevant to the Netherlands, as the thesis focuses on this geographical area. By defining and quantifying these variables, a basis for quantitative analysis of climate risk can be achieved.

Subsequently, the research aims to establish a connection between the portfolio and the actual risks associated with climate change. This involves developing a model that can accurately predict the damages to underlying assets caused by climate-related factors. The damage to underlying assets due to climate change has a substantial effect on the required risk capital, as the value of the assets decreases with damage, leading to higher loss given default rates. The shift in this core credit risk parameter provides an indication of the quantitative influence of climate change on the residential mortgage portfolio.

In conclusion, this research aims to develop an accurate modeling framework that integrates physical climate risks into the risk management practices of financial institutions, with a specific focus on the residential mortgage portfolio. By addressing the core problems identified, including the need for a representative portfolio, quantifying climate-related variables, and establishing the connection between the portfolio and actual risks, this study seeks to provide valuable insights into the financial implications of physical climate risks. The findings will not only contribute to filling the research gap in understanding the impacts on loss given default rates but also offer meaningful guidance for banks, policymakers, and other stakeholders in effectively managing climate-related risks.

1.4 Research objectives

With the core problem and accompanying problem approach of the internship covered, a central research question with corresponding sub-questions is formulated. The main research question regarding this research is:

"What is the predicted increase in Loss Given Default up to 2050 for the residential mortgage portfolio in the banking sector in the Netherlands, resulting from physical climate risks such as flooding, pile rot, and settlement?"

First, this research includes the quantitative estimation of LGD given the above-mentioned climate events. Moreover, the research incorporates the positioning of high-risk areas given the portfolio. Nevertheless, the research does not entail any mitigation solution or approximate risk charge to minimise the influence of these climate events.

Second, the research analyses the impact of climate change on the LGD and Value-to-Loan (VtL) and does not incorporate the PD and consecutive Expected Loss (EL). This is mainly due to the complex nature of PD modeling and the limitation in input parameters such as a bank's portfolio. In future research, the addition of a climate-adjusted PD would be beneficial but due to the limitation of this research, it is not included in the scope of the research.

Lastly, the research is limited to a stagnant portfolio. Therefore, portfolio dynamics such as premature closure and VtL shifts due to macro-economic parameters are disregarded to limit the research to the intrinsic effect of the climate change events.

1.5 Research questions

To answer the main research question, the thesis is divided into several sub-sections each corresponding to a component highlighted in the problem approach. The sub-sections have a set of sub-questions which helps to structure the research.

(i) **Climate risks and regulations.**

The Basel regulatory framework strongly regulates financial institutions across Europe. The Basel framework is divided into three pillars. Currently, the Basel framework excludes ESG risks. However, the EBA has already published directives regarding these risks. Hence, the following research questions are formulated:

- Which climate risk regulations and directives are banks exposed to?
- Which published pillar III physical climate risk directives are currently applicable to the residential mortgage portfolio and what do they enforce?

(ii) **Literature review.**

To identify the current efforts made towards this topic, a literature review should be conducted. This review aims to identify current climate scenarios and climate threats applicable to the Netherlands, as well as methodologies and attempts to quantify these climate risks. Therefore, the following research questions have been formulated:

- What are the specific climate scenarios, risks and hazards relevant to the Netherlands?
- How can the qualitative concept of "climate change" be translated into a quantitative set of variables?
- Which methodologies or approaches are currently utilised to quantify physical climate risks?
- What researches have been conducted to examine how the credit risk of banks is affected by physical climate risks?

(iii) **Generating a residential mortgage portfolio.**

To predict damages to certain buildings and structures, the model requires a portfolio that closely represents an actual bank's portfolio. However, since the internship is not being conducted at the internal risk management department but at an external consultant, banks are not willing to share their highly confidential residential mortgage portfolios. Therefore, constructing a portfolio that somewhat resembles an actual portfolio becomes important. In light of this, the following sub-questions are composed:

- What considerations are taken into account when determining the size and composition of a residential mortgage portfolio?
- What data sources are required to gather the necessary information for constructing a representative portfolio?
- How is data on loan characteristics, such as interest rates, and loan-to-value ratios incorporated into the portfolio?

(iv) **Creating damage patterns across different areas within the Netherlands**

To connect the portfolio with the risks associated with climate change, it is necessary to convert the quantified physical climate risks into estimated damages to underlying assets. This step involves addressing the following sub-questions:

- How are the potential damages to underlyings quantified using the identified climate variables?
- How can real-world data be used to validate the accuracy of the incurred damages to underlyings?

(v) **Connecting incurred damages with risks and required risk capital**

The damage to underlyings due to climate change has a substantial effect on the required risk capital, as the VtL decreases, implying a higher LGD. Hence, it is important to associate the damages with actual figures required by Basel Pillar I. Therefore, the following sub-questions are formulated to establish this connection:

- How are damages to an underlying and VtL associated with LGD?
- What is the overall effect of the physically induced damages on the LGD?
- How does the model tie in with the proposed ESG regulations and directives?

1.6 Research approach

To answer the aforementioned questions, the following research approach will be applied. First, a literature review should be conducted to acquire information regarding the current applicable Basel framework for physical climate risks. Additionally, the literature study should incorporate previous efforts in quantifying these risks. To accurately predict damages over a 30-year period, the literature review should include probable climate scenarios, as the probability and severity of climate events depend on the extent of climate change. Lastly, existing literature on the impact of physical climate events on mortgage credit risk is analysed to identify utilised methodologies, findings, and research gaps in investigating the relationship between climate change and credit risk for the residential mortgage portfolio.

Subsequently, the necessary data can be gathered to construct a residential mortgage portfolio that closely resembles an actual portfolio. This can be achieved by collecting data on VtL from annual reports and approximating the distribution of underlyings associated with residential mortgages based on the population distribution across the Netherlands.

Additionally, data needs to be gathered to quantify acute and chronic climate risks. Accessing current predictive flood risk maps and probabilistic models can provide insights into the frequency and severity of acute climate risks in the future. Moreover, quantification of chronic climate events requires data on the probability of properties being built on appropriate foundation types and the severity of the resulting damage. Both settling and pile rot originate from the same groundwater patterns and hence require similar data for quantifying these qualitative risks. Furthermore, for quantifying both acute and chronic climate events, the climate scenarios obtained in the literature review should be incorporated, as these scenarios significantly impact the prediction of input risks.

The next step in answering the research questions is to develop a modelling framework that incorporates these input variables and predicts the incurred damages over the coming decades. As mentioned earlier in the problem approach, this study will thoroughly investigate existing modelling methodologies and approaches to identify the most effective and widely accepted methodology available in the current literature. The development of the modelling framework will be based on this best-fit methodology, and its accuracy in predicting damages to underlyings will be validated by comparing the results with real-world data.

Lastly, the data is analysed to assess the specific impacts of flooding, pile rot, and settlement on the LGD of the residential mortgage portfolio. Furthermore, it is possible to allocate the physical climate risk to specific regions within the Netherlands in relation to the residential mortgage portfolio.

2 Literature review

The goal of this chapter is to identify possible risks associated with climate risks and previous modeling efforts to express climate risks in actual figures. The chapter begins with an introduction to ESG and briefly mentions import regulations and directives regarding physical climate risks. This is followed by the introduction of several climate scenarios. Subsequently, the applicable climate risks to the Netherlands and their associated quantitative data for climate risk models are presented. Afterwards, the existing methodologies and approaches to model acute and chronic climate events are discussed. Finally, the literature review addresses the existing literature regarding the integration of physical climate change risks into credit risk metrics.

2.1 ESG regulation

Climate risk is embedded within the overarching term ESG. As briefly discussed in the introduction, these regulations regard the social aspects of the financial sector. Within the next two subsections, ESG is elaborated on and the import regulations and directives are addressed.

2.1.1 The Environmental, Social, and Governance framework

Sustainable finance refers to the process of considering environmental, social, and governance factors into account when making financial decisions. Rather than just focusing on maximising stakeholder benefits, ESG factors also consider non-financial terms. This framework seeks to maximise financial returns while accounting for social risks and opportunities [17].

Firstly, the environmental aspect of ESG regards energy consumption, carbon emissions, waste production, and climate change of particular companies. Secondly, the social term addresses the companies relationship with people and other companies. This factor involves terms such as inclusion and diversity. Lastly, the governance factor encompasses the internal system of practices and procedures the company adopts to make effective decisions and comply with the law [18]. The ESG framework is deeply convoluted within a company, just like the factors themselves are intertwined. As of this moment, the thesis will focus on the environmental section of ESG since within this part climate risks are located.

2.1.2 Regulations and directives

Different regulations and directives are issued by the EBA. The content within this thesis is mainly impacted by the standards proposed in: 'Final draft implementing technical standards on prudential disclosures on ESG risks in accordance with Article 449a CRR'. These directives are located within Pillar III of the Basel framework and state that 'The Article 449a of Regulation (EU) No 575/2013 (CRR) requires large institutions with securities traded on a regulated market of any Member State to disclose prudential information on environmental, social and governance risks, including physical risks and transition risks, as defined in the report referred to in Article 98(8) of Directive 2013/36/EU' [19]. Within this directive, the EBA developed a draft implementing technical standards (ITS) specifying uniform formats and associated instructions for the disclosure of ESG information. The different quantitative templates on climate change disclosed within the document are displayed in Figure 2.1 [19].

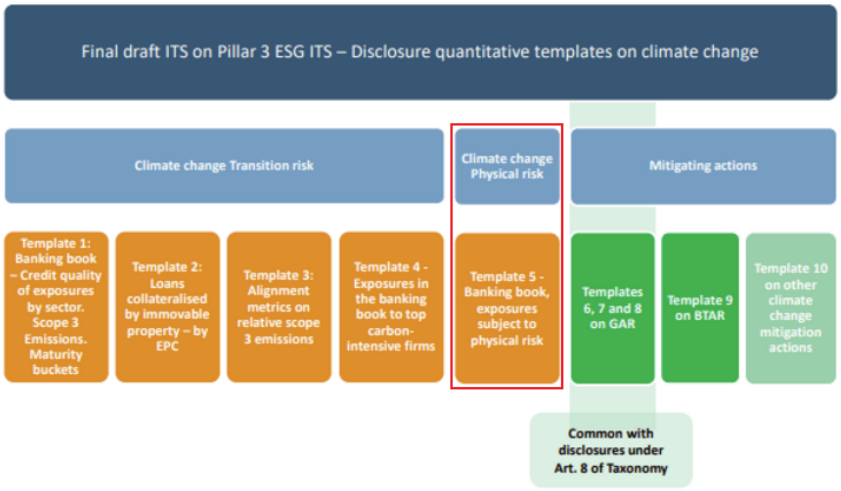

Figure 2.1: *Proposed quantitative templates on ESG from the EBA [19].*

Within this disclosure, template 5 is most important for this research since this thesis solely regards the physical risks of climate change (red contoured in Figure 2.1). The template is depicted in Figure A.1. This template assists banks in evaluating their exposures to both chronic and acute physical climate risks across different assets. However, it only facilitates the quantification of the gross carrying amount of assets which are exposed to either acute or chronic climate change. Hence, the technical standards only quantify the amount exposed to a particular risk and do not evaluate the actual costs the risks bear [20].

2.2 Climate scenarios

Before the actual physical risks are explained, climate scenarios proposed by the NGFS committee are described. The NGFS proposed 72 different climate scenarios. However, in this thesis, the quantity of scenarios is limited to the most important six individual scenarios. In practice, an unlimited number of scenarios exist. However, these six cover the most reasonable spectrum of scenarios.

The scenarios are spread across categories within the NGFS framework. This framework encompasses the quantity of physical risks and the transition pathway incorporated within the climate scenario. A figure illustrating the different quadrants is provided in Figure 2.2, along with a description of these quadrants in Table 2.1.

Table 2.1: *Quadrants employed by the NGFS committee to qualitatively separate climate scenarios [21, 22].*

NGFS Framework	Transition risks	Physical risks	Description
Orderly	Low	Low	These types of scenarios assume an introduction of climate policies at an early stage and become gradually more stringent. Additionally, it presumes there are no substantial discrepancies between policies promulgated by the governing bodies.
Disorderly	High	Low	In the disorderly framework, scenarios are incorporated which explore higher transition risks due to delayed climate policies or inconsistent policies across industries for example. The policies are not gradually introduced but are very stringent upon introduction.
Hot house world	Low	High	These scenarios assume that only a modest number of jurisdictions adopt climate policies to counteract global warming. Nevertheless, global efforts are insufficient to stagnate the global warming resulting in irreversible impacts like sea-level rise.
Too little, too late	High	High	The most extreme scenarios are located within this quadrant. It assumes the governmental bodies do not do enough to meet the set climate goals leading to significant climate related disasters. The presence of physical risks spurs a disorderly transition to a net-zero economy with policies being very stringent upon introduction.

The NGFS proposed six scenarios, none of which are located in the "too little, too late" quadrant. To end up in this quadrant, there needs to be a certain sequence of physical events originating from a scenario in the "hot house world" quadrant. Subsequent to the physical disasters, very stringent regulations should follow, which is highly implausible given the current awareness. Therefore, none of the six scenarios are located within this quadrant. The distribution of the six main scenarios proposed by the NGFS across the framework is provided in Figure 2.2.

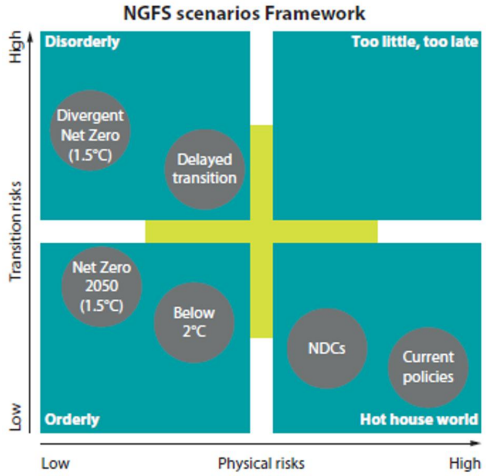

Figure 2.2: *Climate scenarios proposed by the NGFS committee distributed across the quadrants [21].*

Firstly, the most recognisable scenario is the Net Zero 2050 scenario, which aligns with the pathway to a net zero carbon economy outlined in the 2015 Paris Agreement. This scenario entails the least amount of physical risks, with only a limited number of transition risks due to a transparent and unambiguous pathway. Secondly, the Below 2°C scenario follows a similar pathway as the Net Zero 2050 scenario, but with slightly less stringent rules. Consequently, carbon emissions are gradually phased out, in line with the Paris Agreement, resulting in higher physical risks but lower transitional risks. Both of these scenarios are located within the orderly quadrant.

Thirdly, the Divergent Net Zero scenario envisions a carbon-neutral economy around 2050 but with higher costs due to divergent policies across sectors, leading to a more rapid phase-out of oil. However, significant variation in carbon pricing, for example, introduces high transition risks, while the rapid phase-out of oil mitigates an overall temperature increase, thereby limiting the physical risks. Fourthly, the Delayed Transition scenario assumes that annual carbon emissions do not decrease before 2030, requiring strong regulations to limit global warming to 2°C. Consequently, this scenario entails both mild transitional and physical risks. These scenarios are placed within the disorderly quadrant.

Fifthly, the Nationally Determined Contributions (NDCs) scenario encompasses the currently pledged targets aimed at limiting global warming. However, these targets currently lack the backing of implemented policies, directives, or regulations. Nonetheless, governmental bodies have already put these targets forward. Lastly, the NGFS committee proposed a scenario that preserves only the currently implemented policies. Hence, while the physical risks are high, the transition risks are low. Since both the NDC and current policies scenarios exhibit low transition risks but high physical risks, they are located within the hot house world quadrant.

The most important scenarios for this thesis are the Net Zero 2050 and the NDC or current policies scenarios, as these scenarios oppose each other regarding physical risk. Hence, scenarios with the most pronounced contrast in physical risks are of greater interest for this research.

2.3 Climate risks

The Netherlands is exposed to various climate events, such as flooding, hail, and droughts. These weather events can result in property damage and revenue loss. The following chapter will explore the relevant climate events for the Netherlands, discuss the probability of the event occurring, and the typical damages associated with each event.

2.3.1 Flooding

The most significant climate risk faced by the Netherlands is the risk of flooding. Approximately 26% of the country is situated below sea level, with an additional 33% at risk of flooding [5]. This includes densely populated areas, making the potential consequences of water defences failure catastrophic in terms of loss of life and damage to infrastructure. To assess these risks, probability charts can be utilised. A provider of these charts for the Netherlands is the klimaateffectatlas. The charts by the klimaateffectatlas provide information on the probability of a flood based on the inundation depth or determine the maximum inundation depth given a certain probability. The inundation depth refers to the depth of water from the ground level to the water surface. A schematic representation of inundation depth is illustrated in Figure 2.3.

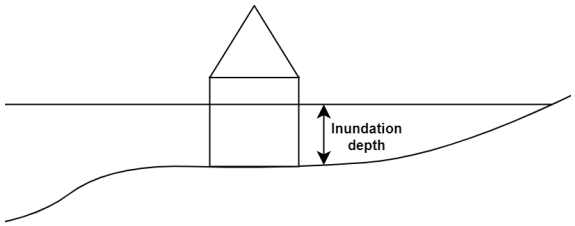

Figure 2.3: *Schematic representation of the inundation depth in case of a flood.*

Besides probability charts, there are also charts representing the maximum inundation depth given the flood probability. The charts that present a fixed inundation depth and varying probability provide a more realistic perspective, while the charts with a fixed probability and variable inundation depth represent a worst-case scenario. These charts aim to estimate the probability of a flood based on high or low climate scenarios. The high and low scenarios used by the klimaateffectatlas are the Gematigd laag (Gl) and Warm hoog (Wh) scenarios, respectively. The Gl scenario aligns with the lower range of the Representative Concentration Pathway (RCP) 2.6 scenario, while the Wh scenario corresponds to the RCP 8.5 pathway. These scenarios are closely linked to the upper range of the net-zero 2050 and NDC scenarios, respectively, as defined by the NGFS [23, 24].

Additionally, the predictions take into account the regulations outlined in the Waterwet 2050, which govern the primary flood barriers. This law sets a maximum allowable flood probability, which the current flood protections do not meet. However, the government is obligated to meet this standard by 2050. The prediction methodology used in these charts is adapted from the 2007/60/EC directive on the management of flood risks. Similarly, the charts depicting maximum inundation depth for a given flood probability utilise the same prediction methodology [23]. An example of both types of charts is presented in Figure 2.4 below. The complete set of flood prediction charts provided by the klimaateffectatlas is appended in Appendix B.

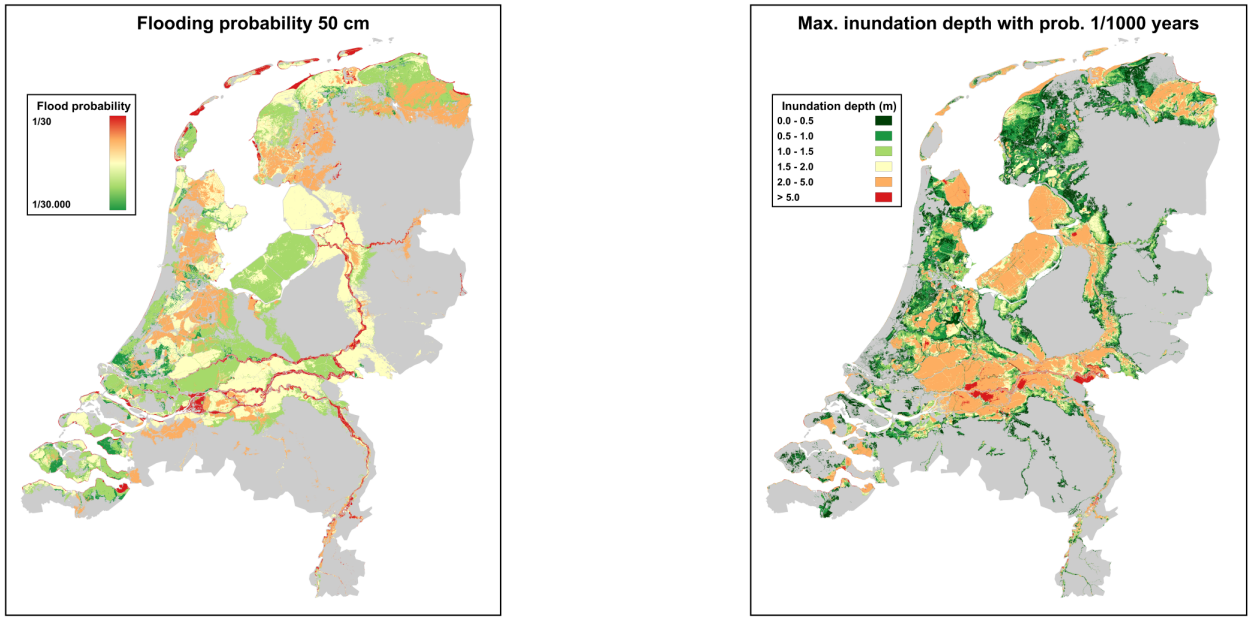

(a) *(b)*

Figure 2.4: (a) *The probability of a flood occurring with an inundation depth of 0,5 m [23]. ,* ***(b)*** *The maximum inundation depth which could be achieved given the probability of flooding equals 1/1000 years [23].*

Both of these maps are closely linked to the distance from a river and the elevation of the terrain relative to sea level. As shown in Figure 2.4a, areas in the eastern parts of the Netherlands have minimal risk of flooding due to climate change. Conversely, regions with high population density, particularly in and around the conurbation in the western parts of the country, face significant flooding risks. However, Figure 2.4b reveals that the most severe inundation depths in an extreme scenario are not concentrated in the conurbation but are more centered around the cities of Den Bosch, Nijmegen, and Arnhem. These cities are situated close to major waterways in the Netherlands, such as the Rijn and the Maas, which are prone to flooding with very high inundation depths, as also visible in Figure B.2a.

These figures are referenced and utilised in various researches, which will be further explained in subsection 2.4. The figures are based on projections of climate conditions, sea level rise, and the strengthening of primary flood defenses. Therefore, they provide estimations that are challenging to validate quantitatively. Consequently, models built upon these figures inherently incorporate these uncertainties.

2.3.2 Droughts

The next climate change risk relevant for the Netherlands is prolonged periods of drought, which directly impacts the agriculture sector by causing water stress. During these periods, the government may impose restrictions on crop field irrigation, resulting in lower crop yields. This puts pressure on loans and increases the probability of default. Additionally, drought periods indirectly affect the residential mortgage portfolio, as phenomena like pile rot and settling can occur. Pile rot refers to the decay of foundation poles, while settling refers to uneven foundation settlement on "op staal" foundations.

Foundation damage commonly occurs in houses built before 1975, particularly those constructed on clay or peat soils with wooden piles or shallow concrete foundations. These structures are sensitive to changes in groundwater levels in different ways. For a detailed overview of the specific mechanisms that can cause damage to residential housing, refer to Table 2.2.

Table 2.2: *Overview of damage mechanisms regarding residential housing with respect to droughts [25, 26].*

Damage mechanism	Description
Pile Rot	Wooden pile foundations tend to rot when exposed to oxygen. The extended periods of drought following climate change causes the groundwater level to drop below the top of the foundation wood. Consequently, the poles start to decay because the poles were exposed to oxygen. Subsequently, the poles decay until the foundation cannot keep up the buoyancy required to withstand the force of the house pressing down causing the structure to settle. This settlement induces cracks within the house and could lead to a complete renovation of the house with the accompanying foundation.
Negative adhesion	Climate change induces settlement of the ground. Clay and peat soils the houses are constructed on tend to stick to the wooden foundation poles. Therefore, the soil pulls the house down with the settlement inducing an uneven foundation. Hence, the walls and the foundation could crack causing massive damage to the structure.
Settlement	If the foundation of a structure settles at an equal rate across the foundation, no damage is induced on the structure. However, when an uneven settlement such as diagonal settlement occurs, the house becomes damaged. Commonly, this damage is associated with structures built 'op staal' and could lead to an extensive renovation of the foundation structure.

Although the literature regarding the quantification of these risks is limited, Costa et al. proposed a methodology to quantify these risks based on the conceptual framework of Hazard-Exposure-Vulnerability [15]. Additionally, Kok [25] published a paper outlining another applicable methodology for quantifying these risks specifically for buildings in the Netherlands. The subsequent section will provide further elaboration on the characteristics and approach of this methodology.

2.4 Climate risk modelling

Currently, the focus of physical climate risk modeling is predominantly on residential mortgage portfolios. This emphasis stems from the fact that banks' balance sheets are primarily composed of these types of mortgages [9, 10, 27]. Additionally, a significant portion of the asset side comprises commercial loans to various industries. However, progress in the development of such models has been limited, as each sector requires a customised approach to assess climate risks. Consequently, these models have not been widely adopted, given the smaller scale of individual branches compared to the overall mortgage portfolio [12].

This subsection is divided into three parts, each addressing climate risk modeling for private residential mortgages. Firstly, the discussion centers around hedonic pricing models. Subsequently, attention is directed towards efforts in flood modeling. Lastly, the focus shifts to the methodologies developed for modeling chronic climate events.

2.4.1 Hedonic pricing models

The effects of floods on a property value can be estimated with a hedonic pricing model (HPM) or a repeat-sales model. Lamond et al. [28] constructed a repeat-sales model to research the impact of flood insurance on residential property prices. As the name suggests, this methodology utilises information on properties which have been sold multiple times. The proposed methodology employs a questionnaire to identify data such as property details, flood history, and insurance costs. The methodology involves distributing questionnaires in three types of areas: those at risk of floods but not recently flooded, areas at risk and recently flooded, and areas not designated as at risk. This approach aims to gather comprehensive insights into flood risk perception and its impact within different geographical contexts. This questionnaire in combination with the assigned flood risks from the Environment Agency in the UK analytically determines the impact of flood probability on the residential property price [28]. Although this methodology sounds interesting to execute and has been successfully employed in previous research on climate change regarding market responses to hurricanes [29], generally, the HPM is the preferred method since it is a more comprehensive and practical approach [30].

HPM models are employed in multiple researches regarding the effects of floods on the prices of residential properties. HPMs utilise a mathematical function that incorporates various parameters known to impact property prices. The general structure of such a model is outlined in Equation 2.1.

$$p = f(Location, Structure, Neighbourhood) \tag{2.1}$$

Wherein, the property price (p) can be represented as a function of various property characteristics such as location, structure, and neighborhood. This function can be further extended to incorporate climate-related parameters, such as flood duration, to better capture the influence of environmental factors on property values. Generally, these functions employ a log-linear setup as presented in Equation 2.2 [31].

$$Ln(p_i) = \beta_0 + \sum \beta_1 FLOOD_i + \sum \beta_2 LOC_i + \sum \beta_3 STR_i + \sum \beta_4 NGH_i + \epsilon \tag{2.2}$$

Applying this model to the property market allows estimation of the extent to which each factor affects the market price of the property. However, a substantial drawback of this model is that it captures a consumer's willingness to pay. Consequently, if property owners perceive no flood risk, it is also reflected in the HPM, leading to potential discrepancies between perceived and actual risks. This downside was demonstrated in a study by Fuerst and Warren-Myers, which examined the implications of sea level rise on property values. The research concluded that the influence of sea level rise is insignificant, even in areas with significant flood risks, suggesting either a lack of consideration or awareness of the risks by the market and purchasers [32].

Nevertheless, several other studies have shown that HPM is a viable approach for assessing the effect of flood probability on property valuation. Multiple studies have focused on properties in the United States, with Pope et al. finding that properties situated in floodplains experience a value reduction ranging from 3.8% to 4.5% [33].

In addition, Bin et al. conducted a study that highlighted the effectiveness of HPM in capturing the influence of perceived flood risk on property prices. Their research differentiated between properties in high and low flood probability areas within floodplains. The study found that properties in high-probability floodplains experienced a decrease in value of 7.8%, while properties in low-probability floodplains only experienced a decrease of 6.2%. This indicates that flood risk perception does influence property value [34].

However, when addressing the research question, both the repeat-sales and hedonic pricing models pose significant implementation challenges. These challenges primarily stem from the need for an extensive set of house characteristics for a hedonic pricing analysis and the requirement of sales prices for the repeat-sales methodology. The effectiveness of the HPM greatly improves with more detailed house characteristics, but obtaining such data can be challenging [35]. Consequently, the general applicability of this model becomes problematic, particularly for properties with varying characteristics and facing different types of flood risks.

Furthermore, quantifying the credit risk associated with climate risk through the impact of risk perception on the model's outcomes may not be a suitable approach. Therefore, the literature explores alternative avenues by examining the current modelling efforts undertaken by banks. These efforts provide valuable insights into the assessment of climate-related risks in the context of credit risk.

2.4.2 Predictive flood modelling

Larger banks, such as ABN Amro, have made investments in creating climate risk models for their residential mortgage portfolio. ABN Amro, for instance, employed a Bernoulli trial method to predict portfolio-specific probability maps. This method involves cross-referencing the spatial charts of their residential mortgage portfolio with flood probability maps. It assigns a flood probability to each individual mortgage and estimates the associated risk using the Bernoulli trial method [12]. In the theory of probability and statistics, a Bernoulli trial is a random experiment with two possible outcomes, "success" and "failure," where the probability of success remains the same in each experiment. The methodology discussed in this text has a long history, dating back to the first paper on the subject published in 1969 [36]. This methodology has been applied in several papers to determine the occurrence of weather events. For example, Hossain et al. utilised Bernoulli trials to predict the occurrence of rainfall [37], and Callaghan and Hughes employed Bernoulli trials to assess flood hazards [38]. While the implementation of this model is straightforward, a notable drawback is the requirement for accurate input flood probabilities to ensure an accurate model.

The probability of a flood occurring is influenced by various factors, such as hydraulic load, defense type, and failure mechanisms. These parameters are closely linked to the design of dikes, which serve as input variables in probability charts [39]. The design of these charts is based on Bayesian probability theory, which allows for the incorporation of expert judgment due to the presence of many unknown parameters that need to be estimated [11]. Generally, these probability estimations provide the likelihood of a flood occurring within a specific time interval. In the Bernoulli trial methodology, these charts are used to determine whether a flood has occurred by comparing a randomly generated number with the probability of a flood occurring.

In literature, numerous models exist for estimating potential flood damages when a flood occurs. Some papers utilise a methodology that incorporates damage functions. One such earlier model, developed by Dutta et al., uses a simple method based on inundation depth and different residential structures to estimate the relative flood damage incurred by each structure [40]. These models have evolved to include additional parameters, such as flow depth, which is particularly relevant for flash floods [41]. However, these flow depth curves are less applicable to the Netherlands as these curves are specifically designed for estimating damage in floods with high flow velocity, which is not relevant due to the limited slope of the terrain.

A significant development for the Netherlands is the creation of damage models by the joint research center (JRC). Huizinga developed a set of inundation depth-damage functions and maximum damage values that can be utilised by all EU countries [42, 43]. These models are relatively simple and hence contain some uncertainty, especially when dealing with multivariate models. However, these curves can provide a reasonably accurate estimate, particularly when data is limited [44]. The Dutch government incorporates these JRC-type damage functions in their methodology for predicting flood damages to buildings. This methodology was initially published in 2005 by Koks et al. and has been continuously developed, with the most recent version dating back to 2017 [45, 46].

Besides these depth-damage functions, more sophisticated methodologies are also employed to predict damages to buildings. For instance, Dottori et al. propose a methodology called In-depth Synthetic Model for Flood Damage Estimation (INSYDE), which utilises 23 input variables, six describing the flood event, and 17 referring to building features. This approach improves the accuracy of damage prediction, enhancing the reliability of the model. However, it is worth noting that the inclusion of additional required parameters may introduce limitations to the practical applicability of the model. Nevertheless, the model has been successfully validated for multiple flood cases in Italy, demonstrating its robust performance and effectiveness [47, 48]. Numerous advanced methodologies have been developed to predict flood damages, and in some cases, they outperform the basic JRC damage function, as shown in a comparative analysis by Arrighi et al. [49]. However, the transferability of these models depends on the similarity between the calibration context and the implementation area. The analysis suggests that simpler models, such as the JRC curves, can provide estimates comparable to more complex models like INSYDE when applied to their appropriate calibration area. Therefore, when considering the research scope limited to the Netherlands, the Standaardmethode 2017 Schade en Slachtoffers by Deltares is deemed a suitable methodology. It is specifically designed for buildings in the Netherlands, offering a simplistic yet tailored approach.

The ABN Amro case study mentioned at the beginning of this subsection employs the Standaardmethode 2017 Schade en Slachtoffers methodology for the prediction of incurred damages ones a flood has occurred. Using this method in combination with the Bernoulli trial methodology, ABN constructed maps for flood risks. A similar Bernoulli method is employed to estimate the risks associated with pile rot. The only notable difference is that the data provided was very granular at the time of publication [12]. An example of the maps constructed with this method is displayed in Figure 2.5 below.

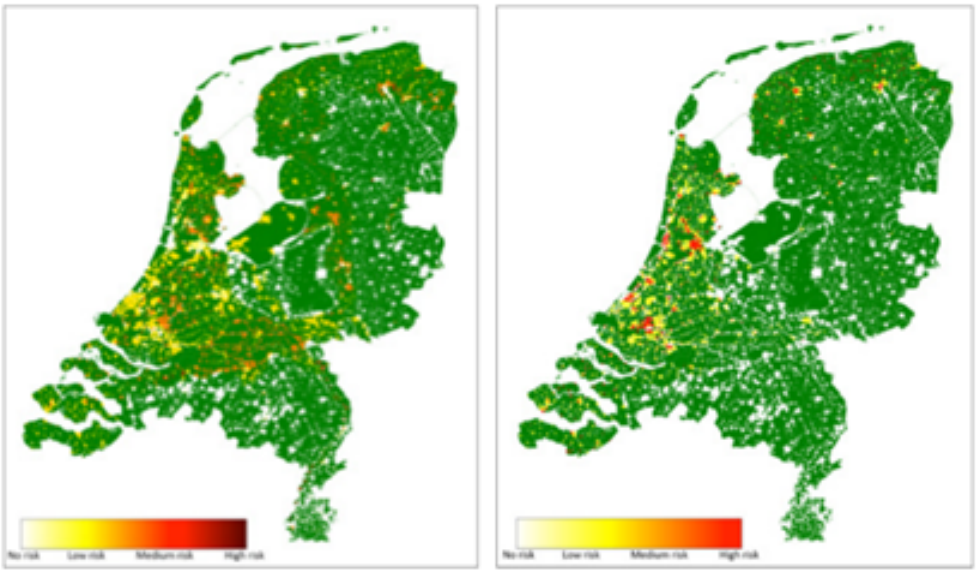

Figure 2.5: *Portfolio-specific probability maps for flooding risk (Left) and pile rot risks (Right) [12].*

Another example of an application of a similar methodology is the case study conducted by the United Nations Environment Program Finance Initiative (UNEP FI). The UNEP FI utilised JBA flooding scores to assess the current flood risk to properties in the UK. The JBA flood score is determined at the property level and takes into account factors such as property elevation, the probability of coastal and river floods. Based on these JBA flooding scores, climate scenarios, and data from a recent global assessment of future changes in flood risk, the UNEP FI developed a model to estimate the impact on the loan-to-value ratio (LtV) by deducting the value of the property due to flood risks.

As a case study, the UNEP FI applied this methodology to a sample of UK residential mortgages. Using this approach, UNEP FI observed an increase in loans with a LtV greater than 80%, with the percentage ranging from 5% to 10%, depending on the climate scenario. It is important to note that the analysis was conducted on a 3% subset of the initial sample, which was most exposed to flood risks [50]. Therefore, the actual impact of floods would be lower, as stated in this research.

Apart from being employed by banks and major research institutions, the Bernoulli trial methodology is also utilised in various research papers. However, these papers use it to estimate the damages incurred in specific regions, including buildings and agricultural land. Unlike this study, which focuses on residential properties across the entire Netherlands, these papers demonstrate the methodology's applicability in approximating flood damages for a particular area

The first notable paper where this methodology is applied is a publication by Hoes et al. The simulation methodology closely resembles the approach employed by ABN Amro. Similarly, the methodology utilises a Bernoulli trial to determine the occurrence of a flood. Additionally, the paper leverages the 'Basisregistratie Adressen en Gebouwen' (BAG) register, a cadastral polygon shape file containing the footprint of 7 million buildings in the Netherlands. The BAG map is cross-referenced with the 'LGN6' map, which specifies land usage, including agricultural purposes. By overlaying these maps, it becomes possible to quantify the damage a flood would cause in a specific area. The paper employs a methodology similar to the Standaardmethode 2017 Schade en Slachtoffers by Deltares to estimate damages to buildings and agricultural land. This approach involves the use of a damage function, which considers the inundation depth multiplied by a base value per square meter. Essentially, the simulation follows an identical methodology and execution compared to the previously discussed ABN Amro simulation. The main difference lies in the data preparation stage, where the ABN Amro simulation uses their own residential mortgage portfolio as input files, while the paper by Hoes et al. utilises a combination of the BAG, Top10NL, BBG, and LGN6 maps to assess the land usage exposed to the flood [51].

The second paper that employs a similar methodology focuses on industrial buildings. In the first part of the paper by Koks et al., a direct loss model is utilised to estimate the direct damages to buildings. This model solely focuses on the actual flood damages incurred and does not employ a Bernoulli trial to determine flood occurrence. However, the direct flood model used in this approach is worth reviewing. The model is based on Equation 2.3.

$$D^{dir} = \sum_{l}^{m} \sum_{n}^{r} a(h_r) D_l^{max} \tag{2.3}$$

Where D^{dir} is total direct damage in the area under consideration, D^{max} is value at risk for land-use category i, $a_i(h_r)$ is a depth-damage function for land-use category i, and h_r is inundation depth of the flood in a particular cell r [52]. Similar to the ABN Amro simulation and the paper by Hoes et al, the direct loss model employs a multiplication between a damage factor depending on the inundation depth and a base value at risk depending on the building affected by the flood. A schematic overview of this simulation is provided in Figure 2.6 where the important part of the simulation for this thesis is the direct model assessment step.

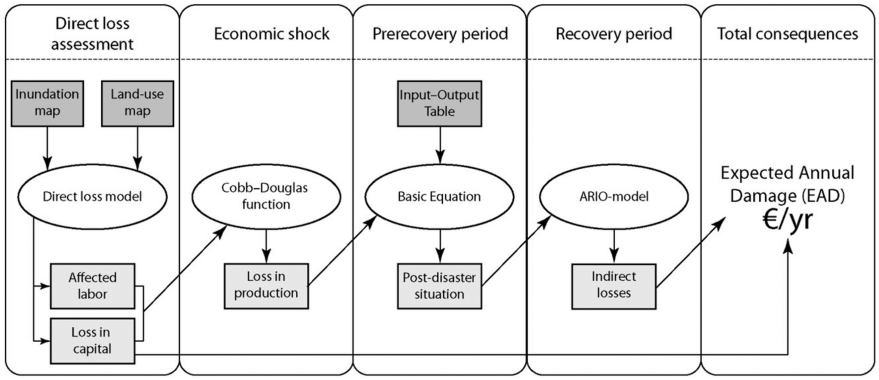

Figure 2.6: *Overview of the different components of the framework. The dark grey squared boxes are the inputs, the ellipses are the different models, and the light grey squared boxes are the model outputs [52].*

The other parts of this flood damage assessment methodology are less applicable to the current thesis since the Cobb-Douglas function is predominantly used for buildings with an industrial function. However, considering the impact of indirect effects of floods in future research could be a significant addition to this field of research. Therefore, an explanation of the second part of the methodology from this paper is added in Appendix C.

While all the previously discussed research papers focus on approximating the incurred damage in the event of a flood, there is limited research on predicting the impact of these damages on the residential mortgage portfolio. Typically, papers that explore the effect of climate change on the portfolio are retrospective, analysing changes after the event has occurred [4, 53]. Forward-looking models are predominantly published by national banks or governmental research organisations. Although there are a few research papers attempting to predict the influence of flooding on the residential mortgage portfolio, the amount of research in this area is limited [54].

A particularly interesting paper by Bikakis examines the impact of climate change on a UK residential mortgage portfolio up to 2080. The study employs a simplistic methodology where the total value of all outstanding residential mortgages in each region is divided by the cumulative value of properties in the same area. This percentage is then multiplied by the Estimated Annual Damages (EAD) for the region. Finally, the total value of mortgage-related EAD is divided by the common equity tier 1 (CET1) to predict the impact of climate change on the required CET1 [55]. The paper utilises the results of a climate risk assessment conducted by Sayers et al., which predicts flood damages to residential properties in different UK regions from 2015 to 2080. Multiple climate scenarios are considered to estimate damages across the full spectrum of potential climate conditions [56]. Bikakis leverages these damages to estimate the EAD.

The results of this multi-step analysis show that under the Present Day climate scenario, 0.01% of the UK's CET1 capital is currently exposed to flood risk. However, this percentage increases to 0.03% under the 4°C Low population growth scenario. These findings highlight a significant portion of the residential mortgage portfolio that is susceptible to climate risks, potentially placing banks beyond their CET1 capital buffer [55].

2.4.3 Risk perception

Physical climate risk is not only determined by damages but also by risk perception. In flood-prone areas, monetisation of the actual damage and the damage to subjective well-being shows that risk perception is twice as damaging to people than the actual physical damage. This change in risk perception shifts demands for houses away from flood-prone areas, thereby changing housing prices [57]. Different researchers have proved this perception indeed exists. However, the extent and duration of the flood perception differ significantly between areas. Exemplary, a Pennsylvania flooding in 1972 saw house prices plummet by 30% in the subsequent months. Contradictory, the 1974 floods in Ontario observed no influence on house prices [58].

The closest representation of the influence of floods on the Dutch perception of floods comes from the 1993 and 1995 Maas floods. Before the floods, there was no significant difference between the house price of the affected area and the non-affected area. However, after the first flood, property values dropped approximately 4%, whereas, after the second flood, the values declined by an additional 2-5 percent [13]. The paper states the effect did not gradually become smaller as the memories of the second flood faded. Nonetheless, commonly, this happens as time progresses, the memories of the flood disappear, and the dispersion between the property values decreases [57]. Refering back to the ABN Amro model earlier discussed, ABN chose to employ a 5% shock to the housing market which temporarily stayed in place after which it disappeared across the following couple of years [59].

The main purpose of adding these micro-economic parameters is to identify adverse movement in important macroeconomic parameters such as gross domestic product (GDP) and the unemployment rate. These variables massively influence the PD [60]. Hence, these parameters are of particular interest to the banks.

Commonly, the above-described tendencies are observed in all simulations regarding climate risks. Firstly, an estimation of incurred damages is made. Subsequently, macroeconomic parameters such as house depreciation due to risk perception are added. Lastly, expected loss and important macroeconomic parameters like GDP are determined. These parameters influence internal PD and LGD models.

2.4.4 Pile rot and settling modelling

As briefly mentioned when identifying the research gap, there is a scarcity of research focusing on modeling damage caused by settling and pile rot. While the literature on quantifying these risks is limited, Costa et al. have proposed a methodology to address this challenge. The methodology is based on a conceptual framework of Hazard-Exposure-Vulnerability, where the hazard characterises the events causing damage, exposure assesses the inventory of the building at risk, and vulnerability defines the degree of physical damage to the building at risk [15]. Together with a paper published by Kok [25], this methodology is the only applicable approach to quantify these risks for buildings in the Netherlands. Therefore, further elaboration on this methodology is necessary.

The methodology employs different hazard levels corresponding to different stages of foundation hazard. The damage level of a house is classified into six distinct categories, ranging from 0 to 5. The classification is based on the degree of hazard to the overall structural integrity, where 0 indicates no hazard and 5 represents a very high level of hazard. The methodology prescribes a certain level of incurred damage after surpassing a hazard level, taking into account the vulnerability of the underlying structure. A detailed description of these categories is provided in Appendix D.

Subsequently, the exposure is based on data regarding the percentage of houses within a certain district built on wooden poles or "op staal." Multiplying the approximated damage category by the percentage of houses on the specific foundation type provides an estimation of the expected risks within a certain area. A combination of the paper by Costa et al., Koks et al., and quantitative efforts by the Klimaateffectatlas provides the expected vulnerability in 2050 and the exposure of neighborhoods in the Netherlands. By multiplying these spatial charts, it is possible to predict the risks on a per-neighborhood basis. The charts displaying the risk due to pile rot and the risk due to settlement are depicted in Figure 2.7a and Figure 2.7b, respectively.

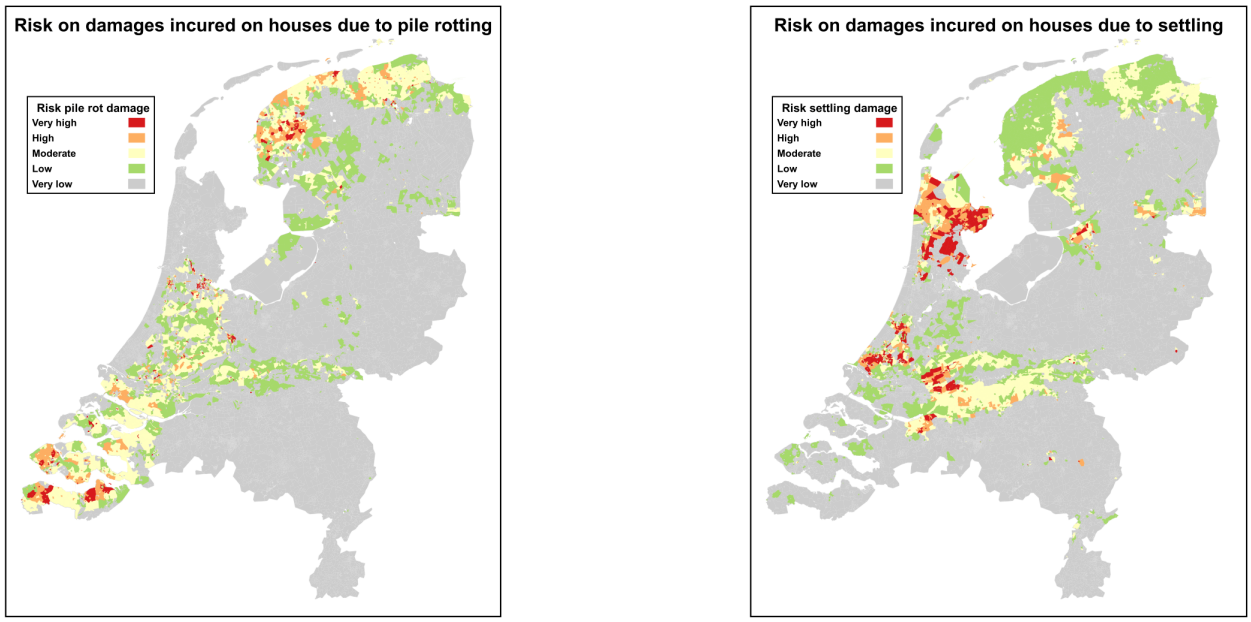

(a) *(b)*

Figure 2.7: ***(a)*** *The qualitative risk associated with damages due to wooden foundation poles [23]. ,* ***(b)*** *The qualitative risk associated with damages due to uneven settlement of the foundation [23].*

Figure 2.7a and Figure 2.7b display the qualitative risks based on the multiplication of exposure and vulnerability. However, when the vulnerability is cross-referenced with the hazard level and multiplied by the exposure, the quantitative risk can be determined. Unlike acute events like flooding, where damages are immediately visible, the deterioration of a foundation is a slow process. As a result, the vulnerability increases over time due to the degradation of the foundation.

The deterioration of the foundation is influenced by various factors, including the duration of drought periods, soil type, and the type of wood used for the piles. However, Costa et al. and Koks et al. assume a linear relationship between the damage level and time, implying a consistent degradation of the foundation over time. By adopting this assumption, it becomes possible to determine the precise timing at which hazard thresholds are exceeded, aligning precisely with the occurrence of damages. Combining this with an estimated base rate per hazard level allows for the calculation of the total damage sustained by a property.

It is important to note that the linear deterioration of the foundation has not been conclusively proven. The methodology proposed by Costa et al. and Koks et al. has been adopted by the Klimaateffectatlas and is also incorporated into the methodology used by ABN Amro [12]. However, there are currently no published papers utilising this methodology or proposing alternative approaches within the existing literature [15, 25].

2.4.5 Climate risk incorporation in credit risks management

This subsection aims to explore the existing literature on the integration of climate effects with the credit risk metrics for the residential mortgage portfolio. A study conducted by Weber et al. investigates the current practices of banks in Europe regarding the inclusion of climate risks in their credit risk management. The research involves sending questionnaires to 205 major banks in Europe to gather information on their current implementation of environmental risks. The study reveals that banks give more consideration to environmental risks during the rating phase compared to other phases of the credit risk management process. Interestingly, during the costing phase, 74% of the banks have only partially or not at all incorporated environmental risks, despite the recommendation that these risks should be considered as these risks impact all phases of the credit management process [61]. It should be noted that this paper was published in 2008, so the banking landscape changed drastically after this period, where banks probably have incorporated more environmental risks in their credit risk management process.

However, despite Weber's paper being outdated, some of its points remain relevant today. Berman's paper echoes this sentiment by emphasising that current flood risk assessment tools are insufficient and outdated in accurately measuring flood risk and the effectiveness of mitigation strategies. Similarly, Monnin's research highlights the absence of climate risks in credit risk analysis but highlights the emergence of new methodologies for integrating these risks [62, 63].

Berman suggests that major banks should take the lead in developing standardised tools and metrics for assessing flood risk and property resilience. These tools will be utilised during the mortgage origination process, ongoing portfolio analysis, and asset management. Furthermore, mortgage loan programs and incentives will be established to incentivise responsible risk mitigation practices. These frameworks aim to enhance climate risk awareness among individuals and facilitate efforts to mitigate such risks, ultimately reducing property owners losses and the associated risk of loan default [62].

These papers primarily focus on the current integration of climate risk in credit risk management and analysis. Subsequently, the following papers explore the impact of various climate events on the residential mortgage portfolio, despite their lack of relevance to the Netherlands. However, the methodologies used to connect climate events with mortgage credit risks could still be applicable for this area.

One paper specifically examines the effect of Hurricane Harvey on mortgage credit risk, employing a difference-in-difference (DiD) approach. This statistical method compares outcomes between two groups before and after a climate event to estimate causal effects. The study investigates the hurricane's influence on default rates and also explores the impact of flood insurance on these rates. Kousky et al. find that in the short term, mortgage delinquencies and forbearance increase regardless of whether the property is insured against floods. However, in the long run, the default rate for mortgages with flood insurance is statistically equivalent to that of undamaged properties, while mortgages without flood insurance are more likely to default compared to the control group. Thus, the results strongly support the notion that flood insurance not only provides financial protection to households but also safeguards banks [53].

While the findings presented in this paper are valuable, one limitation of using the DiD methodology is its reliance on historical data. This makes the methodology an unreliable tool for predicting future credit risks associated with climate change trends [63].

Another relevant to this research is a study by Rossi which examines the influence of hurricane intensity and frequency on mortgage default rates, employing a standard logistic regression model similar to the research conducted by Kousky et al. The regression results support the hypothesis that an increase in hurricane intensity and frequency leads to a higher probability of default. Consequently, if the frequency and intensity of major Atlantic hurricanes rise in the coming decades, as suggested by meteorological research [64, 65], a larger number of borrowers will be affected. This, in turn, is expected to result in higher default rates due to wind and flood damage to residential properties, exposing banks to additional mortgage credit risks [66]. These regression methodologies can be widely applied to various climate events, as demonstrated in studies like Issler et al., where similar regression approaches to those used by Rossi and Kousky et al. are employed to examine the impact of wildfires on mortgage credit risks [67]. Furthermore, Ouazad and Kahn's research confirms this statement, investigating the effects of different natural disasters on the securitisation dynamics of residential mortgage portfolios through a series of identical regressions [68].

The final paper to be discussed in this section is by Calabrese et al. What sets this paper apart from previous contributions is its focus on incorporating the physical characteristics of extreme events as explanatory variables, rather than solely assessing post-damage impacts. Unlike the previous studies, Calabrese et al. aims to account for future changes in risk. To achieve this, the paper employs an additive Cox proportional hazard model, which simultaneously evaluates the effects of multiple factors on mortgage survival probability.

The overall model yields similar results to those obtained by Kousky et al. and Rossi. However, the paper by Calabrese et al. demonstrates the differences in survival curves when weather events are included or excluded from the models. The methodology involves two mortgages: Mortgage A, which is subjected to a Category 3 hurricane with a low flood probability and limited rainfall, and Mortgage B, which experiences a substantial amount of rainfall and a high flood probability. The survival curves for Mortgage A and Mortgage B are illustrated in Figure 2.8a and Figure 2.8b, respectively.

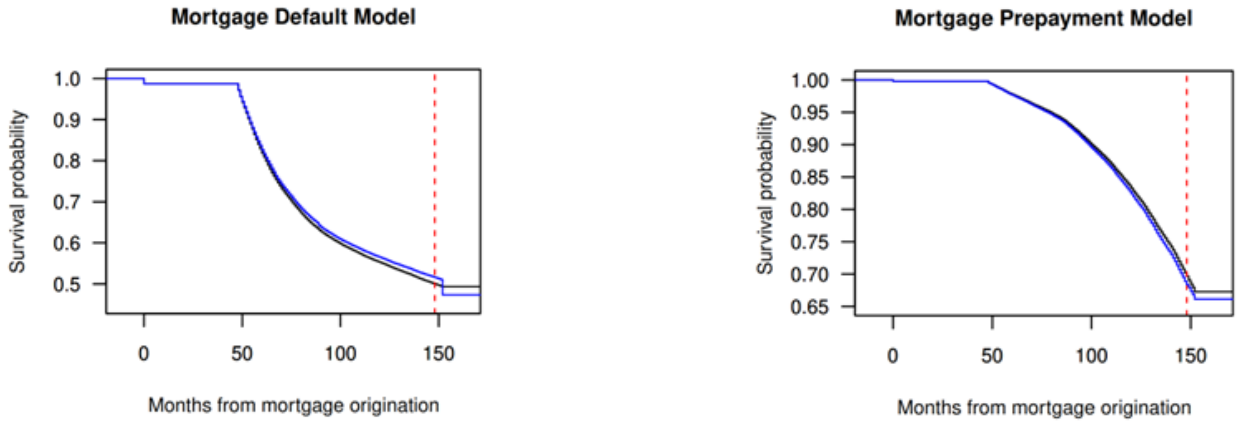

(a) *(b)*

Figure 2.8: ***(a)*** *Survival curves for the Mortgage A as a result of the application of the default model[4]. ,* ***(b)*** *Survival curves for the Mortgage B as a result of the application of the default model [4].*

The survival curves depicted in Figure 2.8 illustrate different scenarios. The black curve represents the baseline survival curve without the inclusion of a weather event, while the blue curve represents the survival curve when a weather event is taken into account. The red dotted line indicates the specific time at which the weather event occurred. Both figures clearly show a significant drop in the survival probability of the mortgage after the weather events, indicating a notable negative influence on the probability of default. These figures demonstrate the impact of these risks on the residential mortgage portfolio, especially with the increasing frequency of such events due to climate change.

The most intriguing aspect of this paper is the scenario analysis conducted by Calabrese et al., which explores the future impacts of climate change using metrics from the 2050 First Street (FS) flood model [69]. This model, developed by Bates et al., employs the RCP 4.5 climate scenario to estimate the projected flood exposure of properties. The scenario analysis incorporates two weather scenarios: scenario 1, which includes 300mm of precipitation in 5 days, and scenario 2, which combines a category 2 hurricane with 200mm of precipitation in 5 days. The prediction results reveal that the default probability increases by up to 36% for scenario 1 and 17% for scenario 2, depending on the city's location, following changes in exposure from FS2020 to FS2050. The highest increases are observed in coastal areas with the greatest flood exposure. Overall, based on these findings, Calabrese et al. assert that climate change will bring about substantial changes in risk. It is noteworthy that RCP 4.5 is considered a relatively mild scenario, and the impacts are expected to escalate significantly in the latter half of the 21st century [4].

3 Portfolio preparation

This chapter will describe the preparation of a dummy portfolio to predict the damages incurred due to climate change. Normally, a bank has information regarding the location, surface area, exposure, and underlying value of its loans. Nevertheless, this information is classified as highly confidential. Therefore, this data is not openly shared with companies outside the bank. Hence, to predict the implications of climate change on the VtL and LGD, a realistic portfolio is required. This chapter explains how a generic portfolio utilised to represents a bank's residential mortgage portfolio is created and the underlying assumptions which are made in the process. A flowchart schematically illustrating the steps explained in this chapter to create the private residential mortgage portfolio is displayed in Figure E.1.

The first step in creating the portfolio is to determine the required size to accurately represent a bank's portfolio. To calculate the required sample size, first, determine the theoretical sample size needed to replicate a portfolio with an infinite population. This initial calculation is crucial since it acts as the basis for finding the sample size required for a portfolio with a finite number of houses. The required samples for a theoretical infinite portfolio can be calculated with Equation 3.1 [70].

$$n = \frac{Z^2 \cdot P(1-P)}{\epsilon^2} \tag{3.1}$$

Subsequently, the number of samples calculated with Equation 3.1 is employed in Equation 3.2 as input parameter n. This equation is designed to calculate the required portfolio size to statistically represent a portfolio with size N.

$$n' = \frac{n}{1 + \frac{Z^2 \cdot P(1-P)}{\epsilon^2 \cdot N}} \tag{3.2}$$

Wherein, Z represents the z-score corresponding to the chosen confidence interval, N stands for the population size of the original portfolio, ϵ denotes the margin of error, which quantifies the degree of random sampling error and provides a measure of acceptable deviation from the true value. Lastly, P represents the population proportion, indicating the proportion of the population in a specific category [70]. In this case, a value of 0.5 is assigned because it is unknown for this specific case and a value of 0.5 maximises the required amount of samples in the portfolio.

In this thesis, the ING portfolio will be employed as the basis of the created portfolio. Currently, the outstandings in the ING residential mortgage portfolio in the Netherlands account for 114,219 million euros [9]. To determine the number of houses in the portfolio, the initial step involves dividing this numerical value by the average Wet waardering onroerende zaken (WOZ) value for residences in the Netherlands. However, simply performing this division of outstanding quantities by the average WOZ value would not provide an accurate estimate. This inaccuracy arises because the reported outstandings in the annual report cover the exposures of the bank, rather than reflecting the valuation of underlying assets. As a result, it is essential to consider the valuation of these underlying assets in relation to the overall exposures. In the annual report, ING provided the distribution of the VtL as shown in Table 3.1.

Table 3.1: *VtL distribution of the 2021 ING residential mortgage portfolio [9].*

VtL	No cover	0-25%	25-50%	50-75%	75-100%	>100%
Percentage	-	-	-	0.5%	7.6%	91.8%

To estimate the average Value-to-Loan (VtL), a normal distribution is fitted to match the tail of the mortgage portfolio. The best-fitting normal distribution to the figures provided in Table 3.1 has an average of 1.303 and a standard deviation of 0.217. This bears the assumption that the VtL is normally distributed, which is difficult to validate without the actual portfolio. However, in literature, modelling of expected loss and probability of default is sometimes conducted with bivariate normal distributions [71]. These figures are indirectly linked to VtL values. Hence, the estimation of a normally distributed VtL seems to be a reasonable assumption.

According to the CBS, the average WOZ value of houses in the Netherlands is €315,000 [72]. Combining the outstanding from ING, average VtL, and the average WOZ value, the size of the residential mortgage portfolio in the Netherlands is estimated to incorporate approximately 472,500 loans. This is a rough estimate of the number of houses in the portfolio. However, the formulation presented in Equation 3.2 reaches the limit of the required sample size for portfolio sizes above 300,000 samples. At this juncture, the sample size required for the theoretical scenario with an infinite number of houses in the portfolio equals the sample size needed for a finite portfolio of over 300,000 samples. Consequently, the precise number of houses in the portfolio becomes less critical, as long as it exceeds 300,000. Using Equation 3.1, the calculation shows the portfolio should contain 4116 sample points given a confidence interval of 99% and a margin of error of 2%.

The second step is to generate the actual coordinates of the points. Randomly generating points within the Netherlands would not provide an accurate representation of a bank's portfolio since houses are not evenly spread across the Netherlands. Therefore, the population density is used to associate each point with specific coordinates. A chart provided by the CBS divides the Netherlands into sections using 100m by 100m squares, each containing information about the population residing in that area [73]. This chart distinguishes between squares on land and squares on water, allowing for the exclusive assignment of coordinates located on land.

To distribute the 4116 sample points randomly, points within the range of 0 to the cumulative total population of the Netherlands are generated. For instance, if the simulation has covered 10 squares, each accommodating 10 people, the cumulative population would be 100. If the subsequent square holds 5 people, the simulation would assign a range of 100 to 105 to this square. If a randomly generated number, such as 102, falls within this range, the simulation would determine a random set of coordinates within the corresponding 100m by 100m square and subsequently incorporate these coordinates into the portfolio. This process continues until a portfolio containing 4116 sample points is constructed. The resulting distribution of points obtained through this methodology is illustrated in Figure 3.1.

Figure 3.1: *Randomly generated points in the residential mortgage portfolio.*

Rationally, the majority of the points in Figure 3.1 are located in the Randstad since the majority of people live in this area. Additionally, major cities like Amsterdam and Rotterdam can be observed due to a substantial cluster of points in close proximity.

With the longitude and latitude of the points determined, the third step is to correlate the previously described climate risk data to the data points. Firstly, the flood probability and maximum inundation depth charts are appended to the data points. The data from the klimaateffectatlas is provided in a Tag Image File Format (TIFF) file and previously depicted in Figure 2.4a. These files consist of approximately 3.25 billion points in a (61775,52880) matrix. To correspond the longitude and latitude coordinates to the x-y data in the matrix, an affine transformation is performed. An affine transformation is a linear mapping method that preserves points, straight lines, and planes. Therefore, the longitude and latitude in the European Petroleum Survey Group (EPSG) 28992 coordinate system can be transformed into x-y coordinates from the flood matrix. With this transformation, the correct flood probability or maximum inundation depth prescribed at the x-y coordinate can be added to the data set.

The fourth step is to assign data regarding pile rot and settling to the portfolio. This data is also from the klimaateffectatlas and is delivered as a geopackage. Geopackages are constructed from small individual multi-polygons covering the entirety of the Netherlands. The circumferences of the polygons are made up of lines between certain longitude and latitude points. Hence, the points within these lines are precisely known. Therefore, it can be determined whether a longitude and latitude from the portfolio is within a polygon. If the randomly generated coordinates of a point are located within the circumference of the multi-polygon, the probability and severity data from the klimaateffectatlas chart are transferred to the data of the point. This methodology applies to both the settling and the pile rot data.

In the fifth step, the points are assigned to a neighborhood with an accompanying code. This code is utilised to group points that are in close proximity to each other. This is necessary since floods do not occur at a single individual location but in a larger area. Consequently, if a house is located in the near vicinity, the likelihood that it is also affected by the flood would be substantial. Therefore, the data set is appended with a unique neighborhood code. The different unique neighborhoods in the Netherlands are provided by the CBS and displayed in Figure 3.2 [74].

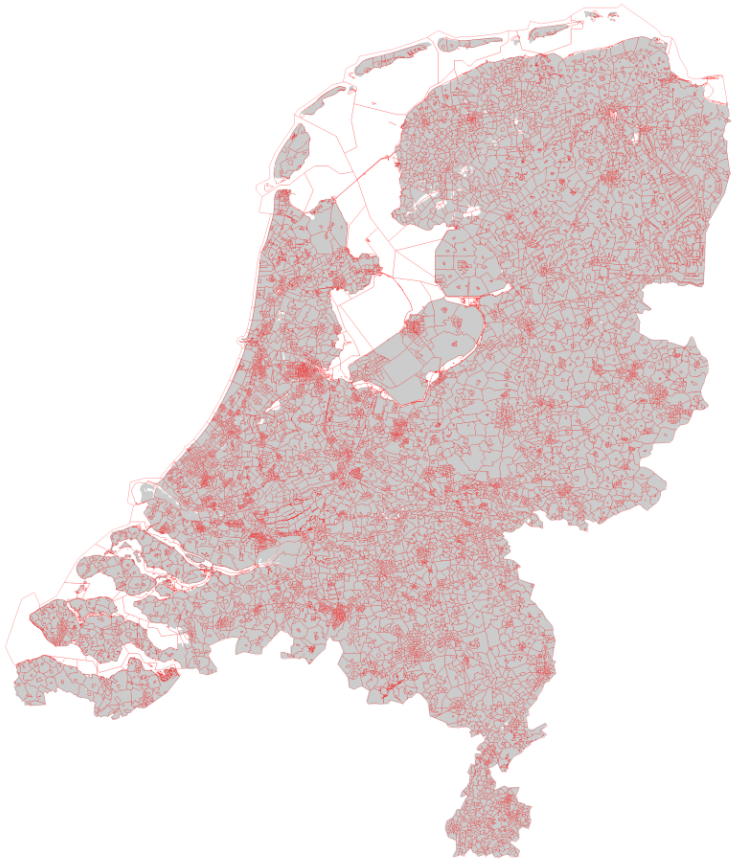

Figure 3.2: *Unique neighbourhoods located within the Netherlands [74].*

The above-described methodology generates a dummy residential mortgage portfolio designed to represent an actual bank portfolio. Additionally, the methodology demonstrates the data preparation required for predicting incurred damages due to climate risk modeling.

4 Modelling structure

This section describes the modeling structure and methodology used to predict the damages due to climate change. The chapter incorporates the explanation of four different models based on the previously constructed portfolio. First, the simulation that predicts the damages incurred due to flooding is described. This simulation utilises the probability given by the inundation depth charts as the basis for calculation. Secondly, a more extreme flood simulation is discussed, which is based on the maximum inundation given the flood probability. Third, the simulation to forecast indirect damages as a result of drought periods is defined. Lastly, the prediction which is responsible for calculating the economic implications of the incurred damages is described. All these individual simulations have a flowchart which are presented in Appendix E.

4.1 Flood simulation with given inundation depth

The quantification of climate risks should incorporate methodologies aimed at predicting physical damage incurred up to 2050, as uncertainties beyond this point significantly increase. Previous literature has outlined efforts to predict the impact of physical climate risks, including hedonic price modeling, repeat-sales modeling, and a combination of the Bernoulli trial methodology with a damage function approach. The latter is preferred for this research because it focuses on prediction, whereas the former methods are retrospective.

The model used to predict flood damage based on inundation depth utilises the portfolio described earlier. The simulation methodology for this prediction closely resembles the approach described by ABN AMRO and applied by Koks et al. to identify flood-affected areas [12, 52]. These methodologies employ a Bernoulli trial to determine the occurrence of a flood at specific locations. Similar trial methodologies have been employed to detect other weather events, as demonstrated in papers by Hossain et al. and Callaghan [37, 38].

For each individual point in the portfolio, a Bernoulli trail is employed to determine whether a flood has occurred based on the assigned flood probability at the location. When the Bernoulli trail yields a success, indicating a flood has occurred, the simulation records the event and calculates the incurred damage based on the damage function methodology put forward by Deltares. This methodology is preferred as it is tailored for properties in the Netherlands and is employed by the Dutch government to determine water policy regulations. The calculation involves multiplying the surface area by the damage factor and the base rate per square meter. While these paragraphs provide a brief overview of the methodology and the reasoning behind its employment, the subsequent paragraphs offer a more detailed description. A flowchart illustrating this simulation can be found in Figure E.2.

The Monte Carlo utilised in this research spans 30 years without dependencies between the years. In this Bernoulli trail methodology, the Monte Carlo simulation draws a random number from a uniform distribution between 0 and 1 for neighborhoods containing a point from the residential mortgage portfolio. It then verifies whether the random sample is lower than the specific flood probability of that point. Therefore, flood damage is assigned to the point. To predict damage to a structure, a JRC-type damage function is employed. Specifically, the simulation utilises the Standaardmethode 2017 Schade en Slachtoffers. These curves are relatively simple, incorporating only inundation depth as a descriptive variable. However, as demonstrated in the comparative analysis by Arrighi et al., these JRC-type curves, designed for specific areas, can yield estimates comparable to those of more sophisticated models [49]. A description of the Standaardmethode 2017 Schade en Slachtoffers methodology is provided in subsection F.1, where the surface area of the residential home and the property type are required for its application.

Both criteria are estimated based on the provided municipality code. The Netherlands is divided into 352 municipalities. CBS provides information regarding the number of houses in different surface area categories for both single- and multi-family homes [75]. Accordingly, a distribution between the percentage of single- and multi-family homes can be constructed. To randomly determine whether the house is a single- or multi-family home, a draw is taken from a uniform distribution between 0 and 1 and compared to the fraction of single-family homes in the municipality. If the sample is below the percentage of single-family homes, the house is assigned as a single-household house. Conversely, if the sample is above the percentage of single-family homes, the house is assigned as a multi-household house.

Subsequently, a random sample from a Weibull distribution is taken, which is prepared based on the CBS data on the surface area of houses in the specific municipality. An example of such a distribution is provided in Figure 4.1 below.

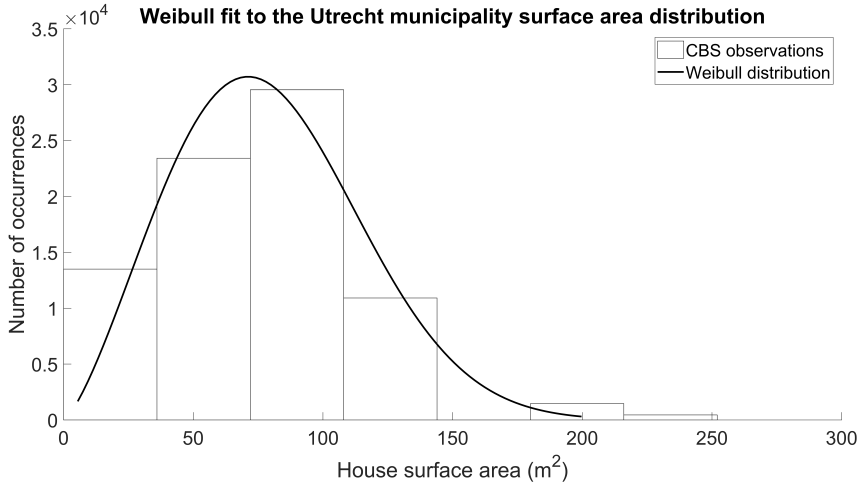

Figure 4.1: *Weibull fit to the surface area distribution for the Utrecht municipality for a single-family house [75].*

A Weibull distribution to fit the data is utilised because the data for each municipality has a unique shape. Typically, municipalities in the north of the Netherlands have a negative kurtosis with a larger tail, whereas the surface area distribution in the randstad are closer to a normal distribution. A Weibull distribution is capable of taking on various shapes, including these extreme forms.

Subsequently, the damage functions from subsection F.1 are utilised to generate a damage factor for the building. Additionally, the Standaardmethode 2017 Schade en Slachtoffers provides the average damage per square meter, as shown in Table F.1. Therefore, the damage to the building is calculated by multiplying the obtained damage factor by the average damage per square meter and the surface area of the building. The resulting damage is discounted with the risk-free rate to obtain the net present value of the damage. This methodology can be summarised in equation form as shown in Equation 4.1.

$$S_i = \sum_{j=1}^{30} \frac{a_{ij} SA_i SN_i}{(1+r)^j} \tag{4.1}$$

Wherein, S represents the incurred damage of building i due to flooding in the simulated 30 years, a denotes the damage factor, SA represents the surface area of building i, SN represents the base rate per square meter, r represents the risk-free rate, and j represents the simulation year ranging from 1 to 30.

Subsequently, it is verified whether there are any additional points located within the neighbourhood. If such points exist, the simulation checks whether the flood probability for this point is also surpassed by the randomly generated Bernoulli trial. If this condition is met, the previously described methodology is repeated until there are no more additional points in the neighbourhood polygon.

4.2 Flood simulation with given flood probability

The flood simulation given the flood probability is constructed using a similar methodology compared to the flood simulation given the inundation depth. The main difference lies in the purpose of the simulation. This simulation aims to represent an unlikely but highly negative scenario. The damage obtained with the maximum inundation depth given the flood probability charts is more extreme than the flood probability given the inundation depth, as certain areas in the map reach maximum inundation depths multiple times higher than the highest given inundation depth utilised in the prediction described in subsection 4.1. This leads to higher damage factors and, consequently, higher damages. Additionally, the modeling setup is designed to enhance the extremity of the scenario. A flowchart describing this particular simulation is appended in Figure E.3.

Similar to the previous simulation, the residential mortgage portfolio serves as the basis for this simulation and the program runs a Monte Carlo simulations over a 30-year period. However, this simulation differs from the previous one in terms of the Bernoulli trial methodology used to assess flood occurrence. In the previous simulation, flood probability was determined by charts that depended on inundation levels. In this methodology, flood probability remains fixed, while the maximum inundation depth varies. The program checks whether each randomly generated draw is lower than the given probability on any of the four provided probability maps from the klimaateffectatlas dataset.

Initially, the random draw is compared to the lowest probability map. If the random draw is lower than the given probability, the associated inundation depth is passed to the damage functions. However, if the random draw is higher than the given flood probability, the draw is compared to the next lowest given flood probability and repeats this process until the draw is checked against all the charts. If a flood probability higher than the randomly generated draw is encountered, a flood probability higher than the randomly generated draw, it writes the corresponding maximum inundation depth from the corresponding flood chart to the damage function. If the random draw exceeds the highest flood probability, the Bernoulli trial determines that no flood has occurred. The different flood probabilities given to the charts are outlined in Table 4.1.

Table 4.1: *Flood probabilities for the inundation depth flood charts provide by the klimaateffectatlas [23].*

Chart Name	Flood Probability
Very small	1/100,000
Small	1/1,000
Medium	1/100
High	1/10

The actual damage calculation is identical to the procedure practiced in subsection 4.1. First, the damage factor is calculated from the inundation depth followed by the overall damage from the multiplication of the surface area, damage factor, and base rate per square meter. Second, the damage is discounted with the risk-free rate. This methodology is comprised in Equation 4.1.

The extremity in this modeling technique arises due to the exploitation of the four charts in one model and the usages of the maximum inundation depth since this greatly improves the frequency of floods and increase the severity of the occurred flood. Consequently, the observed damages from this simulation are expected to be higher compared to the methodology explained in subsection 4.1.

4.3 Indirect damage to the residential mortgage portfolio simulation

The simulation of indirect damages to the residential mortgage portfolio presents a distinct approach compared to the methodologies discussed earlier. This methodology draws upon a framework proposed by Costa et al. [15], previously discussed in the literature review. This methodology employs a continuous increase of the damage, whereas the damage due to floods has a discrete modeling methodology. Although the methodology is rather simplistic, there are currently no alternatives due to the early stage of research on this topic. Therefore, this methodology is deemed the best fitting for this research at the moment. A flowchart illustrating the process of predicting the indirect damages to the residential mortgage portfolio utilising this methodology is presented in Figure E.3.

Similar to the previous predictions, a Monte-Carlo simulation across thirty years is utilised. Currently, the data provided by the klimaateffectatlas includes expectations on the severity level in 2050 [76]. According to the klimaateffectatlas, the pathway to this end-point is relatively linear, which is a fair approximation since the indirect influences are comprised of a continuous degradation, meaning the degradation has a nearly constant rate. The simulation exploits this concept and applies an almost linear pathway of the severity level to the provided end-point.

Similar to the methodology proposed by Costa et al., the severity of the damage is distributed across five damage categories. The five levels of damage which can occur are described in Appendix D. If the vulnerability exceeds a certain hazard level, indicating a specific threshold is surpassed, damage is assigned to the house. The data from the klimaateffectatlas provides expectations on the severity level in 2050 and does not include any uncertainty with the outcome of the simulation. Therefore, to create some randomness in the simulation, the severity at 2050 has been given a three-sigma of half a point. The simulations predicts across thirty years, and hence the variability has to be distributed across the thirty years. To convert the three-sigma of half a point over 30 yeas to a one year one-sigma, the conversion shown in Equation 4.2 is required.

$$\sigma_1 = \sqrt{\frac{\left(\frac{3\sigma_{30}}{3}\right)^2}{30}} = \sqrt{\frac{\left(\frac{3 \cdot 0.5}{3}\right)^2}{30}} = \sqrt{\frac{1}{1080}} \tag{4.2}$$

In the methodology employed in this research, all houses are assumed to start at a severity level of 0. Every simulated year, a random draw from a normal distribution with a mean of the point expected severity at 2050 divided by the number of years in the simulation and a standard deviation of $\sqrt{\frac{1}{1080}}$ is added to the severity level. This creates a relatively linear pathway towards the expected severity in 2050 provided by the klimaateffectatlas. A schematic example of a pathway up to the highest damage level is provided in Figure 4.2.

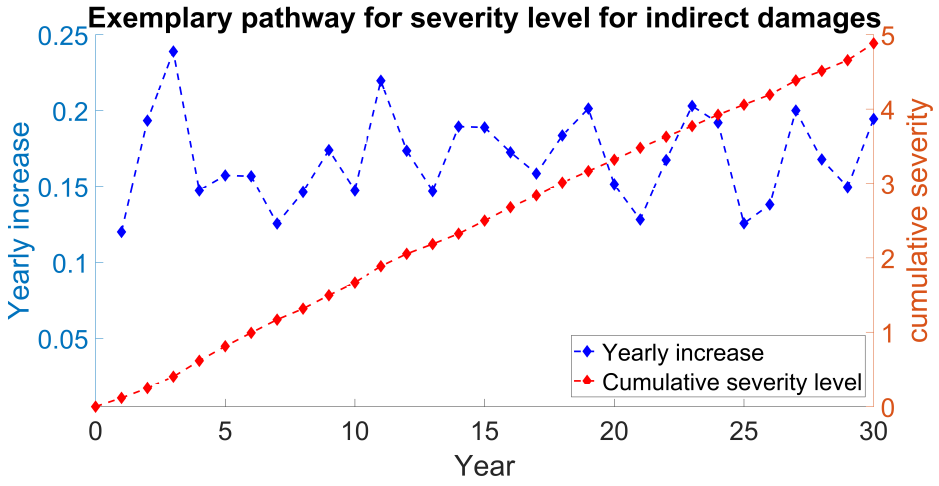

Figure 4.2: *Exemplary pathway for the severity level for indirect damages to the residential mortgage portfolio.*

The severity level for all the data points is yearly increased until it surpasses an integer level. Once this occurs, a damage value is assigned to the house according to Table D.1. This table provides the maximum and minimum repair costs for the incurred damage to the house. By setting the difference between the maximum and minimum costs to six sigma, which covers 99.99966% of the samples, the standard deviation can be estimated. Additionally, the mean is calculated as the average of the maximum and minimum repair costs. The calculated means and standard deviations for the five severity levels are displayed in Table 4.2.

If a point reaches the highest severity level of five before the end of the 30-year simulation, the severity level is kept at five and no more damage is assigned to the point. The underlying assumption for this is that at severity level five, the entire foundation is rebuilt, effectively solving the problem. Furthermore, the methodology assumes no efforts are made to improve the foundation before reaching severity level five. In reality, people might choose to renovate or replace their foundation before severity level five. However, this decision-making process is not incorporated in the methodology due to the lack of available information regarding when and if such decisions are made.

Table 4.2: *Damage categories with accompanying mean and standard deviation for the repair costs.*

Severity level	Mean	Standard deviation
1	1,250	250
2	2,750	750
3	6,000	1,333.33
4	35,000	8,333.33
5	75,000	15,000

To ensure consistent damage estimation across different damage categories, only one random draw is taken from a standard normal distribution. Subsequently, the corresponding probability of this random draw is calculated using the cumulative distribution function (CDF). This probability is matched with the appropriate CDF of the normal distribution based on the just surpassed severity level and the corresponding damage is assigned to the data point. This approach is adopted because the damage to a house is primarily impacted by its surface area. Consequently, the CDF probability of the repair costs remains relatively consistent across severity levels, as it is assumed that the surface area of a house does not change over time.

Subsequently, the net present value (NPV) of the damage is calculated by discounting the incurred damage using the risk-free rate and the year in which the damage occurs. The severity level is increased until the 30-year simulation period is completed. To assess the risk associated with the incurred damages, the total damage to the structure is multiplied by the probability of the house being on the appropriate foundation type for the indirect damage to occur. These incurred damage are then utilised to determine the economic implications of the indirect damages due to climate change.

4.4 Economic implications of the incurred damages

The final part of the simulation utilised in this thesis serves as the central point. It acts as a coordination point, providing information to all the previously mentioned simulations in this chapter, while also receiving the incurred damages from them. Besides, this simulation is responsible for analysing the economic implications resulting from the incurred damage to the portfolio. The flowchart representing the steps in explained in this subsection is provided in Figure E.5.

The analysis of the economic implications of the incurred damage on the portfolio begins by combining the points in the original portfolio with the damage portfolio, which only includes points with a flood probability. The value of the underlying asset is then estimated, representing its market value. However, assigning a market value to a house proves to be challenging due to limited information available on the actual sales price distribution within an area. Typically, only average sales prices for a specific period are publicly available. To properly estimate the value of the underlying asset, the WOZ value is utilised. The average WOZ value for each municipality is publicly available [77], although the actual distribution per municipality is not provided. However, a categorised distribution of the WOZ value for the entire Netherlands is disclosed by the CBS, which can be converted into a Weibull distribution [78]. In order to establish a distribution per municipality, it is assumed that this WOZ-distribution is equal across all the municipalities. However, a shift factor proportional to the average WOZ value of the municipality compared to the national average is added. This adjustment ensures that the distribution's mean aligns with the CBS-provided average for the particular municipality. A random draw from the appropriate distribution function is taken as an approximation of the actual value of the underlying asset.

Subsequently, the exposure at time t based on the underlying asset value and the VtL distribution constructed in section 3 is determined. Next, the damages incurred on the underlying asset due to flooding or indirect causes are deducted from the value of the underlying. Typically, when an underlying asset is repossessed, the bank aims to sell the property quickly, often through an execution auction. Generally, the bank receives less money compared to the current market value of the underlying asset. Therefore, a haircut is applied to the value of the underlying asset. Currently, as per Basel CRE36, banks are allowed to apply a singular haircut based on historical internal data [79]. However, this information is confidential and not publicly available. Thus, an approximation of the haircut is incorporated into the prediction. The estimation is based on the data published in a paper by Leow and Mues [80], where Leow and Mues researched a two-stage LGD model that includes a haircut for repossessed and forced-sold properties. The data is based on the UK housing market, but it is assumed to be a good approximation of the Dutch residential market. The data used by Leow and Mues is presented in Figure 4.3.

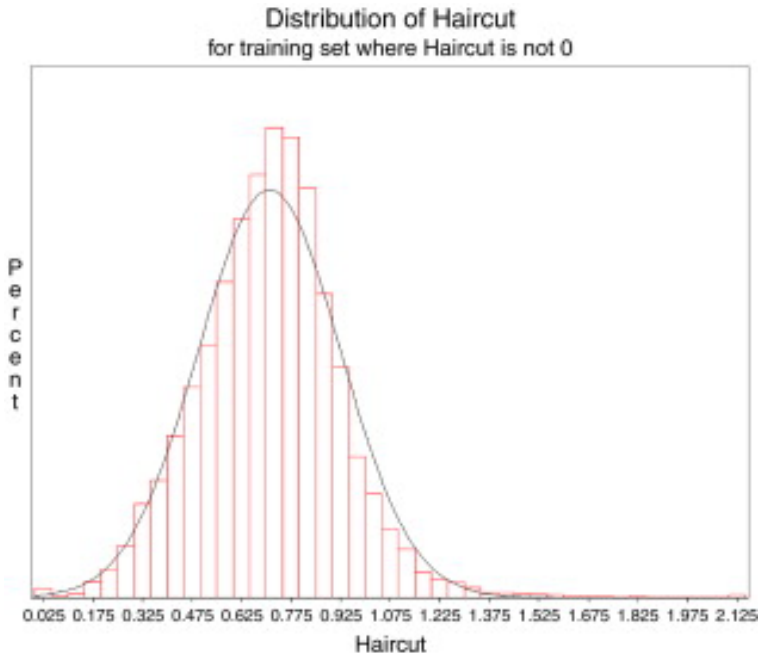

Figure 4.3: *Distributions of observed haircuts in the UK residential market given a repossession and forced sale [80].*

A random draw from this distribution is taken and applied to the value of the underlying asset as a haircut. Subsequently, this recovered value is utilised to generate a new VtL by dividing the repossessed value by the exposure at time t. Additionally, the LGD is calculated by first subtracting the recovered value from the exposure and then dividing this value by the exposure. The LGD cannot be negative since a loss cannot be negative. Therefore, the LGD is programmed to be the maximum of the calculated LGD or zero. The entire calculation performed by the prediction is summarised in Equation 4.3.

$$LGD_{it} = max\left(\frac{EAD_{it} - (1-\beta)\cdot Value\ underlying_{it}}{EAD_{it}}, 0\right) \tag{4.3}$$

Wherein, EAD_{it} represents the exposure at default of loan i at time t, LGD_{it} represents the loss given default of loan i at time t, and β represents the haircut applicable to the underlying. After completing this methodology, the economic implications of the incurred direct and indirect damage are visible.

4.5 Modelling interdependence

This chapter has provided an overview of the individual simulation and the corresponding assumptions. To illustrate the interdependencies between the various simulations and the involved portfolio, Figure 4.4 has been created. This flowchart outlines the data importation and information sharing between different simulations. Clearly, file which calculates the economic implications of the incurred damages serves as the central component of the program. However, it is important to note that the flood simulation based on flood probability is treated as a separate simulation. This design choice was made to ensure a realistic main simulation. As discussed in this chapter, the flood simulation based on flood probability represents an extreme scenario that is highly unlikely to occur. Therefore, this simulation is not included in the main modelling structure.

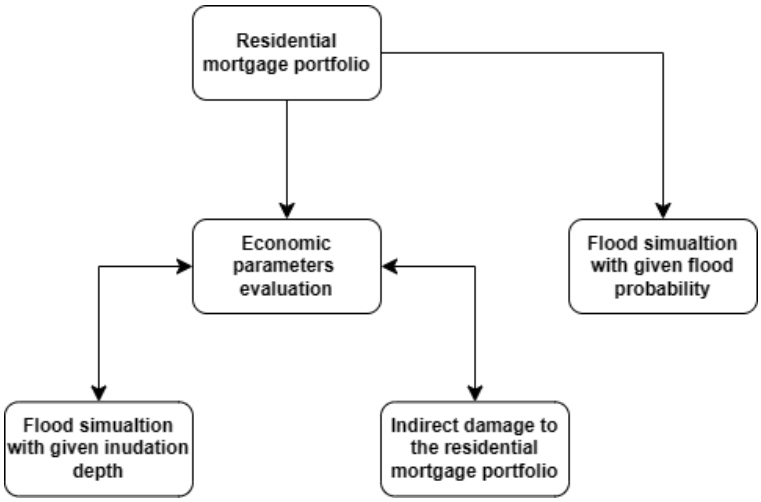

Figure 4.4: *Design and interdependencies of the overall simulation.*

4.6 General remarks on the methodology

Both the modeling of acute and chronic climate events is based on a static model primarily due to the limitations of currently available input parameters. In the Netherlands, the primary source of climate data provides cross-sectional data at specific points in time, such as 2050 and 2100. Consequently, creating a dynamic model with this data is challenging, leading to the decision to employ a static modeling methodology.

The methodology explained in this chapter relies heavily on the input parameters. For example, the flood probability in 2050 is contingent upon expected climate change and expected compliance with the Waterwet 2050. Given the complexity of Earth's climate and long-term uncertainties in politics, these figures are subject to change over time, resulting in significant uncertainty associated with these parameters. Therefore, models of this nature could potentially be run annually using updated and improved input parameters. However, in the context of this research, the validity and realism of the predictions could be questioned due to these uncertainties. Specifically, for the extreme prediction scenario, there may be concerns about its realism. Nevertheless, the assumptions made in these methodologies can only be validated over time, and as such, these uncertainties, although acknowledged, cannot be minimised with current knowledge.

5 Results

This chapter presents the outcomes of the predicting model explained earlier. The results are organised into four sections. Firstly, the direct flood damages are examined, focusing on the impacts of flooding on the residential mortgage portfolio. Secondly, the analysis explores the indirect damages caused by pile rot and settling. Subsequently, the discussion shifts to the influence of these damages on the VtL and LGD. Lastly, the direct damages resulting from the alternative extreme flood modeling methodology are discussed. This subsection incorporates all previous subsections, including the incurred damages and their implications on the VtL and LGD. Additionally, some additional information outside of the scope of the main research is provided which regards the required risk capital and the connection of the results with the current regulatory framework.

The results section is setup to first describes the incurred damages on the portfolio for both the direct as well as the indirect damages. A full description, explanation, and risk allocation of these results are provided in subsection 5.1 and subsection 5.2 after which the main research question is answered in subsection 5.3 based on the results of these two subsections.

5.1 Direct flood damages

In this subsection, the direct flood damages to the residential mortgage portfolio are explained. This section is divided in four distinctive parts where the first parts examines the incurred damages on the portfolio and the distribution these damages. Secondly, a partial validation of the results is discussed. Thirdly, the scaled quantity of damage for the current ING portfolio and the entire Netherlands is generated and analysed. Lastly, the allocation of flood risk patterns across the Netherlands is computed and examined.

In this subsection, an explanation of the direct flood damages to the residential mortgage portfolio is discussed. This section is divided into four distinctive parts, with the first part examining the incurred damages on the portfolio and their distribution. Secondly, a partial validation of the results is discussed. Thirdly, the scaled quantity of damage for houses nationwide is generated and discussed. Lastly, the regions within the Netherlands where the risk of flood damages is discussed.

The direct flood damages to the residential housing are based on three flood probability charts with a given inundation depth. The amount of damage incurred on the structures is dependent on the location of the property, surface area, and inundation depth of the flood. The probability of a flood occurring with a low inundation depth is relatively high, whereas floods with an inundation depth of 2.0 meters rarely occur. To illustrate the difference between these flood charts, a summation of the incurred damages obtained within the 30 years from each Monte Carlo simulation is combined into a histogram. The histogram for the simulation with an inundation depth of 0.2 meters is provided in Figure 5.1.

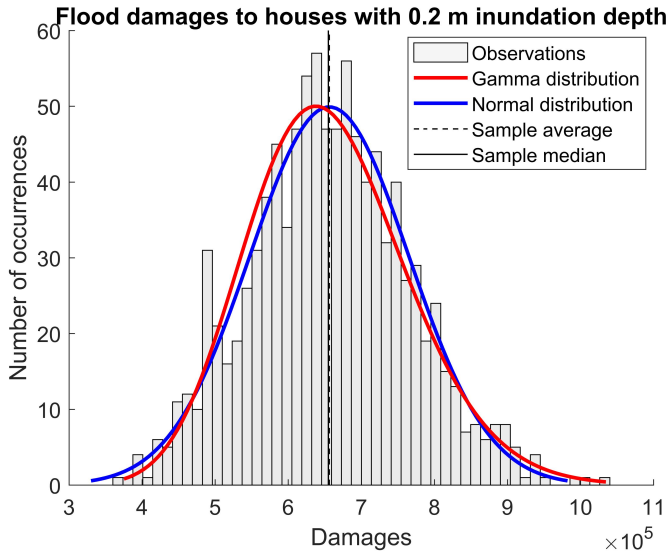

Figure 5.1: *Histogram of flood damages to houses from the Monte Carlo given an inundation depth of 0.2m.*

The histogram from the obtained damages with an inundation depth of 0.2m closely represents a normal distribution. The data matches a normal distribution fit to the observations, which is represented by the blue line. Additionally, the median and mean are approximately identical. Contrarily, the incurred damages histogram from the simulation with an inundation depth of 2.0 meters has a substantially different shape. This histogram is depicted in Figure 5.2.

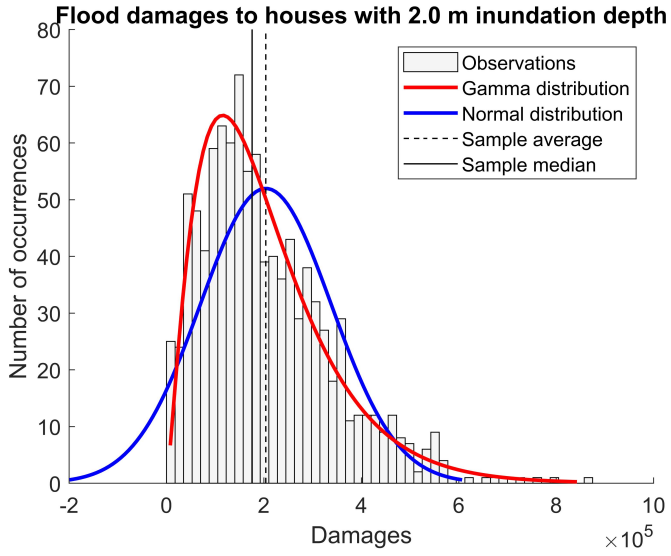

Figure 5.2: *Histogram of flood damages to houses from the Monte Carlo given an inundation depth of 2.0m.*

As can be noticed from Figure 5.2, the histogram of the damages with the inundation depth chart of 2.0 meters becomes positively skewed, i.e., the average is higher than the median. This positive skewness induces a heavy tail on the higher side damages, which could be very dangerous to a bank if ignored [81, 82]. These tails emerge from a statistical property of the Poisson distribution. The Poisson distribution is a statistical probability distribution that models the likelihood of a certain number of events occurring within a specific time interval, given the average rate of occurrence. Hence, the Poisson distribution is discrete since it counts the number of events in a time period. The gamma distribution is a comparable distribution wherein the time until a specified number of events occurs is modeled. Contrarily to the Poisson distribution, the gamma distribution is a continuous probability distribution [83].

Because time is continuous and the number of events is discrete, both Figure 5.1 and Figure 5.2 are fitted with a gamma distribution. The gamma distribution posses the property that if the shape factor goes up the distributions tends to become normally distributed [84]. This shape factor is inherently connected to the time till the next event where the shape parameter goes up if the time to the next event becomes shorter. Because the probability of an event occurring with a given inundation depth of 0.2m is multiple times higher compared to the probability of an event occurring with a given inundation depth of 2.0m, the time between events is smaller and hence a more pronounced gamma distribution is obtained with the prediction given an inundation depth of 2.0m. The observation of a gamma distribution is backed by previous researches on the hydrological flood frequency since these researches have shown frequent usage of Gamma family distributions. Several research concludes these types of distributions are best suitable as inputs for flood frequency models. Therefore, with enough time until the next flood event, the obtained flood frequency curve tends to become a gamma distribution [85, 86]. To better illustrate the effect of the time until the next event, the average flood probabilities in the prepared residential mortgage portfolio are provided in Table 5.1.

Table 5.1: *Average flood probability of the points in the residential mortgage portfolio across the simulated inundation depths.*

Inundation depth (m)	0.2	0.5	2.0
Average flood probability	$5.43 \cdot 10^{-4}$	$3.56 \cdot 10^{-4}$	$4.58 \cdot 10^{-5}$
Average yearly flood occurrence	2.228	1.458	0.188

Table 5.1 displays the average flood probability of the simulation with an inundation depth of 0.2m is almost twelve times as high compared to the simulation with an inundation depth of 2.0m. Hence, the time between events is smaller, and the obtained damages become more normally distributed. In between these two extremes, the simulation with an inundation depth of 0.5m is located. The histogram of this simulation is provided in Figure 5.3.

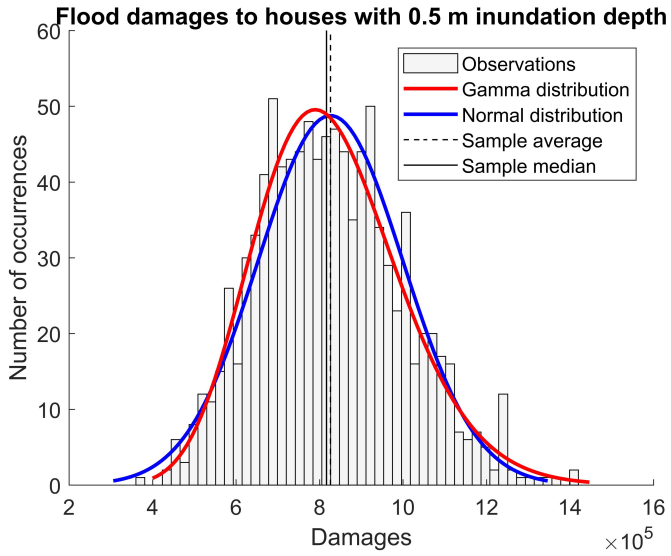

Figure 5.3: *Histogram of flood damages to houses from the Monte Carlo given an inundation depth of 0.5m.*

The histogram in Figure 5.3 is relatively close to a normal distribution. This is in accordance with the expectations since the average flood probability of the simulation with an inundation depth of 0.2m is only one and a half times as high as the simulation with an inundation depth of 0.5m. Therefore, the time in between events is rather similar, and hence the distribution is expected to be comparable. However, to statistically demonstrate the dissimilarities between the simulations, a comparative analysis is constructed with the most important parameters. The results of this analysis are displayed in Table 5.2.

Table 5.2: *Comparative analysis of the statistical import parameters regarding the flood simulation given the inundation depth.*

Inundation depth (m)	0.2	0.5	2.0
Average (€)	656,247	826,308	204,017
Median (€)	654,997	816,770	175,904
Percental difference average and median	0.19%	1.17%	15.98%
Skewness	0.141	0.333	1.039

The skewness of all the simulations displays a positive shift, indicating a heavier right-tailed distribution. Statistically, distributions are considered symmetrical with a skewness below 0.5 [87]. Hence, the simulation with a given inundation depth of 0.2m and 0.5m is recognised as a normal distribution, whereas the simulation with a given inundation depth of 2.0m is regarded as heavily skewed towards the right. This is important to establish in credit risk since the value at risk (VaR) and expected shortfall (ES) are dependent on the right tail skewness of the distribution.

To prepare for the worst-case scenarios, banks have developed the VaR and ES. The VaR can be defined as the maximum possible loss during a time period t after excluding all worse outcomes whose combined probability is at most p. The ES is an adjustment on the VaR by taking the average of the outcomes above the VaR to account for non-normal behavior in the tail. To identify these tail risks, this research incorporates these factors in the analysis of the results. The observed VaR and ES of the pr editions are provided in Table 5.3.

Table 5.3: *Value at risk and expected shortfall regarding the flood simulation given the inundation depth.*

Inundation depth (m)	0.2	0.5	2.0
Average (€)	656,247	826,308	204,017
90% VaR (€)	796,586	1,060,155	388,002
90% ES (€)	851,983	1,149,155	486,618
99.9% VaR (€)	1,003,836	1,407,510	795,136
99.9% ES (€)	1,019,891	1,469,624	857,947

The average, VaR, and ES of the simulation with a given inundation depth are all the highest with the inundation depth set at 0.5m. This originates from a mixture of the inundation depth influencing the damage factor and the probability of the event occurring. The combination of these is the highest in the simulation with the given inundation depth of 0.5m. Later in this subsection, these figures will be employed to adjudicate the financial implications on a bank's portfolio.

First, the numbers the program provides need to be validated against a real case. During the last decades, the Netherlands has suffered relatively few influential floods up to the 2021 flooding in Limburg. To validate the damages from the simulation, this event will be utilised since it is a flood which recently occurred and affected mainly residential properties. The Verbond van Verzekeraars reports about 10,000 claims from people primarily focused on household inventory and structure. These claims amount to a total incurred damage of around 210 million euros, which equals around 21,000 euros per claim [88]. To compare to the simulation, the average damages per claim coming from the program are provided in Table 5.4.

Table 5.4: *Average incurred damage per claim regarding the flood simulation given the inundation depth.*

Inundation depth	Average damage per house (€)
0.2	10,906
0.5	20,455
2.0	38,757

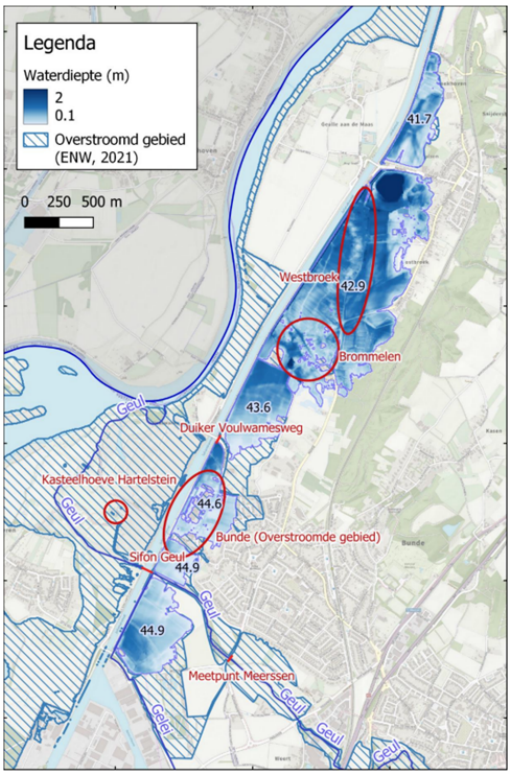

Figure 5.4: *Inundation depth during the 2021 Limburg floods [89].*

The claims originating from the simulation are strongly dependent on the inundation depth. To properly compare the incurred damages from the simulation to the claims from the Limburg flood, the approximate inundation depth of the flood has to be determined. Figure 5.4 depicts the recorded inundation depth during the 2021 Limburg floods. The picture shows the inundation depth is between 0.1m and 2.0m with commonly observed depths between 0.5m and 1.0m. Therefore, the average damage per house from the simulation with a given inundation depth of 0.5m is a good reference to the floods in Limburg. The simulation provides an average damage of €20,455 per house given the house incurred flood damage. Hence, the prediction is verifiable since this number is comparable to the average damage incurred on houses during the Limburg floods.

Additionally, a paper by Ermolieva et al. obtains similar results with a different modeling methodology. Ermolieva et al. utilise a Hazard-Exposure-Vulnerability methodology to predict the flood damages to households for a region around Rotterdam [90]. The results from this paper are provided in Table 5.5. The paper specifically provides the total amount of losses and the number of affected citizens. However, the paper does not include the quantity of affected households. To scale the damages to the amount per household, the damage per citizen is multiplied by 2.13, which represents the average number of residents per household as of 2022 [91].

Table 5.5: *Losses obtained by Ermolieva et al. from floods for a region around Rotterdam [90].*

Flood probability	Total damage	Affected citizens	Damage per citizen	Damage per household
1/10	20,248,656	1,804	11,224	23,908
1/100	54,404,334	7,354	7,398	15,758
1/1000	96,487,015	11,585	8,329	17,740

The model developed by Ermolieva et al., which utilises a different methodology, yields similar results compared to the methodology employed in this thesis. Consequently, the model's results are validated using current available literature on this topic and actual damages from the Limburg floods. However, it is important to note that these analyses do not fully validate the model, as the results of the damage calculation are primarily influenced by the damage functions used in this methodology. The validation of the Bernoulli trial component of the methodology is more challenging, as it relies on the predicted flood probability in 2050, which is dependent on future regulations and made efforts to reduce flood probability.

The setup of the portfolio allows for the allocation of flood risks to a particular area. The program provides the average incurred flood damages per point across all the Monte Carlo iterations. This average indicates the flood risk a certain point bears. The incurred damages to each point are loaded into a program called QGIS. QGIS creates a heatmap based on the amount of incurred damages within a circle of 20 kilometers. The greater the amount of incurred damages within a radius of 20km, the greater the flood risk of the area. Figure 5.5a and Figure 5.5a display the heat maps for the simulation with a given inundation depth of 0.2m and 2.0m, respectively.

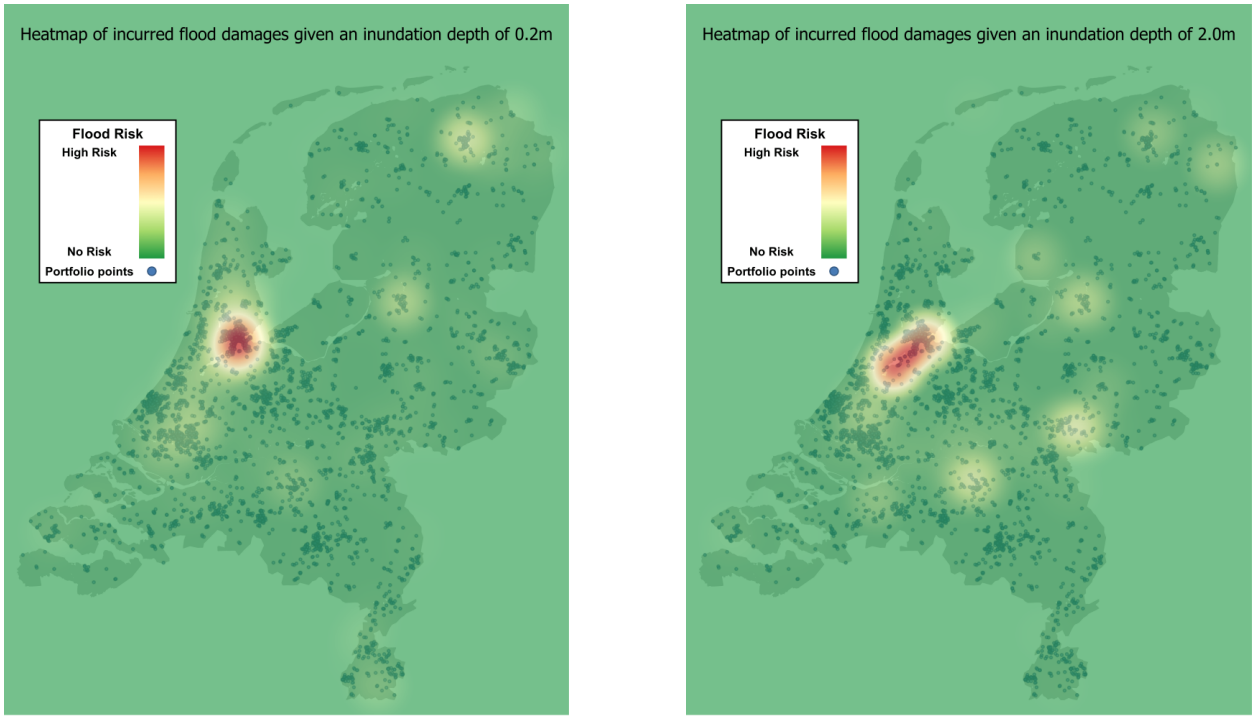

(a) *(b)*

Figure 5.5: (a) *Heatmap of incurred flood damages on the residential mortgage portfolio given an inundation depth of 0.2m.,* ***(b)*** *Heatmap of incurred flood damages on the residential mortgage portfolio given an inundation depth of 2.0m.*

The areas with the greatest flood risks, as indicated by heat maps, are situated near Amsterdam. Especially, the simulation given an inundation depth of 0.2m has almost all risks concentrated around Amsterdam. Other areas that bear some flood risks are the regions around Zwolle, Groningen, and Rotterdam. However, this is only marginal compared to the Amsterdam area. The risk being allocated to one particular area is a consequence of the population density, population size, and flood probability. With a population of around 900,000, the municipality of Amsterdam has roughly 250,000 more residents than the second-ranked city of Rotterdam. Additionally, the municipality of Amsterdam is rated as the fourth densest municipality in the Netherlands [92]. Combining this with a relatively high flood probability as visible in Figure B.1a, the risks are predominantly located in this area.

Comparably, the simulation with a given inundation depth of 2.0m has the majority of the risks around the Amsterdam area. However, the other areas with a medium flood risk are cities located close to the rivers such as the Ijsel, Waal, and Rijn. Primarily, this is induced due to the high flood probability around these rivers. Additionally, the population density around Arnhem, Zwolle, and Den Bosch elevates the risks.

The flood risk allocation from the simulation given an inundation depth of 2.0m is predominantly dependent on the flood probability since according to Figure B.1b, a substantial part of the major cities within the Netherlands has a flood probability of zero. Contrarily, the simulation given an inundation depth of 0.2m is mainly dependent on the population size and density since a substantial portion of the Netherlands has a relatively high flood probability. The simulation with a given inundation depth of 0.5m provides a heat map that is almost identical to the heat map of the simulation with a given inundation depth of 0.2m. Similar to the heat map of the simulation given an inundation depth of 0.2m, the distribution of the flood risk is primarily induced due to the population size and density. The heat map of this simulation is provided in Figure 5.6.

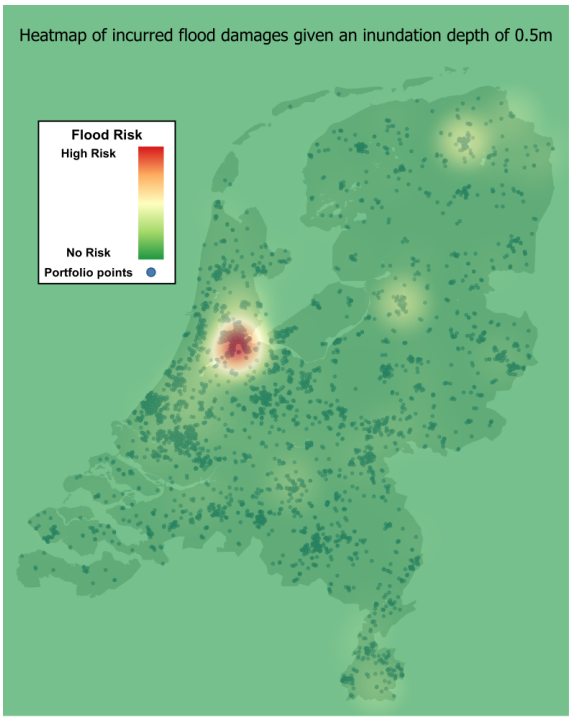

Figure 5.6: *Heatmap of incurred flood damages on the residential mortgage portfolio given an inundation depth of 0.5m.*

The difference between the simulation with a higher inundation depth is induced by the flood type. Commonly, the smaller inundation depths are induced by coastal flooding, whereas the damages in the simulation given an inundation depth of 2.0m are caused by river floods. This contrast is visible in the probability charts since the probability of a flood occurring with a given inundation depth of 2.0m is almost solely associated with areas around the major rivers in the Netherlands, whereas the probability chart given an inundation depth of 0.2m has a positive probability assigned to almost half of the points in the Netherlands.

The heat maps exhibit a diverse portfolio of regions with a significant risk of flooding. Nevertheless, the most predictable region is not embraced in the heat map. Specifically, the Maas area in Limburg is allocated with a low amount of risk. However, the previous three major floods all occurred within this province. Therefore, a logical question is why? The answer has to do with the preparation of the portfolio and the probability charts. The probability charts do display a very high probability of a flood occurring near the Maas in Limburg. However, the area around the Maas with a high probability is incredibly narrow. The widest span of flood probability along the Maas in Limburg reaches up to 2.5km from the riverbank, while in most segments, the flood probability extends only 1km from the bank. Hence, a substantial portion of the houses in Limburg does not have a flood probability since even within cities, houses are not always located within 1km of the river. Consequently, the program does not recognise the Maas in Limburg as a high-risk area since the impacted area around the Maas is relatively small, and therefore, a considerable amount of damage is not obtained from this area. This observation highlights the limitation of using a simulated portfolio instead of an actual bank's portfolio. Additionally, this highlights the problems associated with utilising a smaller portfolio which significantly decreases the granularity of the results.

A simplistic validation of these results can be achieved by comparing the results with literature regarding the possible damage in a protected area per kilometer of primary flood defense. A paper by Ten Brinke et al. evaluates these numbers for the Netherlands and finds that the provinces of Friesland, Groningen, and Noord-Holland bear significant potential flood risks, with the largest risks being allocated to Zuid-Holland [93]. These provinces also appear in the analysis performed in this thesis regarding flood risks. Although these results provide an indication the results are valid, a proper validation with these results from Ten Brinke et al. is not possible since the results from the paper regard the possible damages per kilometer of primary flood defense, whereas the employed methodology in this research predicts the possible damages per square kilometer of land. Hence, the paper by Ten Brinke et al. provides an indication that the model performs well. However, a full validation cannot be achieved with these results.

To generate a flood risk for an entire bank portfolio, the simulated portfolio should be scaled. Currently, the simulation is based on a portfolio with 4116 samples. Therefore, the average damage is scaled to this number of houses. However, the size of the sample is established so that it would be representative of a portfolio with an infinite number of houses. Hence, the damages incurred on the sample portfolio can be linearly interpolated to the ING portfolio and a nationwide portfolio. The interpolated numbers for these portfolios are provided in Table 5.6.

Table 5.6: *Average incurred damages for different interpolated portfolios regarding the flood simulation given the inundation depth.*

Inundation depth	Average damage (Portfolio) (€)	Average damage (ING portfolio) (M€)	Average damage (Nationwide) (M€)
0.2	656,247	76	1,289
0.5	826,308	95	1,623
2	204,017	24	401

Currently, the Netherlands has 8.05 million registered houses, which would incur between 400 million and 1.6 billion euros of flood damage in the upcoming 30 years according to the prediction. Scaled to the residential mortgages in the Dutch ING portfolio, this equals damages between 24 and 95 million euros. In relation to the outstanding amount of the ING mortgage portfolio, which is 113,846 million euros, the figure of 95 million euros is relatively insignificant. However, further discussion on the impact of these damages, combined with indirect climate risks, is provided at the end of this chapter.

5.2 Indirect damages

In this subsection, the indirect flood damages to the residential mortgage portfolio are explained. Similar to the previous section, this section is divided in parts. First, the incurred damages on the portfolio and the distribution of these damages are examined. Secondly, the validity of the obtained results are discussed. Thirdly, the scaled quantity of damage for the current ING portfolio and the entire Netherlands is generated and analysed. Lastly, the allocation of both settling and pile rot risks to specific areas in the Netherlands is generated and examined.

As discussed in the literature review, the indirect damages to the Dutch residential mortgage portfolio are induced by pile rot and settlement. The extent of damage to the structure depends on the cumulative severity level assigned by the simulation. The employed prediction methodology for these types of damages utilises a Hazard-Exposure-Vulnerability framework. An example of this methodology is illustrated in Figure 4.2. The resulting damage to the structure is subsequently multiplied by the probability of the house being constructed on a suitable foundation that is prone to pile rot or settlement. The input parameters from the Klimaateffectatlas offer high and low scenarios for both pile rot and settlement. The resulting damages caused by pile rot using both the high and low scenarios are depicted in Figure 5.7a and Figure 5.7b, respectively.

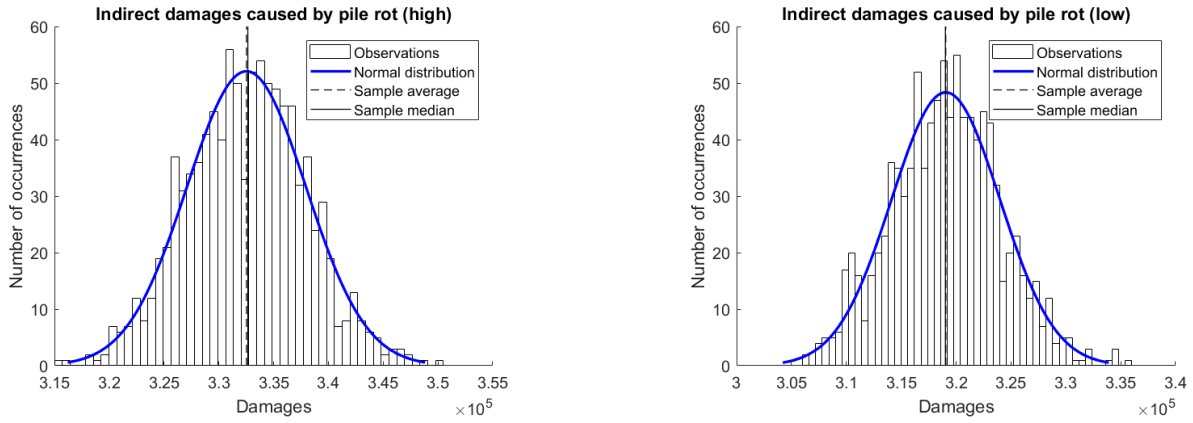

(a) *(b)*

Figure 5.7: ***(a)*** *Histogram of incurred pile rot damages with the high scenario provided to the prediction.,* ***(b)*** *Histogram of incurred pile rot damages with the low scenario provided to the prediction.*

The simulation predicts damages caused by pile rot that follow a normal distribution. This result is expected since pile rot is presumed to be a continuous process, leading to a gradual increase in damage to the structure. Therefore, the incurred damages are anticipated to exhibit a histogram that follows a normal distribution. In both Figure 5.7a and Figure 5.7b, the average and median values are very close to each other, indicating a normal distribution. Additionally, the skewness values of 0.095 and 0.102 for Figure 5.7a and Figure 5.7b, respectively, further support the observation of a normal distribution. The second indirect damage mechanism is the settlement of a house. Similar to the pile rot damages, there are high and low scenarios. The observed damage distribution of the high and low scenarios are depicted in Figure 5.8a and Figure 5.8b, respectively.

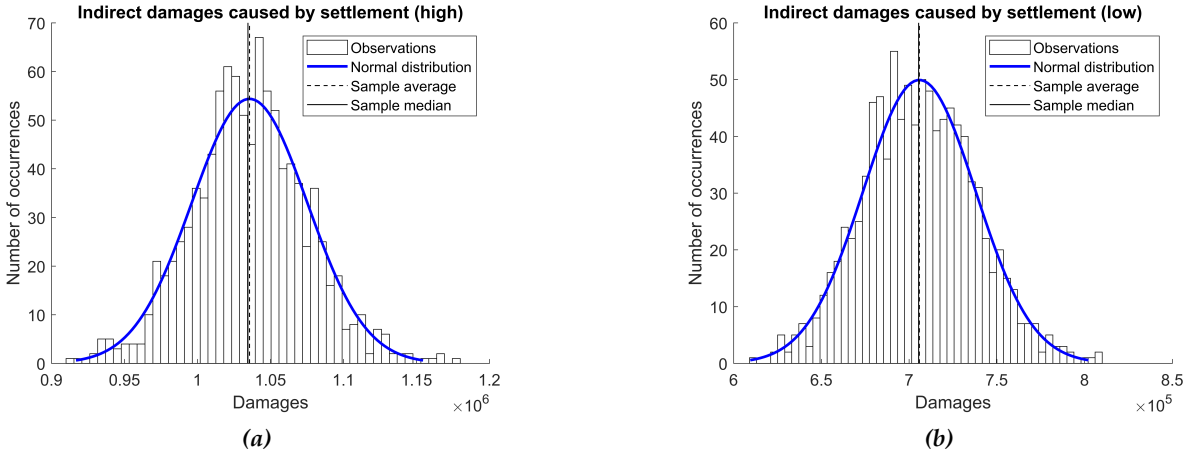

(a) *(b)*

Figure 5.8: ***(a)*** *Histogram of incurred settling damages with the high scenario provided to the simulation.,* ***(b)*** *Histogram of incurred settling damages with the low scenario provided to the simulation.*

Both histograms depicting the damages caused by settling exhibit a normally shaped distribution, similar to the pile rot damages. The skewness values for the high and low scenarios are relatively low, measuring 0.124 and 0.119, respectively. The similarity in the shape of the distributions can be again attributed to the continuous nature of the settling damage mechanism.

However, it is worth noting that the total amount of damage incurred due to settling is approximately three times higher compared to the damage caused by pile rot. This indicates that settling poses a greater risk in terms of potential damage to the structure. The most relevant figures representing the indirect damages from both pile rot and settling are summarised in Table 5.7.

Table 5.7: *Simulated indirect damages to the residential mortgage portfolio.*

Indirect damage	Scenario	Average damage (€)	90% VaR (€)	99.9% VaR (€)
Pile rot	High	332,523	339,294	348,674
Pile rot	Low	319,023	325,325	334,404
Settlement	High	1,035,242	1,083,620	1,147,042
Settlement	Low	705,871	746,967	807,370

The difference between the indirect damages caused by settling and pile rot can be attributed to the year of construction of the houses. Wooden foundation piles, which are susceptible to pile rot, were primarily used in buildings constructed before 1975. This means that more than half of the houses in the Netherlands are already excluded from the risk of pile rot damage [75]. Furthermore, even among the buildings from this period, only a fraction of them are actually built on wooden piles and are therefore susceptible to pile rot.

In contrast, a significant portion of houses in the Netherlands is constructed on shallow concrete foundations, making them more prone to settling. As a result, the multiplication of the incurred damage and the probability of the house being built on the appropriate foundation is considerably higher with the settling mechanism compared to the pile rot mechanism.

To support this statement, data on the average severity and average probability of houses being subjected to the indirect damage mechanisms is generated from the simulated portfolio. This data provides confirmation of the higher risk associated with settling compared to pile rot.

Table 5.8: *Average severity level and occurrence probability of the houses in the residential mortgage portfolio.*

Indirect damage	Parameter	Average
Pile rot	Severity High	0.973
	Severity Low	0.949
	Probability	6.90%
Settlement	Severity High	0.578
	Severity Low	0.477
	Probability	66.71%

Table 5.8 displays the average occurrence probability of pile rot, which is ten times lower compared to the occurrence probability of settlement. However, the average severity level for pile rot is twice as high. As a result, the average damage due to pile rot is higher, despite the lower probability of occurrence. These differences in severity and probability lead to variations in the incurred damages. Although the overall damages from pile rot are lower, a bank could still consider a higher risk premium if a house is deemed susceptible to pile rot compared to a house susceptible to settlement since the average incurred damage per point is higher. Nevertheless, this is only applicable if there is decided to do a case-by-case calculation of a climate risk premium instead of applying a general risk premium for a specific area.

Furthermore, Table 5.8 explains the relatively similar incurred damages in both scenarios for the indirect damage due to pile rot. The divergence between severity levels in the high and low scenarios is relatively small, resulting in rather similar damages. In contrast, there is a more significant difference in settlement damages between the scenarios, as reflected in the severity level with noticeable variance.

Validating the incurred indirect damages is challenging due to insufficient documentation on foundation damages caused by pile rot and settling. However, as a reference, Deltares conducted research on expected foundation damages up to 2050, which estimated a total range of 5 to 39 billion [25]. Currently, the damages are based on the generated residential mortgage portfolio. To properly compare these results, the incurred damages should be scaled to the national level. The linear scaling of the portfolio is provided in Table 5.9.

Table 5.9: *Average incurred damages for different interpolated portfolios regarding pile rot and settling.*

Indirect damage	Scenario	Average damage (Portfolio) (€)	Average damage (ING Portfolio) (M€)	Average damage (Nationwide) (M€)
Pile rot	High	332,523	38	653
Pile rot	Low	319,023	37	627
Settlement	High	1,035,242	119	2,033
Settlement	Low	705,871	81	1,386

The combined damages from both high scenarios amount to 2.65 billion euros, which is significantly lower than the lowest value provided by Deltares. However, it is important to note that the damages from the simulation are discounted using a risk-free rate of 5%. This discounting takes into account the year in which the damages occur. Currently, the simulation is set up such that each foundation starts at a severity level of zero and can escalate to level five after 30 years. As shown in Table 4.2, the damage incurred by a house increases exponentially with the severity level. Therefore, the higher repair costs occur towards the end of the 30-year period. Consequently, the damages could be discounted by up to 75%. Thus, the actual damages are higher than what is displayed in Table 5.9.

As a reference, a prediction without the risk-free rate was also conducted, resulting in an average combined indirect damage of €3,643,305. Scaled to the number of houses in the Netherlands, the total indirect damages amount to 7.2 billion. This falls within the range provided by Deltares. However, it is important to note that this is not a validation of the model since the actual numbers are currently unknown and difficult to validate since research regarding this topic is limited.

Similar to flood damages, the location of the damages is crucial. The damages obtained are associated with specific coordinates, allowing QGIS to create heat maps depicting the density of damage. The heat maps for settling and pile rot can be seen in Figure 5.9a and Figure 5.9b, respectively.

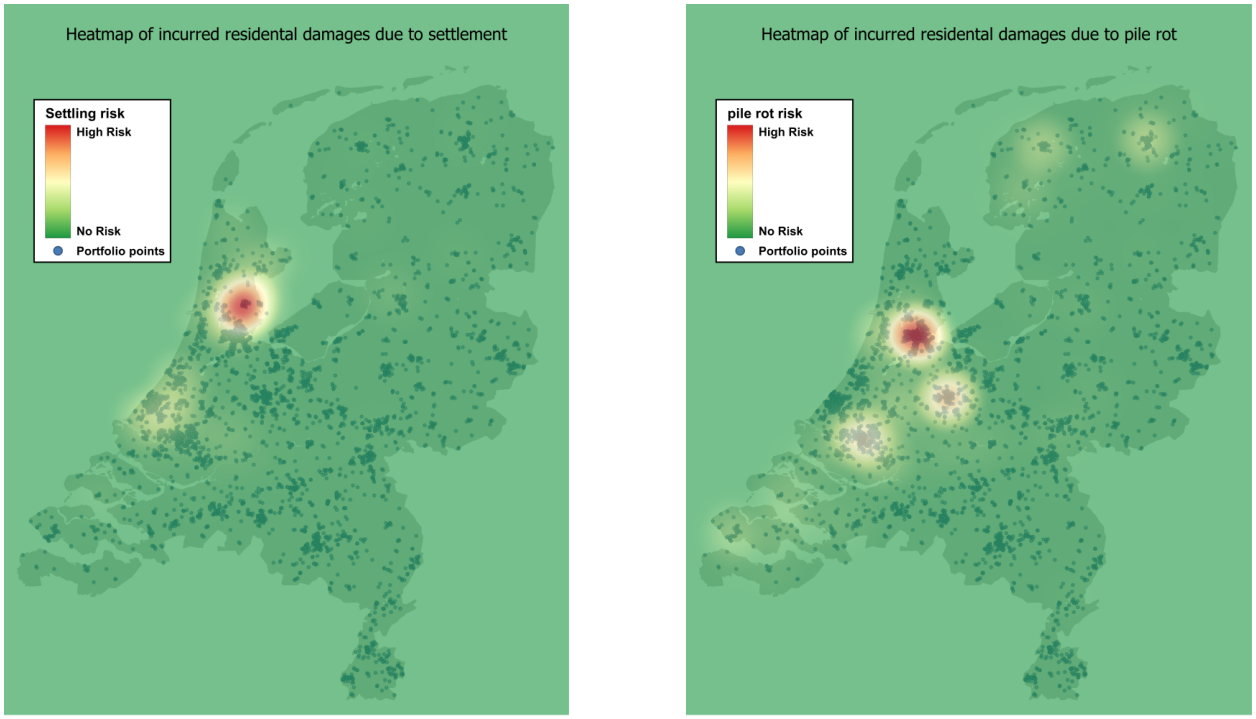

(a) *(b)*

Figure 5.9: (a) *Heat map of settling damages on the residential mortgage portfolio.,* ***(b)*** *Heat map of pile rot damages on the residential mortgage portfolio.*

The settling risk is highly concentrated around Purmerend, primarily due to the assigned probability and severity levels in this city. The multiplication of these numbers determines the settling risk, and ranking this multiplication reveals the top ten riskiest points. Interestingly, all ten points are located within the municipalities of Purmerend, Landsmeer, and Volendam, which are adjacent to the high-risk area. This indicates that the settling risk is less dependent on population density and size but highly dependent on the risk factor shown in Figure 2.7. Other municipalities with an increased risk of settling can be found around Delft, Den Haag, and Zoetemeer. In these areas, a relatively high probability and severity risk, combined with a high population density and size, contribute to the settling risk.

On the other hand, the risk associated with pile rot is more widespread across the Netherlands but still concentrated in major cities. Similar to the flood risks, the highest pile rot risks are associated with Amsterdam. City centers, in general, pose a relatively high-risk area due to the age of the buildings. There is a clear distinction in construction years for neighborhoods in Amsterdam [94], with older city centers having a higher probability of being built on wooden foundations. Consequently, the probability of pile rot occurring in these city centers is high. However, unlike the settling risk, pile rot risks are not confined to a specific area. Nevertheless, the population density, population size, and presence of older buildings contribute to the allocation of pile rot risks mainly in the major cities of the Netherlands. Besides Amsterdam, cities such as Rotterdam, Utrecht, Leeuwarden, and Groningen have also been assigned a medium pile rot risk by the prediction.

5.3 Economic implications of climate risks

In the previous two subsections, the direct and indirect damages to the portfolio were discussed. This subsection utilises these results to connect the predicted damage incurred due to climate change to VtL and LGD. In this section, first, VtL and LGD values are generated for all the scenarios that are passed through the prediction algorithm. Second, the validity of the obtained LGD distributions is discussed. Finally, heatmaps depicting the shift of LGD from the baseline values are generated, allowing identification of regions with the highest climate risks associated with the region.

In this section, the damages discussed in the previous subsections are categorised into three scenarios: the original case, the average damage scenario, and the 99.9% worst-case scenario. The original case serves as a baseline, where no damage is assigned. In the average scenario, the average damage obtained from the Monte Carlo simulation is allocated to each household. This entails summing up the damages incurred over the 1000 Monte Carlo simulations and dividing the total by 1000. As a result, the damage per household is relatively low, but nearly all loans in the portfolio are affected.

Conversely, the 99.9% worst-case scenario utilises the 99.9% VaR from both the direct and indirect simulations. Consequently, the direct damages in this scenario are significantly higher compared to the average case, but the number of affected households is lower.

The first important economic parameters is the VtL. This parameter indicates the proportion of the underlying property value in relation to the loan exposure. As the damage to a house occurs, the value of the underlying property decreases in proportion to the extent of the damage, thus adjusting the VtL. A histogram is created for the scenario involving high indirect damage simulation, along with direct damages resulting from the simulation with an inundation depth of 0.2m. The histogram is presented in Figure 5.10.

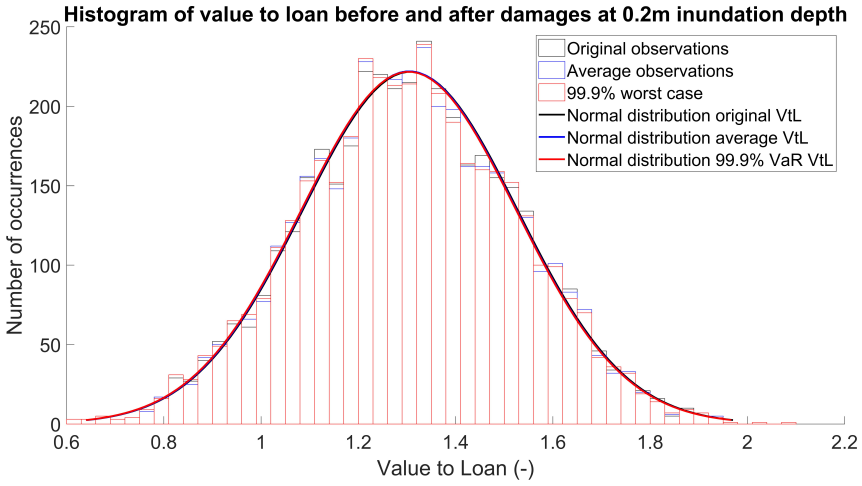

Figure 5.10: *Histogram of the VtL before and after direct and indirect damages from the simulation with a high indirect scenario and the flood simulation with an inundation depth of 0.2m.*

Figure 5.10 shows that the VtL distributions in all three scenarios are almost overlapping. However, it is important to note that even a small shift of a few basis points (BPS) can have an impact on the required capital of a bank. To highlight these shifts, Table 5.10 provides the changes in VtL for all the scenarios. These scenarios are based on the generated baseline VtL, which allows for a simplified comparison between them.

Table 5.10: *Key figures of the VtL and LGD from the simulation on the residential mortgage portfolio.*

Sim number	Inundation depth (m)	Indirect scenario	Scenario	Average VtL (-)	Average LGD (-)	Percent change VtL (BPS)	Percent change LGD (BPS)
Base	-	-	Base case	1.3068	0.1678	0.0	0.0
1	0.2	High	Average	1.3042	0.1688	20.2	55.2
2	0.2	High	99.9% VaR	1.3035	0.1690	24.9	71.0
3	2.0	High	Average	1.3047	0.1686	15.8	44.1
4	2.0	High	99.9% VaR	1.3038	0.1691	22.9	73.7
5	0.5	High	Average	1.3040	0.1688	21.4	59.3
6	0.5	High	99.9% VaR	1.3029	0.1694	29.5	94.2
7	0.2	Low	Average	1.3046	0.1686	16.8	45.1
8	0.2	Low	99.9% VaR	1.3040	0.1689	21.2	61.1
9	2.0	Low	Average	1.3052	0.1684	12.4	34.2
10	2.0	Low	99.9% VaR	1.3043	0.1688	19.1	55.2
11	0.5	Low	Average	1.3044	0.1687	18.0	49.3
12	0.5	Low	99.9% VaR	1.3034	0.1692	25.7	84.3

As anticipated, the highest average VtL is associated with the economic implication from the flood simulation with an inundation depth of 0.5m and the high indirect scenario (simulation numbers 6 and 5). In the average scenario, there is a percentage shift of 21.4 BPS from the baseline average VtL, while the 99.9% worst-case scenario has a deviation of 29.5 BPS. It is evident that the VtL is closely tied to the damages incurred over the 30-year period. Thus, the simulation with the highest average damage and VaR exhibits the largest negative shift in VtL. However, the deviations between the different scenarios are difficult to discern from Figure 5.10 due to their small magnitude. Nevertheless, these small shifts should not be disregarded, particularly when considering the impact on the LGD. In fact, the shifts in LGD are considerably larger compared to those in VtL. Figure 5.11 illustrates the distribution of LGD resulting from the flood simulation with an inundation depth of 0.5m, where the high indirect scenario is considered (simulation numbers 5 and 6).

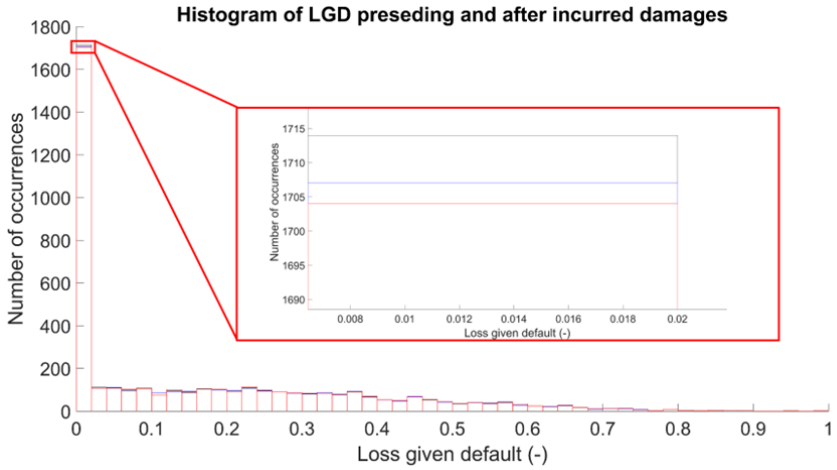

Figure 5.11: *Histogram of the LGD before and after direct and indirect damages from the simulation with a high indirect scenario and the flood simulation with an inundation depth of 0.5m.*

To validate the histogram, the shape of the graph is compared to the historical recovery rates of loans provided by Moody's. The data provided is from 2007, which means it is slightly outdated. However, the current overall recovery rate is approximately comparable to the recovery rate in 2007 [95]. Therefore, this data is used as an indication of the prediction validity. The comparison between the values from the baseline simulation and the values from Moody's is presented in Figure 5.12.

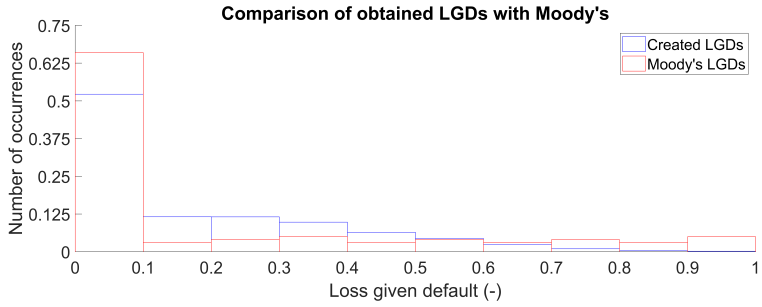

Figure 5.12: *Comparison between the base case LGD with the LGD in 2007 provided by Moody's [96].*

The data from Moody's does not exactly match the data from the simulation. However, considering the number of assumptions involved in establishing the LGD distribution, the shape of both histograms looks similar. The main difference lies in the tail distribution, with the created distribution having a normally distributed tail while Moody's distribution has a more uniform distribution in the tail. However, when considering the ING portfolio, the VtL tail follows a normal distribution, favoring the sample's normally distributed tail over the data provided by Moody's. As a result, the data cannot be validated with complete certainty, but it appears to be reasonably close to the actual values obtained by banks.

To illustrate the differences in LGD between the scenarios, the percentage change from the base case is presented in Table 5.10. The LGDs tell a similar story to the VtLs, with relatively small shifts. However, as a comparison, a model constructed by DMFCO concluded that the loss due to floods in the Netherlands accounted for less than half a basis point per year [97]. In comparison, the prediction shows the highest decrease in LGD of 15.8 BPS observed in scenario 6. This shift occurs over a 30-year timeframe, suggesting an annual loss due to climate risk of approximately 0.5 BPS. Hence, the relatively small shift in the LGD due to climate change is also observed by other researches.

Moving on to the allocation of the highest decrease in LGD, the municipalities with the greatest average shift in LGD represent the highest risk associated with physical climate risk. The municipalities are divided into seven categories based on the difference between the base case and the obtained LGD from scenario 5. Scenario 5 is chosen to ensure all points with a flood probability are assigned damage. If scenario 6 is used, the LGD shift becomes heavily dependent on one or two flood damages in a municipality, which does not accurately represent the physical climate risk. Furthermore, the fifth scenario exhibits the largest shift in LGD among all the averaged scenarios, further emphasising the visualisation of climate risk. To ensure a sufficient sample size for an accurate representation, municipalities with less than five data points are excluded from the dataset. The LGD shift per municipality is depicted in Figure 5.13a.

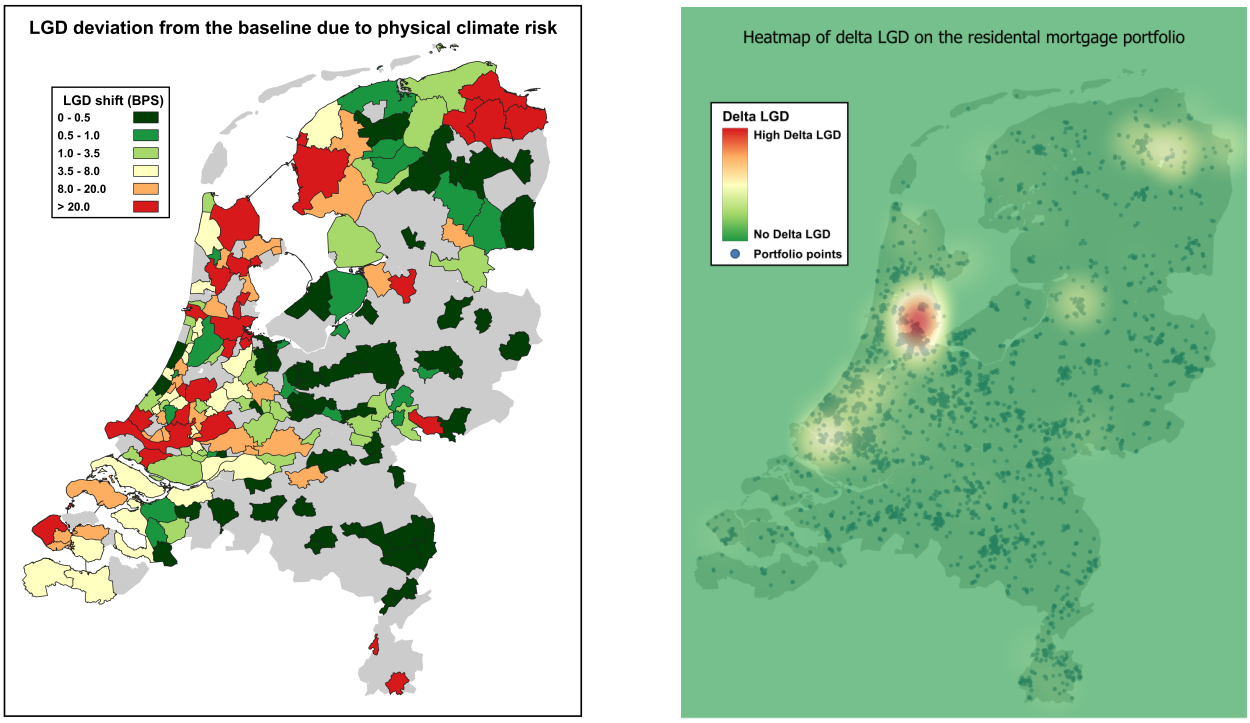

(a) *(b)*

Figure 5.13: ***(a)*** *LGD shift for every municipality from scenario 5 of the residential mortgage portfolio given five points exist within the municipality.,* ***(b)*** *Heat map of LGD shift from scenario 5 of the residential mortgage portfolio.*

The highest climate risk for acquiring a new mortgage is associated with the red-colored municipalities in Figure 5.13a. The municipalities with the highest combined physical climate risk are Landsmeer, Purmerend, and Oldambt, while Amsterdam and Rotterdam are ranked relatively lower at 24th and 23rd, respectively. However, the probability of obtaining a mortgage in these cities is significantly higher compared to acquiring one in Oldambt. Therefore, a heat map is created to account for the proximity of points with a shift in LGD, as shown in Figure 5.13b.

Similar to the incurred damages, the combination of population size, population density, and a medium to high-risk level contributes to the majority of LGD shifts being concentrated around Amsterdam. Upon closer examination, the high LGD shifts also extend into the region just north of the city of Amsterdam, where the municipalities of Landsmeer and Purmerend are located. The depiction of risk is not only influenced by population size and density but also by the increased likelihood of physical climate-related damages. Similarly, the medium LGD shifts around Groningen also extend into the region where the municipalities of Midden-Groningen and Oldambt are situated. These municipalities rank among the top five with the highest physical climate risk but lack in population density and size. Other areas with a moderate influence on the LGD are the municipalities around Rotterdam and The Hague, as well as the municipality of Zwolle. These areas of the Netherlands have the greatest impact on the LGD in the developed portfolio.

Throughout this chapter, it is evident that density and size have a significant influence on the risk assigned to a specific region. Therefore, the physical climate risks observed by a bank are highly dependent on the portfolio owned by the bank. However, the physical climate risk on a portfolio is not solely determined by its density and size. The location of the house also plays a crucial role, particularly concerning direct physical climate risks. Nonetheless, banks can use Figure 5.13a as a guideline to identify municipalities with an increased physical climate risk. Furthermore, this figure can be utilised to diversify the portfolio and reduce risk by encouraging customers to take a mortgage in municipalities categorised as grey in the figure, offering them a discount on the interest rate. Conversely, banks may charge a higher rate in municipalities with increased climate risks (red municipalities) to mitigate some of the inherent risks associated with the location of the mortgage.

5.3.1 Required risk capital

To assess the necessary risk capital that a bank should hold, the calculation of the climate risk-adjusted PD is essential. However, due to the complexity of the PD calculation, it is beyond the scope of this research. Nonetheless, investigating climate-adjusted PD is an intriguing avenue for future research in this field. The LGD, PD, and exposure at Default all play a role in determining the EL of a portfolio. The formula for calculating the EL is presented in Equation 5.1.

$$EL_{it} = EAD_{it} \cdot PD_{it} \cdot LGD_{it} \tag{5.1}$$

Subsequently, to determine the necessary capital provisions for covering physical climate risks, an Internal Rating Based (IRB) or Standardised approach can be employed. The standard procedure is partly regulated by Basel, specifically BIS-CRE 35 and BIS-CRE 36 [79, 98]. The PD also plays a role in determining the loan's stage. In accordance with the International Financial Reporting Standards (IFRS) 9, a loan can be downgraded from an investment-grade loan (Stage 3) to a lower-grade loan. This downgrade can occur when climate risks are incorporated into the Expected Credit Loss (ECL). It is important to note that this change in stage from a Stage 2 to a Stage 1 loan can significantly impact the capital requirement, as the loan is then subject to a 12-month ECL instead of a lifetime ECL. As a result, the capital requirement increases due to the loan degradation [99].

5.3.2 Connection to the current regulatory framework

As discussed in the literature review, the current regulations and directives primarily focus on the Basel Pillar III implementation of technical standards, which specify uniform formats and instructions for the disclosure of ESG information. However, these standards only incentivise banks to disclose the extent of their exposure to physical climate risks.

At present, there are no climate-related constraints on capital requirements imposed on banks under the Pillar I framework [16]. Nevertheless, the Basel framework already incorporates certain requirements that encourage supervisors to consider climate-related financial risks. These requirements are primarily based on the BIS-CRE 20.75 paragraph, which emphasises the need for a prudently conservative appraisal of property value, excluding expectations of price increases and considering potential market price sustainability over the loan's duration [100]. This implies that the LtV ratio should be adjusted to account for potential damage effects or value losses associated with climate-related financial risks. However, these regulations currently lack specificity and are challenging to enforce in their current form [101].

Therefore, while banks are making efforts to estimate the physical risks they face, the current regulations and directives do not mandate the integration of these risks into internal PD and LGD models. Consequently, banks assess these risks separately, as their incorporation would require higher risk capital, as demonstrated in this thesis, resulting in lower Return on Equity (ROE) and potentially harming the bank's competitiveness. As a result, the developed models or similar approaches to assess the impact of physical climate risks, lacking support from current regulations and directives, are unlikely to be implemented due to their potential negative impact on bank's competitiveness.

However, it is anticipated that these risks will be incorporated into the Basel framework in the coming years. The implementation process is already underway, with Basel publishing several principles aimed at enhancing the climate-risk components of existing Pillar II supervisory review processes [102, 103].

5.4 Direct flood damages with a given flood probabilities

This section presents the results from the most extreme simulation conducted as part of this research. The section is structured similarly to the previous subsections. First, it discusses the incurred damages and their accompanying distribution. Second, it explores the adjusted VtL and LGD for all the different input scenarios. Lastly, generated heatmaps are used to identify regions with the highest climate risks according to this modeling methodology.

The resulting damages from this prediction are illustrated in Figure 5.14 below. As can be seen from this histogram, the damages predicted utilising this approach are notably higher when compared to the damages obtained from the configuration used for a specific inundation depth.

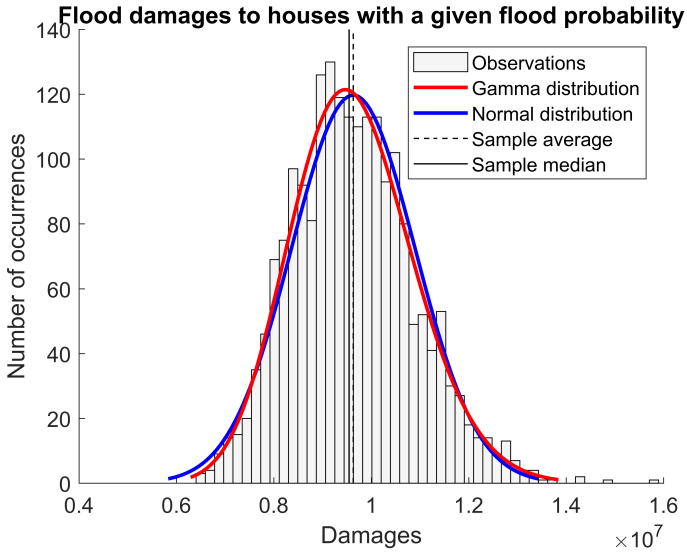

Figure 5.14: *Histogram of flood damages to houses from the Monte Carlo given a flood probability.*

Unlike the previous flood results, the distribution of the resulting damages follows a normal distribution. This can be attributed to the phenomenon discussed earlier, where the time between events causes the gamma distribution to approximate a Gaussian distribution. The simulation setup allows for relatively short intervals between events, resulting in damages that are normally distributed. However, the key focus of this simulation lies in the severity of the average incurred damages and the 99.9% VaR. A comparison between the averages obtained from the simulation with a specific inundation depth and this extreme simulation is presented in Table 5.11.

Table 5.11: *Comparison between the incurred damages from simulations with a given inundation depth and the simulation with a given flood probability.*

Simulation given	Inundation depth (m)	Average (€)	99.9% VaR (€)	99.9% ES (€)
Inundation depth	0.2	656,247	1,003,836	1,019,891
Inundation depth	0.5	826,308	1,407,510	1,469,624
Inundation depth	2.0	204,017	795,136	857,947
Flood probability	-	9,630,762	14,825,398	15,355,046

The damages obtained from the prediction with a specific flood probability are approximately 12 times higher compared to the simulation with an inundation depth of 0.5m. This difference is attributed to the frequency of flood occurrences and the average depth of inundation. In this prediction, the entire portfolio experienced an average of around 5.5 flood events per year. In comparison, the simulation with an inundation depth of 0.2m had approximately 2 flood events per year with the same portfolio. This disparity arises from the modelling methodology, particularly the comparison of randomly drawn samples using four probability charts.

Moreover, the average damage incurred during a flood in this simulation is €57,732. In comparison, floods with an inundation depth of 2.0m result in an average damage of €38,757 per affected property. The difference in incurred damage stems from the variation in inundation depth. The probability charts are constructed based on the maximum inundation depth that could be reached during a flood. Especially, the charts featuring lower flood probabilities indicate large areas with inundation depths exceeding 2.0 meters. Consequently, these floods are more severe and result in more extensive damage, given that the damage factor is solely influenced by the inundation depth while the other parameters remain constant. Hence, the average damage sustained by a property during a flood is higher.

The economic implications of these damages are calculated using the same methodology as the economic implications with a given inundation depth. To ensure proper comparison between the samples, the same baseline is utilised as in the previous subsection. The results of this comparison are presented in Table 5.12.

Table 5.12: *Comparison between the LGD shifts from the simulations with a given inundation depth and the simulation with a given flood probability.*

Sim number	Simulation	Indirect scenario	Scenario	Average VtL (-)	Average LGD (-)	Percent change VtL (BPS)	Percent change LGD (BPS)
Base	-	-	Base case	1.3068	0.1678	0.0	0.0
5	Inun 0.5m	High	Average	1.3040	0.1688	21.4	59.3
6	Inun 0.5m	High	99.9% VaR	1.3029	0.1694	29.5	94.2
11	Inun 0.5m	Low	Average	1.3044	0.1687	18.0	49.3
12	Inun 0.5m	Low	99.9% VaR	1.3034	0.1692	25.7	84.3
13	Flood prob	High	Average	1.2924	0.1734	110.5	334.5
14	Flood prob	High	99.9% VaR	1.2867	0.1780	153.9	603.5
15	Flood prob	Low	Average	1.2928	0.1733	107.1	324.1
16	Flood prob	Low	99.9% VaR	1.2872	0.1778	150.2	593.5

As anticipated based on the incurred damages, the LGD is significantly higher in comparison to the simulation with an inundation depth of 0.5m. The marginal shift of 15.8 BPS observed in simulation number 6 becomes a shift of 101.3 BPS in scenario 14. Consequently, the economic implications of this simulation are significantly greater. Furthermore, the balance between direct and indirect damages is altered. In the simulation with an inundation depth of 0.5m, the relative ratio of average direct to average indirect damages is approximately 0.6. In contrast, the simulation with a given flood probability exhibits a ratio of around 7.0 between direct and indirect damages. As a result, the indirect damages become almost negligible in this prediction, as the shift in LGD is predominantly driven by flood damages alone. This is evident in the difference in the percentage change between simulations 13 and 15, for instance. The transition from a high indirect scenario to a low indirect scenario leads to a decrease of 10.4 BPS in the percentage change of LGD, representing a relative change of approximately 3.1%. In comparison, the shift between simulations 5 and 11 is 10.0 BPS, corresponding to a relative change of 16.9%. Therefore, the influence of indirect damages is less significant in this simulation setup compared to the more realistic setup. The distribution of LGD risk across municipalities also reflects this observation. The LGD risk per municipality and the heat map of LGD shifts can be seen in Figure 5.15a and Figure 5.15b, respectively.

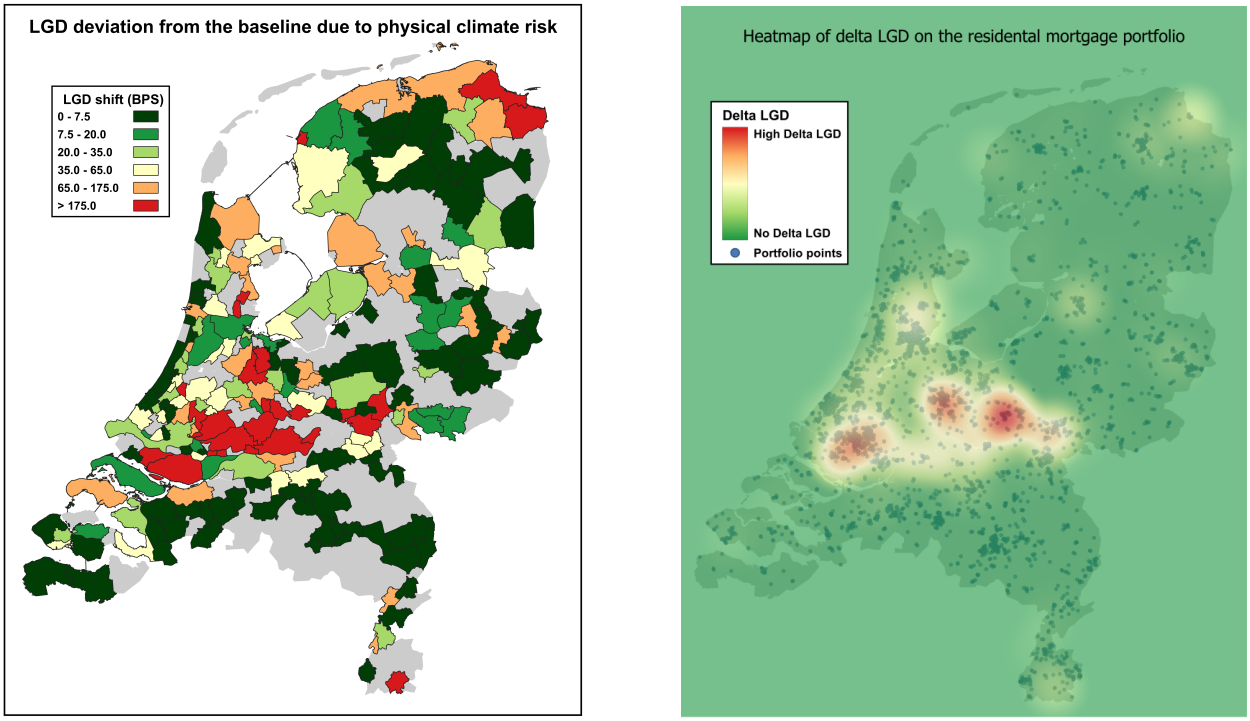

(a) *(b)*

Figure 5.15: ***(a)*** *LGD shift for every municipality from scenario 13 of the residential mortgage portfolio given five points exist within the municipality.,* ***(b)*** *Heat map of LGD shift from scenario 13 of the residential mortgage portfolio.*

When comparing Figure 5.13a and Figure 5.15a, the municipality with the highest shift in LGD changes completely. In Figure 5.13a, Landsmeer has the highest LGD shift, but in Figure 5.15a, it is ranked only 12th. Conversely, Veenendaal, which is ranked 173rd in the prediction with a given inundation depth, has the highest LGD shift in this prediction. This highlights the significant influence of direct damages on LGD in this simulation.

A similar pattern can be observed in Figure 5.13b compared to Figure 5.15b. Specifically, the economic impact of climate change on LGD shifts away from the Randstad towards the middle of the Netherlands. The areas around the major waterways in the country are deemed particularly vulnerable to economic risks in this prediction. This shift in risk pattern is due to the inundation depth depicted in the risk charts, as seen in Figure 2.4b. The inundation depth around the major waterways is the highest in the Netherlands. Since the economic risk is primarily driven by flood risk, the municipalities with the highest inundation depth also have the highest economic risk.

However, it is important to note that this scenario is currently irrelevant, as the existing primary flood barriers are capable of limiting the frequency and depth of floods. Nonetheless, in an extreme scenario with rapid sea level rises and a lack of government incentives to comply with the Waterwet 2050, this scenario could become relevant. Nevertheless, as discussed in the framework of the NGFS, it is unlikely that this scenario will be reached since it requires a sequence of events that are highly implausible. Nonetheless, this scenario is valuable for discussion as it represents a situation where direct climate risks dominate over indirect risks. Additionally, it emphasises the importance of well-managed primary and secondary flood barriers within the Netherlands.

6 Conclusion

This research aimed to assess the impact of physical risks associated with climate change on the LGD for the Dutch residential mortgage portfolio. Additionally, it aimed to address the literature gap concerning the connection between incurred damages due to climate change and their implications for banks. Currently, existing literature primarily focuses on identifying incurred damages, with limited attention given to their economic implications. To address the research question, five stages with subsections were established.

Firstly, this research establishes a solid foundation by examining the existing ESG regulations, climate scenarios, and relevant climate events specific to the Netherlands. Secondly, various research approaches are explored, aiming to identify methodologies available for predicting the incurred damages due to climate changes and understanding the current research landscape regarding weather events impact on the residential mortgage portfolio.

Among the diverse methodologies proposed in literature to assess flood damages for specific regions, the Bernoulli trial modelling approach is chosen. This approach, combined with depth-damage curves specifically tailored for the Netherlands, is considered the most suitable for this research. It serves as the methodology to predict flood damages accurately. Additionally, the Hazard-Exposure-Vulnerability methodology, as proposed by Costa et al. and Koks et al., is applied to quantify indirect damages to residential properties. To facilitate the utilisation of these methodologies, a dummy portfolio is constructed by integrating various public databases. Consequently, the predicted damages are assessed, highlighting their implications on both the Value-to-loan and Loss Given Default resulting from climate change.

Using this methodology, the residential mortgage portfolio incurred the highest amount of flood damage in the probability charts given an inundation depth of 0.5m. The portfolio consisting of 4116 points resulted in an average flood damage of €826,308, with a 99.9% VaR of €1,407,510. The indirect damages on the same portfolio resulting from pile rot and settlement, calculated under a high scenario, amount to an average total damage of €332,523 and €1,035,242, respectively. Therefore, 62.5% of the cumulative average damage incurred is attributed to these indirect phenomena.

Considering both direct and indirect damages, the average VtL decreased from 1.3068 (in the base case) to 1.3040 (with average damages) and 1.3029 (with the 99.9% VaR damages). Simultaneously, the average LGD increased from 16.78% (in the base case) to 16.88% (with average damages) and 16.94% (with the 99.9% VaR damages), resulting in relatively modest economic implications. The reductions in VtL and LGD are primarily concentrated around the Randstad, with Amsterdam being particularly exposed to high economic risks due to a combination of relatively high climate risks and a dense population. Without taking population density and size into account and concentrating solely on the on VtL and LGD shifts from the baseline, the municipalities of Landsmeer, Purmerend, and Oldambt stand out for having the highest combined physical risks. Therefore, acquiring a new mortgage in these municipalities entails the highest physical climate risks associated with the loan according to the prediction.

As an extreme scenario, a simulation with a given flood probability and maximum inundation depth was conducted. The results yielded an average flood damage of €9,630,762, along with a 99.9% VaR of €14,825,398. Consequently, the indirect damages become almost insignificant. The economic implications reveal a decrease in the VtL ratio to 1.2924 and 1.2867, alongside an increase in LGD to 17.34% and 17.80% for the average and 99.9% VaR scenarios, respectively. The economic implications highlight significant economic consequences associated with this scenario. However, this scenario is currently irrelevant due to the effectiveness of the existing primary flood barriers in limiting the number of floods and inundation depth. Nevertheless, in an extreme scenario characterised by rapid sea level rises and a lack of government incentives to comply with the Waterwet 2050, such a scenario could become relevant. The domination of direct damages focuses the risk more around the major rivers, where the maximum inundation depths are the highest.

To answer the main research question: *What is the predicted increase in Loss Given Default up to 2050 for the residential mortgage portfolio in the banking sector in the Netherlands, resulting from physical climate risks such as flooding, pile rot, and settlement?'*, the analysis reveals several key insights.

Overall, the findings indicate that climate change has a relatively limited impact on the LGD, with changes of up to 15BPS. This limited impact is observed across all scenarios except for the extreme scenario applied to the residential mortgage portfolio. In this extreme scenario, notable and significant increases in the LGD were observed, indicating the potential vulnerability of the portfolio under severe climate-related conditions. This scenario highlights the need for more extensive stress testing in the simulation, as it could generate scenarios where the incurred damages are enormous, resulting in substantial economic implications. However, it is crucial to carefully consider the severity and validity of these stress scenarios before implementing them in the prediction, as this substantially impacts the economic implications.

7 Recommendations

Current simulation

The prediction discussed in this thesis incorporates some assumptions and features that could be improved in future research. First, to enhance the reliability of the program, proper validation of the generated simulation is required. Currently, the outcomes of the program are validated against the obtained flood damages in the 2021 Limburg floods and previously conducted researches. However, properly validating the prediction is challenging due to the lack of information and the prediction's area-specific nature.

As a point of discussion in the context of the current simulation, it is important to note both the portfolio generation and modeling structure rely on highly specific parametric assumptions. Sometimes, the basis for these assumptions lacks a strong foundation in actual data, resulting in an oversimplification of the problem. Additionally, these assumptions are often presumed to follow a normal distribution, which may not hold true for certain distributions. This presumption reduces the consideration of tail risks, as normal distributions have limited tail risk. Consequently, the current predictions have significant limitations in identifying these risks. Given that climate risks are closely tied to extreme tail events, particularly in relation to flooding in specific areas, it is advisable to enhance the current assumptions of normality for some of the parameters used in the prediction.

Another important point for discussion concerns the use of a static modeling methodology. This simplification is a result of the limited availability of input data related to flood, pile rot, and settling risks. However, the static nature of the prediction simplifies the interconnection between years, which is common in realistic scenarios. Therefore, a recommendation would be to develop a more dynamic modeling methodology in which results from the previous year (i-1) influence the input parameters for the current year (i). Additionally, in the next subsection, a dynamic modeling methodology that takes into account changes in the economic landscape and the bank's portfolio is discussed.

Simulation Expansion

The first recommended expansion to properly assess the impact of climate change on a bank involves incorporating the PD into the simulation. This inclusion would not only enable the prediction of the LGD but also facilitate the estimation of the necessary risk capital required to address climate risks in accordance with Basel Pillar I regulations.

Moreover, this addition becomes particularly essential if other portfolios are to be included in the prediction. The current model lacks consideration for any influence on the mortgage when the LGD equals one, denoting a lack of underlying collateral. However, in these cases, the PD would increase while the LGD remains at one. While this scenario doesn't apply to private residential mortgages due to the inherent collateral involved, it does hold true for other portfolios like loans to the general industry.

To improve the results of this thesis and gain a better understanding of the tail risks associated with climate risks, stress testing of the simulation is required. Currently, the simulation incorporates a limited number of extreme scenarios that could have significant influence on this topic. In particular, extreme floods can have a substantial impact on economic implications for the portfolios, as demonstrated in the simulation with a given flood probability.

To refine the simulation results, an actual portfolio from a bank would be necessary. Access to an actual portfolio would remove current uncertainties in the prediction, such as the height of exposure, current value of the underlying property, exact positioning of the underlying property, and loan stage, for example. Currently, these values are approximated using parameters like the WOZ-value for the value of the underlying property. However, this value is a rough estimation and thus has significant associated uncertainty.

Without access to a highly classified bank's portfolio, the simulation could utilise the BAG register to improve the estimation of the underlying property. Currently, the simulation takes a random sample to generate the surface area of the underlying property. However, a SPARQL query could be used to accurately retrieve the surface area of a house. Subsequently, a cross-reference between the surface area and the cumulative surface area distribution function of the municipality can be made to estimate the cumulative probability of the sample. This probability can then be inserted into the cumulative distribution function of the WOZ-value to generate an accurate value of the underlying property based on point coordinates.

The next recommendation is the inclusion of macroeconomics in the model. As discussed in the literature, the influence of macroeconomic parameters in the case of a flood is substantial. For instance, the residential mortgage portfolio faces the risk that the perception of increased flood risk could adversely impact the value of the underlying properties. The introduction of these indirect losses could significantly increase the acute climate risks associated with climate events, as displayed by Koks et al. in the literature review [52].

The last two recommendations in this regard are the inclusion of additional climate events and a dynamic portfolio. Besides floods, the Netherlands experiences additional climate effects that are not considered in this thesis. These events include additional storms often accompanied by heavy rainfall, as well as wildfires resulting from prolonged drought periods. Currently, modeling wildfires presents a significant challenge, primarily due to their frequent ignition by human activities [104]. However, to accurately predict the damages caused by climate change, these events need to be incorporated into the prediction.

The final recommendation for expanding the simulation is to introduce a dynamic portfolio. Currently, the portfolios in this thesis are static, meaning the VtL and LGD remain the same over time. This is a drastic simplification since customers pay off their debts, the bank takes on new mortgages, and macroeconomic conditions change over time. Therefore, adding a dynamic portfolio where mortgages are paid off prematurely and new mortgages are obtained could enhance the simulation. However, this would be challenging to model and would require historic data on previous mortgage foreclosures, for example.

As a general remark, to overcome some of the aforementioned challenges, a bank could decide to implement the incurred damages from the simulation as input into their respective PD and LGD models. If the prediction is executed with an actual bank's portfolio, the incurred damages can be incorporated into these models, which are already well-refined and validated.

Data

The final recommendation is both a recommendation and a critical observation. The generated simulation heavily relies on input data from the klimaateffectatlas. This data is the result of a collaboration between the government, consultancies, and universities. While these institutions are dependable, there are other data vendors for flood risk assessment, such as HKV consultants, which have developed a Real-Time Flood Risk Assessment tool based on accurate flood charts [105]. Therefore, a proper selection of data vendors would provide valuable insights.

Furthermore, the underlying climate scenario plays a crucial role in the data. The data obtained from the Klimaateffectatlas is derived from climate change scenarios put forth by the KNMI. These scenarios significantly influence the input data, thus warranting further research to identify the specific climate scenarios upon which the data is based. The prediction's dependency on these input parameters is significant, emphasising the need for a thorough assessment of the input data. Moreover, this implies an inherent risk or uncertainty linked to the prediction due to the substantial reliance on these input parameters.

To partially mitigate the limitations imposed by input parameters, it is advisable to conduct the proposed predictions on an annual basis, for instance. Climate change dynamics are influenced by human behaviour, resulting in fluctuations, making the input parameters subject to yearly variations. Consequently, by running predictions using updated data, more accurate forecasts for future years can be attained. Therefore, it is recommended to periodically execute, evaluate, and enhance these prediction methodologies on an annual basis to ensure that predictions remain aligned with the latest information concerning input parameters.

References

[1] BIS. *Basel Committee on Banking Supervision Principles for effective supervisory colleges*. 2022.

[2] S. Gao, F. Meng, Z. Gu, Z. Liu and M. Farrukh. *Mapping and Clustering Analysis on Environmental, Social and Governance Field a Bibliometric Analysis Using Scopus*. 2021. DOI: 10.3390/su13137304.

[3] M. Brei, P. Mohan and E. Strobl. 'The impact of natural disasters on the banking sector: Evidence from hurricane strikes in the Caribbean'.
In: *The Quarterly Review of Economics and Finance* 72 (2019), pp. 232–239. ISSN: 1062-9769. DOI: 10.1016/j.qref.2018.12.004.

[4] R. Calabrese, T. Dombrowski, A. Mandel, R. K. Pace and L. Zanin.
'Impacts of extreme weather events on mortgage risks and their evolution under climate change: A case study on Florida'. In: *SSRN Electron. J.* (September 2021). ISSN: 1556-5068. DOI: 10.2139/ssrn.3929927.

[5] Planbureau voor de Leefomgeving. *Low probabilities - large consequences*.
Accessed: 2022-11-10. URL: https://themasites.pbl.nl/o/flood-risks/.

[6] KNMI. *Zeespiegelstijging*.
https://www.knmi.nl/kennis-en-datacentrum/uitleg/zeespiegelstijging.

[7] M. Grimwade. 'How climate change may impact operational risk'.
In: *Journal of Operational Risk* (2022). DOI: 10.21314/jop.2022.023.

[8] M. Westcott, J. Ward, S. Surminski, P. Sayers, D. N. Bresch and B. Claire.
'Be Prepared: Exploring Future Climate-Related Risk for Residential and Commercial Real Estate Portfolios'. In: *The Journal of Alternative Investments* 23.1 (June 2020), pp. 24–34. DOI: 10.3905/jai.2020.1.100.

[9] ING bank. *ING Bank annual report 2021*. 2022.

[10] De volksbank. *De volksbank annual report 2021*. March 2022.

[11] S. N. Jonkman, M. Kok and J. Vrijling.
'Flood Risk Assessment in the Netherlands: A Case Study for Dike Ring South Holland'.
In: *Risk analysis : an official publication of the Society for Risk Analysis* 28 (September 2008), pp. 1357–1374. DOI: 10.1111/j.1539-6924.2008.01103.x.

[12] Dutch Central Bank. 'Climate risk and the financial sector: sharing of good practices'.
In: *The Sustainable Finance Platform* (2020).
URL: https://www.dnb.nl/media/zvunexjb/climate-risk-and-the-financial-sector-sharing-of-good-practices-_tcm46-389956.pdf.

[13] V. E. Daniel, R. J. G. M. Florax and P. Rietveld.
'Floods and Residential Property Values: A Hedonic Price Analysis for the Netherlands'.
In: *Built Environment* 35.4 (2009), pp. 563–576. DOI: 10.2148/benv.35.4.563.

[14] M. Bosker, H. Garretsen, G. Marlet and C. van Woerkens.
'Nether Lands: Evidence on the Price and Perception of Rare Natural Disasters'.
In: *Journal of the European Economic Association* 17.2 (April 2019), pp. 413–453.
ISSN: 1542-4766. DOI: 10.1093/jeea/jvy002.

[15] A. L. Costa, S. Kok and M. Korff.
'Systematic assessment of damage to buildings due to groundwater lowering-induced subsidence: methodology for large scale application in the Netherlands'. In: *Proceedings of the International Association of Hydrological Sciences* 382 (April 2020), pp. 577–582.
DOI: 10.5194/piahs-382-577-2020.

[16] Genest, Benoit. *7 Proposals to integrate climate risk into capital requirements*. June 2020.
URL: https://www.tcfdhub.org/wp-content/uploads/2020/06/2020-05-Climate-Risk-CH-Convictions.pdf.

[17] R. Boffo and R. Patalano. *ESG Investing: Practices, Progress and Challenges*. Tech. rep.
OECD Paris, 2020, p. 88.
URL: https://www.oecd.org/finance/ESG-Investing-Practices-Progress-Challenges.pdf.

[18] W. Henisz, T. Koller and R. Nuttall. 'Five ways that ESG creates value'.
In: *McKinsey Quarterly* November (2019), pp. 1–12.
URL: https://www.mckinsey.com/$%5Csim$/media/McKinsey/Business%20Functions/Strategy%20and%20Corporate%20Finance/Our%20Insights/Five%20ways%20that%20ESG%20creates%20value/Five-ways-that-ESG-creates-value.ashx.

[19] European Banking Authority. *Final draft implementing technical standards on prudential disclosures on ESG risks in accordance with Article 449a CRR*. Tech. rep. 2022, p. 124.
URL: https://www.eba.europa.eu/sites/default/documents/files/document_library/Publications/Draft%20Technical%20Standards/2022/1026171/EBA%20draft%20ITS%20on%20Pillar%203%20disclosures%20on%20ESG%20risks.pdf.

[20] *Annex I - Templates for ESG prudential disclosures*. European Banking Authority.
URL: https://www.eba.europa.eu/implementing-technical-standards-its-prudential-disclosures-esg-risks-accordance-article-449a-crr.

[21] *NGFS Scenarios for central banks and supervisors*. Tech. rep.
Network for Greening the Financial System, 2022, pp. 1–48.

[22] *A Call for Action: Climate Change as a Source of Financial Risk*. Tech. rep.
Network for Greening the Financial System, 2019, pp. 1–40.
URL: https://www.ngfs.net/en/first-comprehensive-report-call-action.

[23] Klimaateffectatlas. 2021. URL: https://www.klimaateffectatlas.nl/nl/.

[24] Royal Netherlands Meteorological Institute. *KNMI'14-klimaatscenario's*. Tech. rep.
Ministerie van infrastructuur en waterstaat, 2021. URL:
https://www.knmi.nl/kennis-en-datacentrum/achtergrond/knmi-14-klimaatscenario-s.

[25] S. Kok and L. Angelova. *Impact droogte op funderingen*. Tech. rep. Deltares, 2020.
URL: https://www.verzekeraars.nl/media/7875/20200930-rapport-impact-droogte-op-funderingen.pdf.

[26] E. Schreurs. 'Deterioration of Timber Pile Foundations in Rotterdam'.
PhD thesis. Delft University of Technology, 2017, p. 172.

[27] Rabobank. *Annual Report 2018*.
https://media.rabobank.com/m/77a1773024ad55cb/original/annual-report-2018-pdf.pdf.
March 2019.

[28] J. Lamond, D. Proverbs and A. Antwi. 'The impact of flood insurance on residential property prices: Towards a new theoretical framework for the United Kingdom market'. In: *Journal of Financial Management of Property and Construction* 12.3 (December 2007), pp. 129–138. DOI: 10.1108/13664380780001099.

[29] D. G. Hallstrom and V. K. Smith. 'Market responses to hurricanes'. In: *Journal of Environmental Economics and Management* 50.3 (2005), pp. 541–561. ISSN: 0095-0696. DOI: 10.1016/j.jeem.2005.05.002.

[30] J. Triplett. 'Handbook on Hedonic Indexes and Quality Adjustments in Price Indexes'. In: *OECD Directorate for Science, Technology and Industry* (September 2004). DOI: 10.1787/643587187107.

[31] N. H. Ismail, M. Z. A. Karim and B. H. Basri. 'Flood and Land Property Values'. In: *Asian Social Science* 12.5 (April 2016), p. 84. DOI: 10.5539/ass.v12n5p84.

[32] F. Fuerst and G. Warren-Myers. 'Sea Level Rise and House Price Capitalisation'. In: (2019). DOI: 10.13140/RG.2.2.29209.67687.

[33] J. C. Pope. 'Do Seller Disclosures Affect Property Values? Buyer Information and the Hedonic Model'. In: *Land Economics* 84.4 (September 2008), pp. 551–572. DOI: 10.3368/le.84.4.551.

[34] O. Bin, J. B. Kruse and C. E. Landry. 'Flood Hazards, Insurance Rates, and Amenities: Evidence From the Coastal Housing Market'. In: *Journal of Risk & Insurance* 75.1 (March 2008), pp. 63–82. DOI: 10.1111/j.1539-6975.2007.00248.x.

[35] A. Owusu-Ansah. 'A review of hedonic pricing models in housing research'. In: *A Compendium of International Real Estate and Construction Issues* 1 (February 2013), pp. 17–38. URL: https://www.researchgate.net/publication/287232776_A_review_of_hedonic_pricing_models_in_housing_research.

[36] W. Kirby. 'On the Random Occurrence of Major Floods'. In: *Water Resources Research* 5.4 (August 1969), pp. 778–784. DOI: 10.1029/wr005i004p00778.

[37] F. Hossain, E. N. Anagnostou and A. C. Bagtzoglou. 'On Latin Hypercube sampling for efficient uncertainty estimation of satellite rainfall observations in flood prediction'. In: *Computers & Geosciences* 32.6 (July 2006), pp. 776–792. DOI: 10.1016/j.cageo.2005.10.006.

[38] D. P. Callaghan and M. G. Hughes. 'Assessing flood hazard changes using climate model forcing'. In: *Natural Hazards and Earth System Sciences* 22.8 (August 2022), pp. 2459–2472. DOI: 10.5194/nhess-22-2459-2022.

[39] J. Vrijling. 'Probabilistic design of water defense systems in The Netherlands'. In: *Reliability Engineering & System Safety* 74.3 (December 2001), pp. 337–344. DOI: 10.1016/s0951-8320(01)00082-5.

[40] D. Dutta, S. Herath and K. Musiake. 'A mathematical model for flood loss estimation'. In: *Journal of Hydrology* 277.1-2 (June 2003), pp. 24–49. DOI: 10.1016/s0022-1694(03)00084-2.

[41] S. Fuchs, M. Heiser, M. Schlögl, A. P. Zischg, M. Papathoma-Köhle and M. Keiler. 'Short communication: A model to predict flood loss in mountain areas'. In: *Environmental Modelling & Software* 117 (March 2019). DOI: 10.1016/j.envsoft.2019.03.026.

[42] J. Huizinga. *Flood damage functions for EU member states*. Tech. rep. Lelystad: HKV Consultants, 2007.

[43] F. Carisi, K. Schröter, A. Domeneghetti, H. Kreibich and A. Castellarin. 'Development and assessment of uni- and multivariable flood loss models for Emilia-Romagna (Italy)'. In: *Natural Hazards and Earth System Sciences* 18.7 (July 2018), pp. 2057–2079. DOI: 10.5194/nhess-18-2057-2018.

[44] M. Amadio, A. R. Scorzini, F. Carisi, A. H. Essenfelder, A. Domeneghetti, J. Mysiak and A. Castellarin. 'Testing empirical and synthetic flood damage models: the case of Italy'. In: *Natural Hazards and Earth System Sciences* 19.3 (2019), pp. 661–678. DOI: 10.5194/nhess-19-661-2019.

[45] M. Kok, H. Huizinga, A. Vrouwenvelder and W. van den Baak. *Standaardmethode2005 Schade en Slachtoffers als gevolg van overstromingen*. Tech. rep. HKV Lijn in Water en TNO Bouw, 2005.

[46] K. Slager and D. Wagenaar. *Standaardmethode 2017 Schade en slachtoffers als gevolg van overstromingen*. Tech. rep. 11200580-004. Deltares, 2017.

[47] F. Dottori, R. Figueiredo, M. L. V. Martina, D. Molinari and A. R. Scorzini. 'INSYDE: a synthetic, probabilistic flood damage model based on explicit cost analysis'. In: *Natural Hazards and Earth System Sciences* 16.12 (2016), pp. 2577–2591. DOI: 10.5194/nhess-16-2577-2016.

[48] D. Molinari and A. Scorzini. 'On the Influence of Input Data Quality to Flood Damage Estimation: The Performance of the INSYDE Model'. In: *Water* 9 (September 2017), p. 688. DOI: 10.3390/w9090688.

[49] C. Arrighi, F. Ballio, F. Carisi, F. Castelli, A. Domeneghetti, A. Gallazzi, M. Galliani, F. Grelot, P. Kellermann, H. Kreibich, D. Molinari, G. Samprogna Mohor, M. Mosimann, S. Natho, C. Richert, K. Schröter, A. Scorzini, A. Thieken and A. P. Zischg. 'A comparative analysis of flood damage models: lessons learnt and future challenges'. In: March 2021. DOI: 10.3311/FLOODRisk2020.9.15.

[50] NatWestGroup. *Assessment of flood risk to a sample of UK residential mortgages*. Tech. rep. UNEP FI, September 2020. URL: https://www.unepfi.org/wordpress/wp-content/uploads/2020/09/Charting-a-New-Climate-UNEP-FI-TCFD-Banking-Physical-Risk.pdf.

[51] O. Hoes, M. Tariq and N. V. de Giesen. 'Online estimation of flood damage in The Netherlands'. In: (2014), pp. 553–558. URL: http://repository.tudelft.nl/view/ir/uuid:9ba7618d-ef72-4f78-9e61-c797a65d3051/.

[52] E. E. Koks, M. Bočkarjova, H. de Moel and J. C. J. H. Aerts. 'Integrated Direct and Indirect Flood Risk Modeling: Development and Sensitivity Analysis'. In: *Risk Analysis* 35.5 (May 2015), pp. 882–900. ISSN: 02724332. DOI: 10.1111/risa.12300.

[53] C. Kousky, M. Palim and Y. Pan.
'Flood Damage and Mortgage Credit Risk: A Case Study of Hurricane Harvey'.
In: *Journal of Housing Research* 29.sup1 (November 2020), pp. 86–120.
DOI: 10.1080/10527001.2020.1840131.

[54] S. Dietz, A. Bowen, C. Dixon and P. Gradwell.
''Climate value at risk' of global financial assets'.
In: *Nature Climate Change* 6.7 (April 2016), pp. 676–679. DOI: 10.1038/nclimate2972.

[55] T. Bikakis. 'Climate Change, Flood Risk and Mortgages in the UK: a Scenario Analysis'.
In: *The New School Economic Review* 10.1 (April 2020).
URL: https://nsereview.org/index.php/NSER/article/view/45.

[56] P. Sayers, M. Horritt, E. Penning-Rowsell and A. McKenzie.
Climate Change Risk Assessment 2017: Projections of future flood risk in the UK. Tech. rep.
London, October 2015.
URL: https://www.theccc.org.uk/wp-content/uploads/2015/10/CCRA-Future-Flooding-Main-Report-Final-06Oct2015.pdf.pdf.

[57] P. Hudson, W. J. W. Botzen, J. Poussin and J. C. J. H. Aerts.
'Impacts of Flooding and Flood Preparedness on Subjective Well-Being: A Monetisation of the Tangible and Intangible Impacts'.
In: *Journal of Happiness Studies* 20.2 (2019), pp. 665–682. ISSN: 1573-7780.
DOI: 10.1007/s10902-017-9916-4.

[58] A. A. Aliyu, A. I. Garkuwa, I. M. Singhry, M. S. Muhammad and H. M. Baba. 'Impact of Flooding on residential property values: A review and analysis of previous studies'.
In: *Proceedings of the Academic Conference of Nightingale Publications & Research International on Sustainable Development* 2 (2016), pp. 1–13.

[59] M. Abcouwer, L. Erasmus and S. Phlippen.
Economic impact assessment of future flooding in the Netherlands. Tech. rep. ABN Amro, 2020, p. 17. URL: https://assets.ctfassets.net/1u811bvgvthc/2esFD3ceYP32geq2fLtsbz/b9ffbd9e30d6fbaddc7589ee7a4fa3b7/201207-Economic-impact-assessment-of-future-flooding-in-the-Netherlands-1.pdf.

[60] J. Wong, L. Fung, T. Fong and A. Sze.
'Residential mortgage default risk and the loan-to-value ratio'.
In: *Hong Kong Monetary Authority Quarterly Bulletin* December (2004), pp. 35–45.
URL: https://www.hkma.gov.hk/media/eng/publication-and-research/quarterly-bulletin/qb200412/fa3.pdf.

[61] O. Weber, M. Fenchel and R. W. Scholz. 'Empirical analysis of the integration of environmental risks into the credit risk management process of European banks'.
In: *Business Strategy and the Environment* 17.3 (2008), pp. 149–159. DOI: 10.1002/bse.507.

[62] M. Berman. 'Flood Risk and Structural Adaptation of Markets: An Outline for Action'.
In: *Federal Reserve Bank of San Francisco* (October 2019).
URL: https://www.frbsf.org/community-development/publications/community-development-investment-review/2019/october/flood-risk-and-structural-adaptation-of-markets-an-outline-for-action/.

[63] P. Monnin. 'Integrating Climate Risks into Credit Risk Assessment - Current Methodologies and the Case of Central Banks Corporate Bond Purchases'. In: *SSRN Electronic Journal* (2018). DOI: 10.2139/ssrn.3350918.

[64] E. L. Levin and H. Murakami. 'Impact of Anthropogenic Climate Change on United States Major Hurricane Landfall Frequency'. In: *Journal of Marine Science and Engineering* 7.5 (May 2019), p. 135. DOI: 10.3390/jmse7050135.

[65] C. Wang, Q. Li, H. Zhang and B. Ellingwood. 'Modeling the Temporal Correlation in Hurricane Frequency for Damage Assessment of Residential Structures Subjected to Climate Change'. In: *Journal of Structural Engineering* 143 (May 2017). DOI: 10.1061/(ASCE)ST.1943-541X.0001710.

[66] C. Rossi. 'Assessing the impact of hurricane frequency and intensity on mortgage delinquency'. In: *Journal of Risk Management in Financial Institutions* 14.4 (September 2021), pp. 426–442. URL: https://www.ingentaconnect.com/content/hsp/jrmfi/2021/00000014/00000004/art00009#trendmd-suggestions.

[67] P. Issler, R. H. Stanton, C. Vergara-Alert and N. E. Wallace. 'Mortgage Markets with Climate-Change Risk: Evidence from Wildfires in California'. In: *SSRN Electronic Journal* (2019). DOI: 10.2139/ssrn.3511843.

[68] A. Ouazad and M. E. Kahn. 'Mortgage Finance and Climate Change: Securitization Dynamics in the Aftermath of Natural Disasters'. In: *The Review of Financial Studies* 35.8 (November 2021). Ed. by S. V. Nieuwerburgh, pp. 3617–3665. DOI: 10.1093/rfs/hhab124.

[69] P. D. Bates, N. Quinn, C. Sampson, A. Smith, O. Wing, J. Sosa, J. Savage, G. Olcese, J. Neal, G. Schumann, L. Giustarini, G. Coxon, J. R. Porter, M. F. Amodeo, Z. Chu, S. Lewis-Gruss, N. B. Freeman, T. Houser, M. Delgado, A. Hamidi, I. Bolliger, K. McCusker, K. Emanuel, C. M. Ferreira, A. Khalid, I. D. Haigh, A. Couasnon, R. Kopp, S. Hsiang and W. F. Krajewski. 'Combined Modeling of US Fluvial, Pluvial, and Coastal Flood Hazard Under Current and Future Climates'. In: *Water Resources Research* 57.2 (February 2021). DOI: 10.1029/2020wr028673.

[70] T. P. Ryan. *Sample Size Determination and Power*. 1st ed. Wiley, 2013. ISBN: 978-1118437605.

[71] Y. Kim. 'Modeling of commercial real estate credit risks'. In: *Quantitative Finance* 13.12 (December 2013), pp. 1977–1989. ISSN: 1469-7688. DOI: 10.1080/14697688.2011.592854.

[72] CBS. *Gemiddelde WOZ-waarde van woningen in 2022 8,6 procent hoger*. https://www.cbs.nl/nl-nl/nieuws/2022/35/gemiddelde-woz-waarde-van-woningen-in-2022-8-6-procent-hoger. January 2022.

[73] CBS. *Kaart van 100 meter bij 100 meter met statistieken*. https://www.cbs.nl/nl-nl/dossier/nederland-regionaal/geografische-data/kaart-van-100-meter-bij-100-meter-met-statistieken. 2021.

[74] CBS. *Wijk- en buurtkaart 2021*. https://www.cbs.nl/nl-nl/dossier/nederland-regionaal/geografische-data/wijk-en-buurtkaart-2021. 2021.

[75] CBS. *Voorraad woningen; gemiddeld oppervlak; woningtype, bouwjaarklasse, regio*. https://opendata.cbs.nl/statline/#/CBS/nl/dataset/82550NED/table?fromstatweb. October 2022.

[76] S. Kok. *Technische toelichting risicokaarten funderingen*. Tech. rep. Deltares, 2021, p. 27.

[77] CBS. *Gemiddelde WOZ-waarde van woningen op 1 januari; eigendom, regio*. https://opendata.cbs.nl/statline/#/CBS/nl/dataset/85036NED/table?ts=1675865308204. November 2022.

[78] Allecijfers. *Ranglijst van de hoogste en laagste gemiddelde woningwaarde van de gemeenten in Nederland*. https://allecijfers.nl/ranglijst/hoogste-en-laagste-woningwaarde-per-gemeente-in-nederland/. 2023.

[79] BIS. *CRE36 - IRB approach: minimum requirements to use IRB approach*. https://www.bis.org/basel_framework/chapter/CRE/36.htm?inforce=20230101&published=20221208#paragraph_CRE_36_20230101_36_83. December 2022.

[80] M. Leow and C. Mues. 'Predicting loss given default (LGD) for residential mortgage loans: A two-stage model and empirical evidence for UK bank data'. In: *International Journal of Forecasting* 28.1 (January 2012), pp. 183–195. ISSN: 01692070. DOI: 10.1016/j.ijforecast.2011.01.010.

[81] L. Ji, K. S. Tan and F. Yang. 'Tail dependence and heavy tailedness in extreme risks'. In: *Insurance: Mathematics and Economics* 99 (2021), pp. 282–293. ISSN: 0167-6687. DOI: https://doi.org/10.1016/j.insmatheco.2021.03.016.

[82] V. V. Acharya, L. H. Pedersen, T. Philippon and M. Richardson. 'Measuring Systemic Risk'. In: *The Review of Financial Studies* 30.1 (October 2016), pp. 2–47. ISSN: 0893-9454. DOI: 10.1093/rfs/hhw088.

[83] J. Frost. *Gamma Distribution: Uses, Parameters & Examples*. https://statisticsbyjim.com/probability/gamma-distribution/. August 2021.

[84] L. M. Leemis and J. T. McQueston. 'Univariate Distribution Relationships'. In: *The American Statistician* 62.1 (February 2008), pp. 45–53. DOI: 10.1198/000313008x270448.

[85] S. Yue. 'A bivariate gamma distribution for use in multivariate flood frequency analysis'. In: *Hydrological Processes* 15.6 (2001), pp. 1033–1045. DOI: 10.1002/hyp.259.

[86] C. Ilinca and C. G. Anghel. 'Flood Frequency Analysis Using the Gamma Family Probability Distributions'. In: *Water* 15.7 (April 2023), p. 1389. DOI: 10.3390/w15071389.

[87] B. McNeese. *Are the skewness and kurtosis useful statistics?* https://www.spcforexcel.com/knowledge/basic-statistics/are-skewness-and-kurtosis-useful-statistics. February 2016.

[88] V. van verzekeraars. *Overstroming en droogte: schade en verzekeringen*. https://www.verzekeraars.nl/verzekeringsthemas/klimaatbestendig-nederland/overstroming-en-droogte. July 2023.

[89] J. De Jong and N. Asselman. *Analyse overstromingen Geulmonding*. Tech. rep. 11207700-000-ZWS-0013. Deltares, April 2022. URL: https://www.waterschaplimburg.nl/publish/pages/7013/analyse_overstromingen_geulmonding.pdf.

[90] T. Ermolieva, T. Filatova, Y. Ermoliev, M. Obersteiner, K. M. de Bruijn and A. Jeuken. 'Flood Catastrophe Model for Designing Optimal Flood Insurance Program: Estimating Location-Specific Premiums in the Netherlands'. In: *Risk Analysis* 37.1 (March 2016), pp. 82–98. DOI: 10.1111/risa.12589.

[91] CBS. *Huishoudens nu*. https://www.cbs.nl/nl-nl/visualisaties/dashboard-bevolking/woonsituatie/huishoudens-nu. 2023.

[92] CBS. *Regionale kerncijfers Nederland*. https://opendata.cbs.nl/statline/#/CBS/nl/dataset/70072ned/table?dl=6B145. December 2022.

[93] W. B. M. ten Brinke, B. A. Bannink and W. Ligtvoet. 'The evaluation of flood risk policy in the Netherlands'. In: *Proceedings of the Institution of Civil Engineers - Water Management* 161.4 (August 2008), pp. 181–188. DOI: 10.1680/wama.2008.161.4.181.

[94] K.-B. de Haan. *De groei van Amsterdam vanaf 1850*. https://maps.amsterdam.nl/bouwjaar/?C=52.354838,4.914920&Z=11.75&T=1&L=5,6,7,8,9,10,11,12&K=52.3756027,4.7302972. February 2023.

[95] N. Rainone, N. Brumma and R. Crecel. *ObservedRecoveryRatesDashboardCorporates*. Tech. rep. Blobal Credit Data, May 2022. URL: https://www.globalcreditdata.org/wp-content/uploads/2022/05/GCD-Corporates-RR-Dashboard-2022.pdf?_gl=1*q3a40y*_ga*MTM2ODY2NTQ1MC4xNjc3NTE0NzQx*_ga_Q8THTBL8L4*MTY3NzUxNDc0MS4xLjAuMTY3NzUxNDc0MS4wLjAuMA..&_ga=2.242180161.2144940475.1677514742-1368665450.1677514741.

[96] K. Emery, R. Cantor, D. Keisman and S. Ou. 'Moody's Ultimate Recovery Database Summary'. In: *Moody's* (April 2007). URL: https://www.moodys.com/sites/products/defaultresearch/2006600000428092.pdf.

[97] E. Hilten van and C. Saskia. *Overstromingsrisico Nederlandse Hypotheekbeleggingen*. Tech. rep. DMFCO, 2022. URL: https://dmfco.nl/site-dmfco/storage/files/1516/whitepaper_dmfco_-_overstromingsrisico_nederlandse_hypotheekbeleggingen.pdf.

[98] BIS. *CRE35 - IRB approach: treatment of expected losses and provisions*. https://www.bis.org/basel_framework/chapter/CRE/35.htm. March 2020.

[99] IASB. *International Financial Reporting Standard 9*. Tech. rep. December 2021. URL: https://www.ifrs.org/content/dam/ifrs/publications/pdf-standards/english/2022/issued/part-a/ifrs-9-financial-instruments.pdf?bypass=on.

[100] BIS. *CRE20 - Standardised approach: individual exposures*. https://www.bis.org/basel_framework/chapter/CRE/20.htm. December 2022.

[101] BIS. *Frequently asked questions on climate-related financial risks*. December 2022. URL: https://www.bis.org/bcbs/publ/d543.pdf.

[102] L. Williams. *Basel Climate Principles Will Raise Reputational Risk for Banks*. June 2022. URL: https://www.fitchratings.com/research/banks/basel-climate-principles-will-raise-reputational-risk-for-banks-30-06-2022#:~:text=The%5C%20Basel%5C%20principles%5C%20stipulate%5C%20the,climate%5C%2Drelated%5C%20credit%5C%20risk%5C%20profiles..

[103] BIS. *Principles for the effective management and supervision of climate-related financial risks*. June 2022. URL: https://www.bis.org/bcbs/publ/d532.pdf.

[104] J. B. Barreiro and T. Hermosilla. 'Socio-geographic analysis of the causes of the 2006's wildfires in Galicia (Spain)'. In: *Forest Systems* 22.3 (November 2013), p. 497. DOI: 10.5424/fs/2013223-04165.

[105] M. Hartman. *Real time flood risk assessment*. https://www.hkv.nl/en/news/real-time-flood-risk-assessment/. December 2020.

[106] N. Najibi and N. Devineni. 'Recent trends in the frequency and duration of global floods'. In: *Earth Syst. Dyn.* 9.2 (2018), pp. 757–783. ISSN: 2190-4979. DOI: 10.5194/esd-9-757-2018.

[107] *Klimaatschadeschatter Rapportage 2020*. Tech. rep. NKWK, 2020, p. 65. URL: https://www.klimaateffectatlas.nl/l/nl/library/download/urn:uuid:adc26919-0bb3-433e-9690-952c01280b14/klimaatschadeschatter+rapportage+2020+versie+7+december.pdf?format=save_to_disk&ext=.pdf.

[108] H. Kreibich, P. K, I. Seifert-Dähnn, H. Maiwald, U. Kunert, S. J, M. B and A. Thieken. 'Is flow velocity a significant parameter in flood damage modelling?' In: *Natural Hazards and Earth System Sciences* 9 (October 2009). DOI: 10.5194/nhess-9-1679-2009.

[109] K. De Bruijn, D. Wagenaar, K. Slager, M. De Bel and A. Burzel. *The updated and improved method for flood damage assessment SSM2015: explanation, motivation and comparison to HIS-SSM (SSM2015)*. Tech. rep. Delft: Deltares, 2015.

Appendix A Template for ESG prudential disclosures

Variable: Geographical area subject to climate change physical risk - acute and chronic events		Gross carrying amount (Mln EUR)												
		of which exposures sensitive to impact from climate change physical events												
		Breakdown by maturity bucket					of which exposures sensitive to impact from chronic climate change events	of which exposures sensitive to impact from acute climate change events	of which exposures sensitive to impact both from chronic and acute climate change events	Of which Stage 2 exposures	Of which non-performing exposures	Accumulated impairment, accumulated negative changes in fair value due to credit risk and provisions		
		<= 5 years	> 5 year <= 10 years	> 10 year <= 20 years	> 20 years	Average weighted maturity							of which Stage 2 exposures	Of which non-performing exposures
A - Agriculture, forestry and fishing														
B - Mining and quarrying														
C - Manufacturing														
D - Electricity, gas, steam and air conditioning supply														
E - Water supply; sewerage, waste management and remediation activities														
F - Construction														
G - Wholesale and retail trade; repair of motor vehicles and motorcycles														
H - Transportation and storage														
L - Real estate activities														
Loans collateralised by residential immovable property														
Loans collateralised by commercial immovable property														
Repossessed colalterals														
Other relevant sectors (breakdown below where relevant)														

Figure A.1: *Template 5: Banking book - Climate change physical risk: Exposures subject to physical risk. [20]*

Appendix B Probability and inundation depth charts employed during the simulation

The different probability charts employed during the simulation are displayed in the figures below.

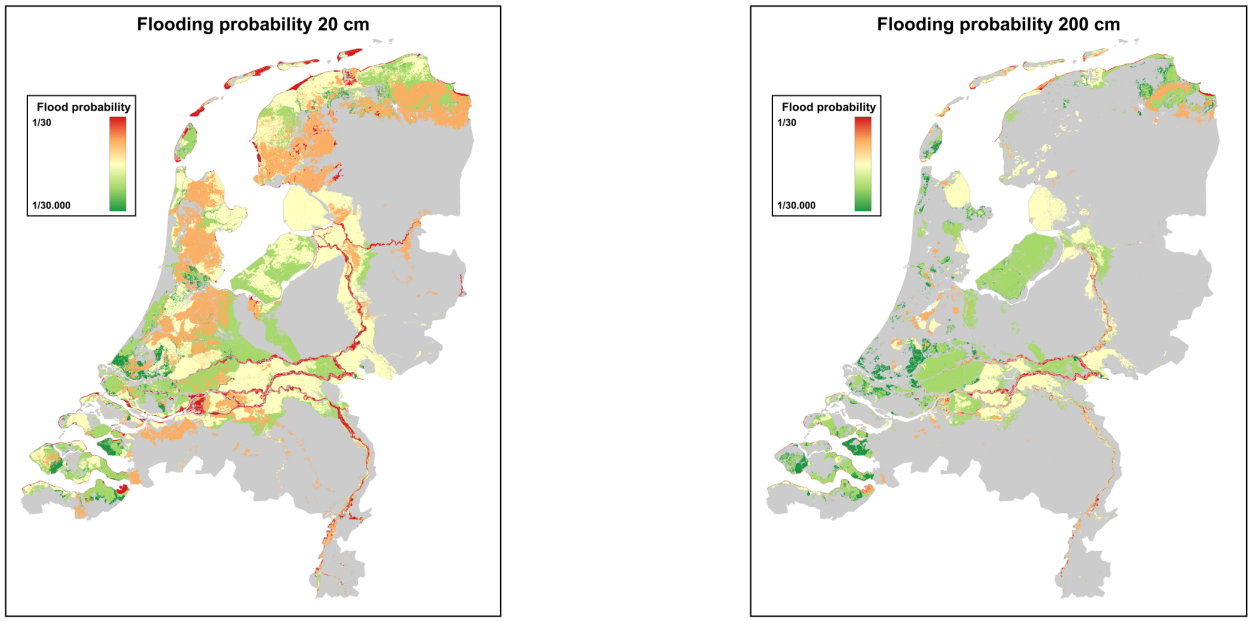

(a) *(b)*

Figure B.1: ***(a)*** *The probability of a flood occurring with an inundation depth of 0,2 m [23]. ,* ***(b)*** *The probability of a flood occurring with an inundation depth of 2 m [23].*

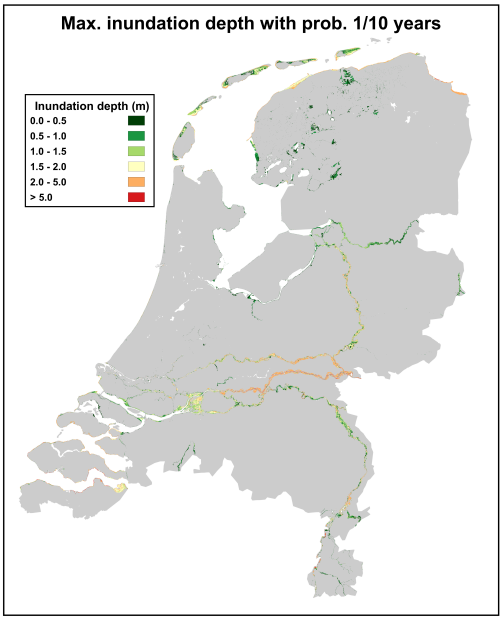

(a)

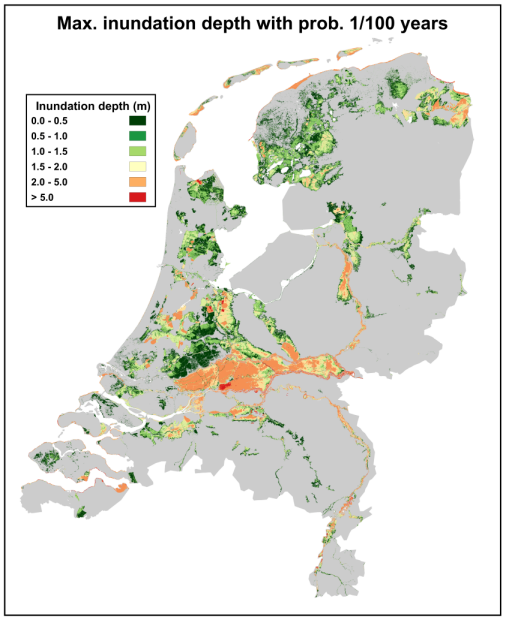

(b)

Figure B.2: ***(a)*** *The maximum inundation depth which could be achieved given the probability of flooding equals 1/10 years [23]. ,* ***(b)*** *The maximum inundation depth which could be achieved given the probability of flooding equals 1/100 years [23].*

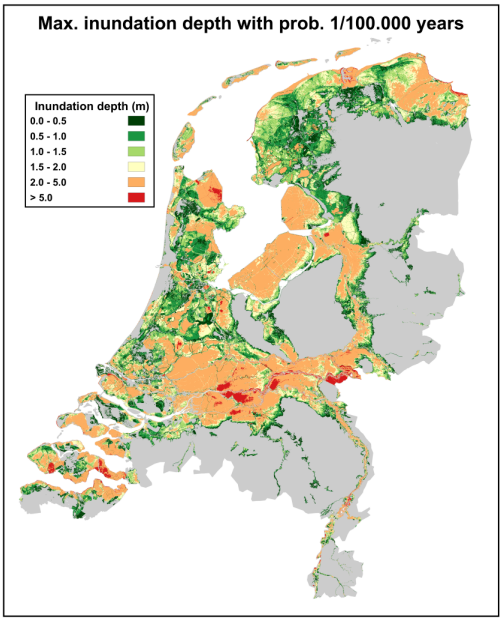

Figure B.3: *The maximum inundation depth which could be achieved given the probability of flooding equals 1/100.000 years [23].*

Appendix C Extended Literature review

As mentioned in the main text, an interesting contrast between the style of modeling employed by koks et al. and the previously discussed methods involves the calculation of indirect damage in the model. Specifically, the economic shock and recovery period play a crucial role in these types of models, as floods can halt production for extended periods. Therefore, the recovery period becomes important when modeling industrial flood damages. Koks et al. developed a simulation that encompasses both the initial damage to physical assets and the indirect losses resulting from missed production. To reinforce the modeling methodology, a schematic overview of this simulation is once again presented in Figure C.1.

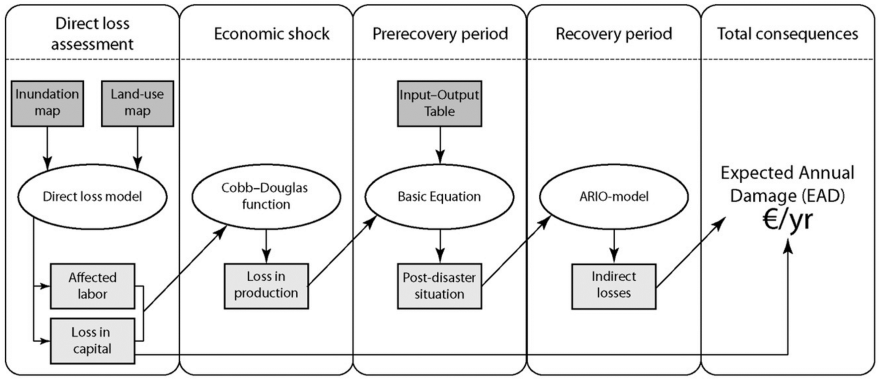

Figure C.1: *Overview of the different components of the framework. The dark grey squared boxes are the inputs, the ellipses are the different models, and the light grey squared boxes are the model outputs [52].*

In the first step, the direct model discussed in the main portion of this thesis is utilised to estimate the damages caused by the flood. In addition to direct damages, this model also provides outputs for the loss in capital and the affected quantity of labor. These outputs are then utilised as inputs for the Cobb-Douglas production function, which calculates the loss of production. The model is calibrated with industry-specific elasticities (α and β) to estimate the production losses based on the losses in capital and labor.

Subsequently, this loss in production, along with an input-output table, is used in basic equations to estimate the pre-recovery damages. The pre-recovery period encompasses the time it takes for the floodwaters to recede. Recent floods in Europe have demonstrated that it can take a considerable amount of time for the flood to subside, hindering or even disrupting daily activities in factories [106]. Therefore, these basic equations include the necessary post-catastrophe information regarding disproportions, which refer to a distorted predisaster economic connection and the inability of total output to directly meet the final demand. These disproportions depict the so-called post-disaster situation.

Finally, this situation is input into an input-output (I-O) model, where the recovery phase takes place. The recovery phase is a period of time during which the factory gradually restarts production but still lacks some of the original capital or labor. As a result, production slowly increases until it reaches the pre-flood level. The I-O model considers the regional economy, consisting of households and various industries that exchange, import, produce, and export goods. Additionally, it takes into account the interactions between sectors through the demand and supply of consumption goods. Consequently, the simulation provides estimates for both indirect and direct losses, which can be associated with the expected annual amount of damage incurred due to a flood [52].

As previously stated in the main text, this thesis does not incorporate the indirect results discussed in this paper, as the impact of indirect flood damage on the residential mortgage portfolio is relatively minor compared to, for instance, an industrial building. Nonetheless, the paper offers valuable insights into the modeling methodologies currently being developed by researchers and helps identify existing research gaps.

Appendix D Damage categories foundation risks

An important factor incorporated in the prediction and the probability charts is the damage factor. This factor estimates the damage a structure will incur if foundation damages occur. The factor is split into six categories ranging from 0 to 5. The different categories and their accompanying damage estimations are displayed in Table D.1.

Table D.1: *Overview of the damage classes with their accompanying required repairs and associated costs [107].*

Damage class	Required repairs	Min repair cost (€)	Max repair cost (€)
0	No repairs	-	-
1	Painting	500	2.000
2	Painting, outer wall cracks	500	5.000
3	Painting, outer wall cracks, plastering	2.000	10.000
4	Painting, outer wall cracks, plastering, new floors, window-frames repairs	10.000	60.000
5	Painting, outer wall cracks, plastering, new floors, window-frames repairs, foundation repairs	30.000	120.000

The figures provided in Table D.1 are based on the average floor space of a house in the Netherlands. These figures are used to estimate the risks associated with each neighborhood within the Netherlands and to approximate the damage the house has incurred within the simulated time span.

The expected damage category a house is predicted to fall into by 2050, as provided by the Klimaateffectatlas, is estimated based on several parameters. The damage factor for houses constructed on wooden poles is determined by the following criteria. Firstly, the local average lowest groundwater level charts estimate the decrease in the groundwater level in the upcoming 30 years. As the average groundwater level decreases, the piles become more exposed to oxygen, accelerating their deterioration. Secondly, the average depth of the pile heads below ground level is considered. Similarly, the deeper the piles are drilled into the surface, the less the poles will be exposed to oxygen, reducing the speed of deterioration. Lastly, the soil type is used to approximate the damage factor. Different soil types can counteract or enhance the pile rot mechanism. For example, clay grounds tend to prevent oxygen from penetrating the soil, whereas sandy soils do not possess this characteristic. The soil type within each neighborhood is determined from the GeoTOP model provided by the national registration of subsoil.

Similarly, the settlement damage factor is based on three factors. Firstly, settlement velocity maps are used to estimate the damage factor. The reasoning behind this is that a higher settlement velocity increases the opportunity for the house to develop foundation failures. Secondly, different house characteristics are considered along with correction factors. For example, a correction factor for the quality of the foundation is applied based on the average construction year within the neighborhood. Therefore, a neighbourhood with older houses receive a higher correction factor compared to a neighbourhood with newer houses. Lastly, the soil type is taken into consideration again. For example, the swelling and shrinking of clay soils increase the probability of settlement. In addition, the preceding loading of the soil is taken into account in determining the damage factor [76].

Appendix E Simulation flowcharts

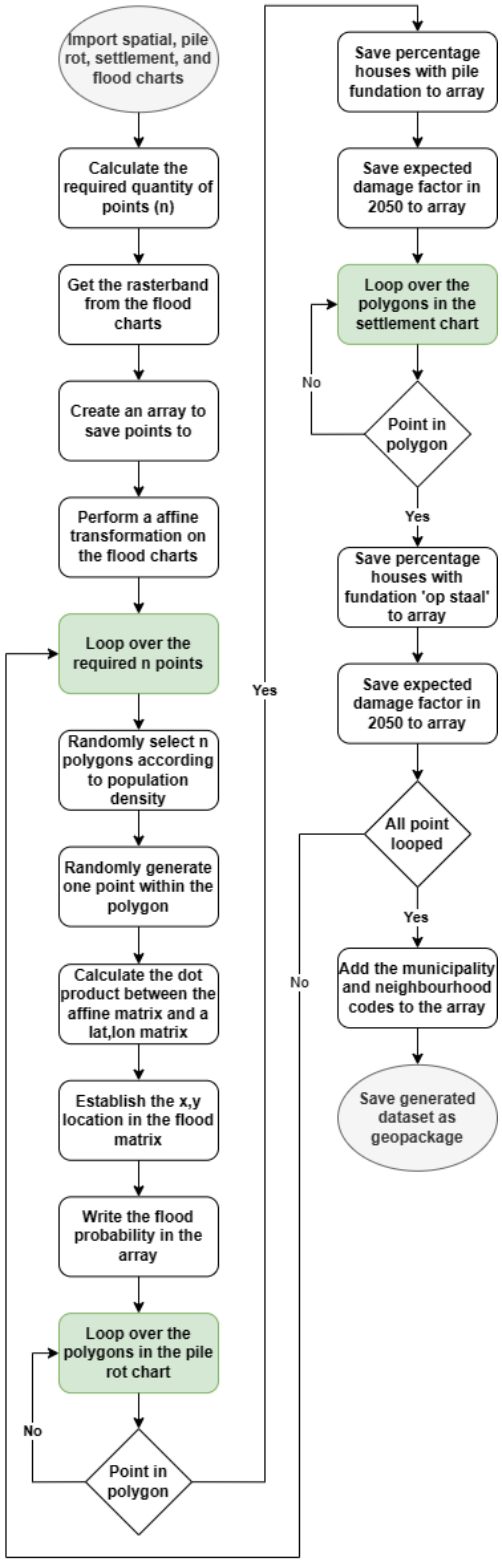

Figure E.1: *Simulation flowchart to prepare the residential mortgage portfolio.*

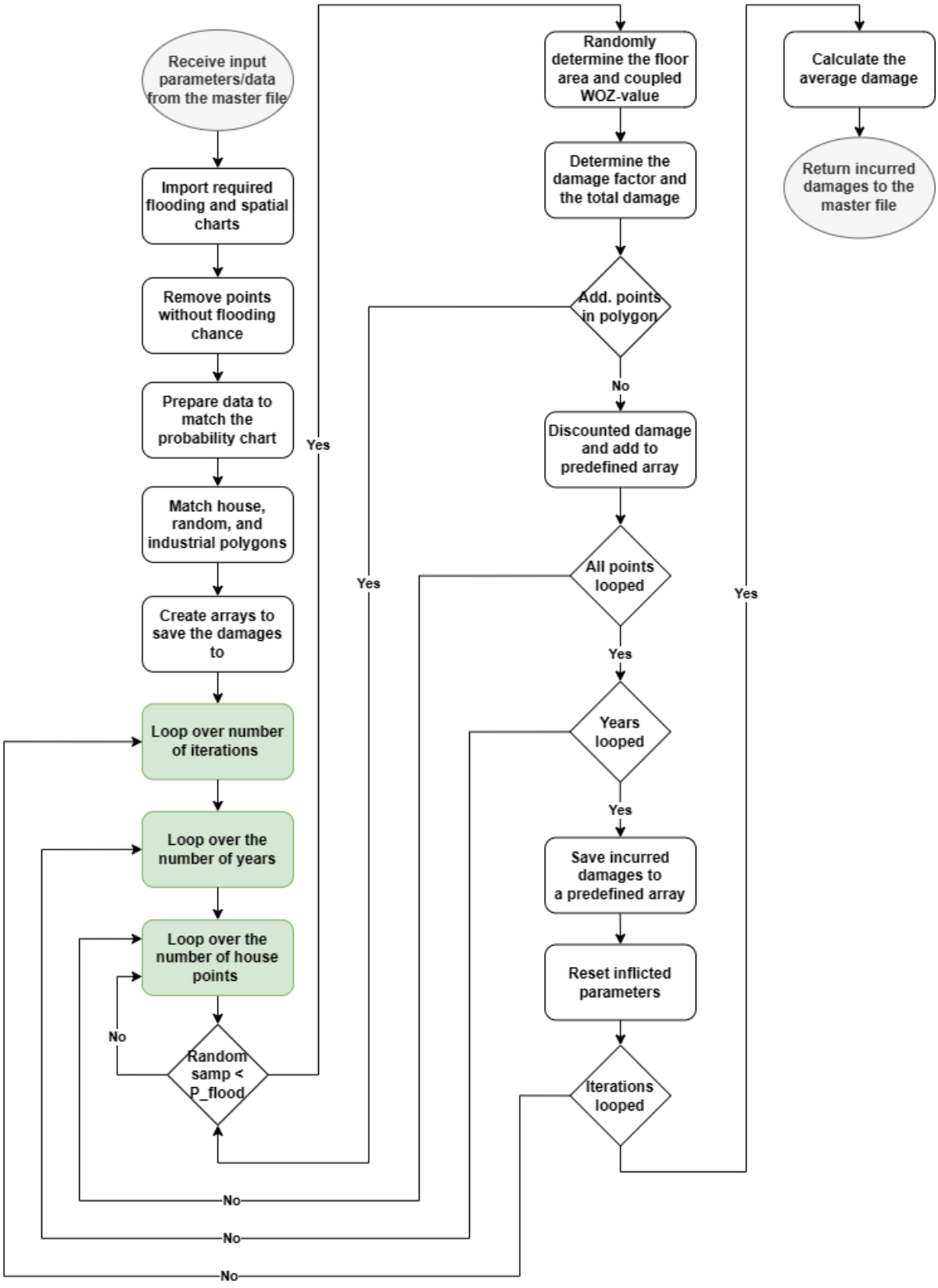

Figure E.2: *Simulation flowchart to estimate flood damages given the inundation depth.*

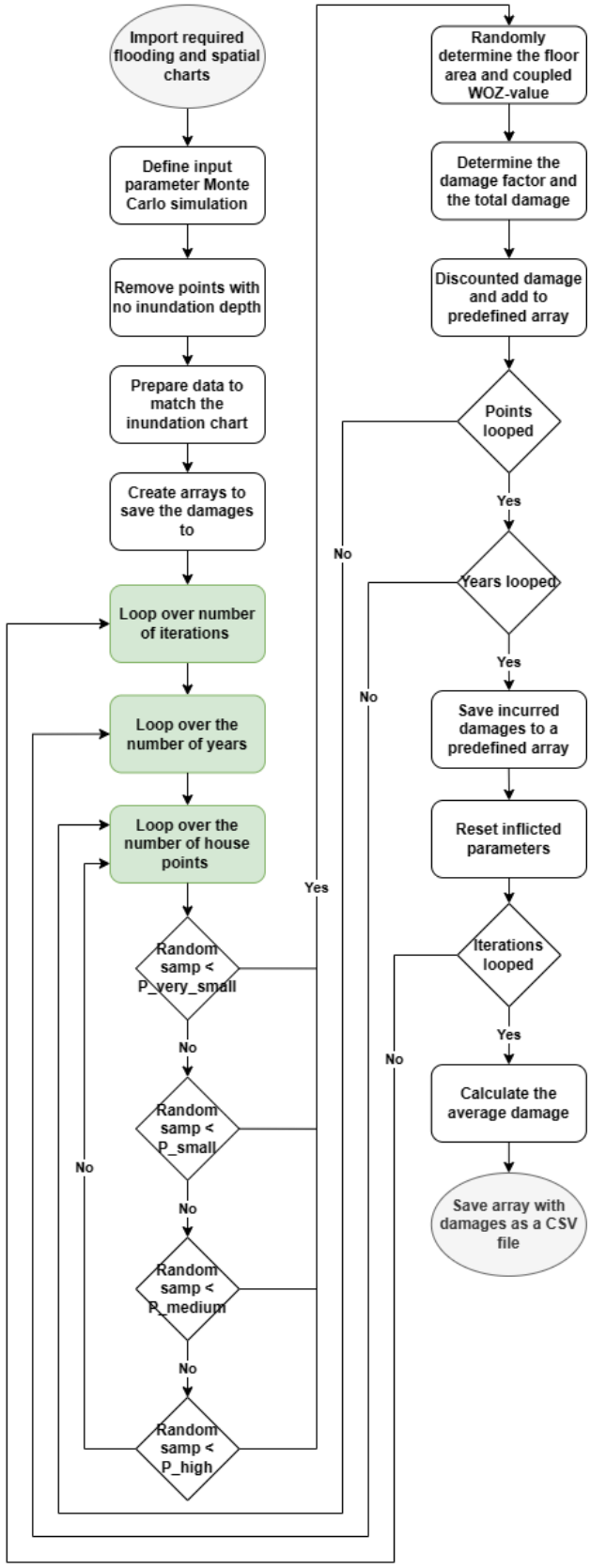

Figure E.3: *Simulation flowchart to estimate flood damages given the flood probability.*

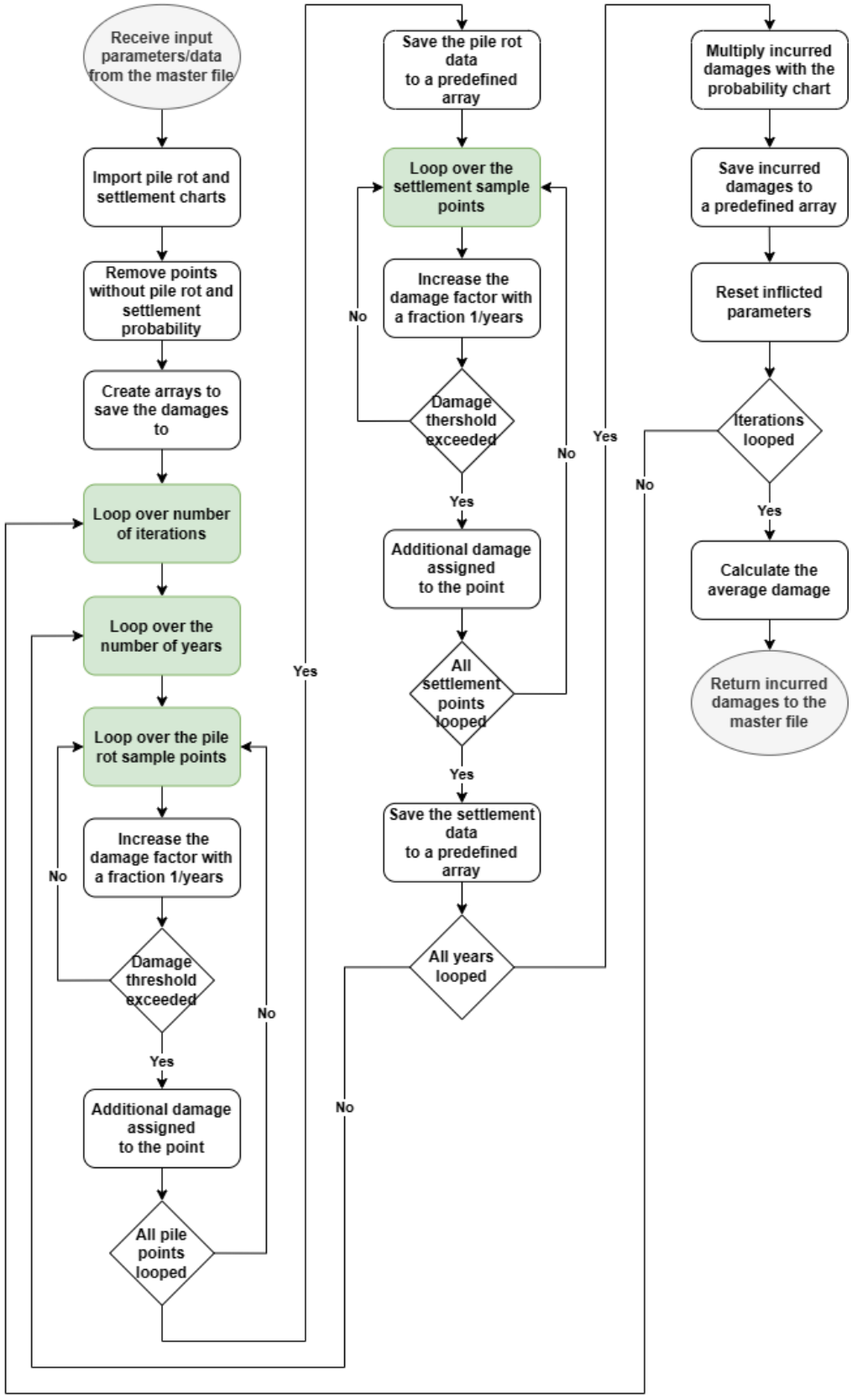

Figure E.4: *Simulation flowchart to estimate indirect damages.*

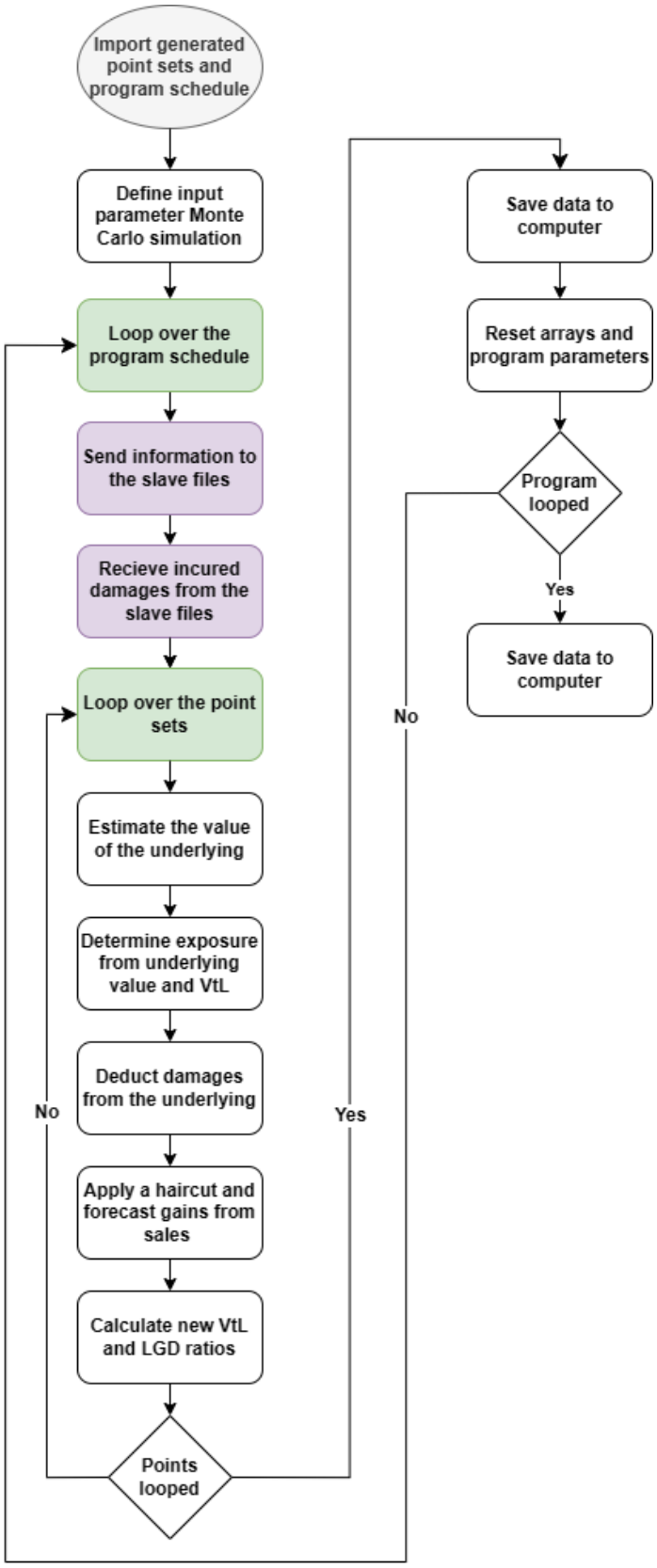

Figure E.5: *Simulation flowchart to estimate the economic implications of the incurred damages.*

Appendix F Flood damage methodology

F.1 Standaardmethode 2017 Schade en Slachtoffers

To adjudicate the damage a building has sustained during floods, the Dutch government together with Deltares developed a damage indication methodology. This rather simple methodology employs damage indicators, building surface areas, and base rates. The basis for this damage model is a combination of previously published models and actual flood damage observations. This methodology is tailor-made for the Netherlands. Hence, the prices and damage curves are specifically created to serve the Netherlands and would not provide an appropriate indication for other countries. The equation the methodology is built upon is provided in Equation F.1 below.

$$S_i = \sum_{i=1}^{n} a_i SA_i SN_i \tag{F.1}$$

Wherein, S is the total incurred damage, a is the damage factor, SA is the surface area of the building, and SN is the base rate per unit of damage. The most substantial influence on the damage sustained due to flooding is the damage indicator. This indicator provides a percentage of the original price per meter which is endured as damage by the building. In this methodology, the damage indicator is solely dependent on the inundation depth of the flood. Obviously, the methodology provides a rough estimation of the actual damage encountered since parameters such as flood duration and flow velocity are also important in floods [106, 108]. However, it provides a relatively good approximation of the damages since the damage-depth curves are specifically calibrated for the Netherlands.

Deltares has provided these types of damage indicators for several types of buildings and houses. The report splits different buildings/structures into four distinct categories. Nevertheless, only two categories are relevant to this thesis. Specifically, the report separates the damages incurred on businesses from damage on residential buildings. The business buildings are further divided into the building purpose implemented in the BAG.

The residential building category is divided based on single-family homes and multi-family homes. Furthermore, the damage indicator graphs differentiate between apartments depending on the floor where the apartment is located. The ground, first, and higher floors each have their separate damage indicator graph, whereas the base damage is identical. Additionally, a damage function regarding the household inventory is included in the report. The shape of this function is equal for all the different households and hence is independent of the apartment floor. Nevertheless, the beginning of the curve shifts by 2.5 meters depending on the apartment floor since the household inventory is not damaged if the water does not reach the apartment. For example, if an apartment is located on the third floor, the damage factor remains 0 until the flood reaches an inundation depth of 7.5 meters. The last damage function important for this thesis pertains to the structure of a house. This damage is relevant to houses designed for single families. The damage functions regarding apartments and households are provided in Figure F.1a and Figure F.1b, respectively.

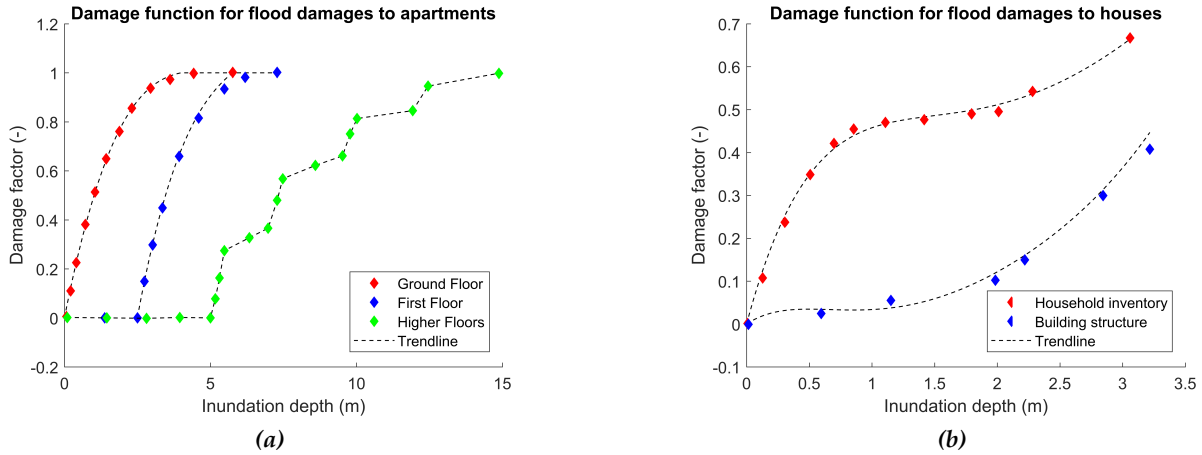

Figure F.1: ***(a)*** *The damage function of flood damages to appartments,* ***(b)*** *The damage function of flood damages to the household inventory and building structure [46].*

The last piece of required information delivered by the Standaardmethode 2017 Schade en Slachtoffers is the base rate per unit incurred during a flood. This information is based on a report by Bruijn et al. published in 2015 [109]. A summary of the most important figures from this report are provided in Table F.1.

Table F.1: *Maximum damage per category per unit [46].*

Category	Unit	Direct Damage
Building structure	m^2	1,000
Household inventory	Object	70,000